Universidad de Alcalá

FRIEDRICH-ALEXANDER UNIVERSITÄT ERLANGEN-NÜRNBERG

Characterization of peripheral nociceptors during chronic secondary pain: experimental studies in mice

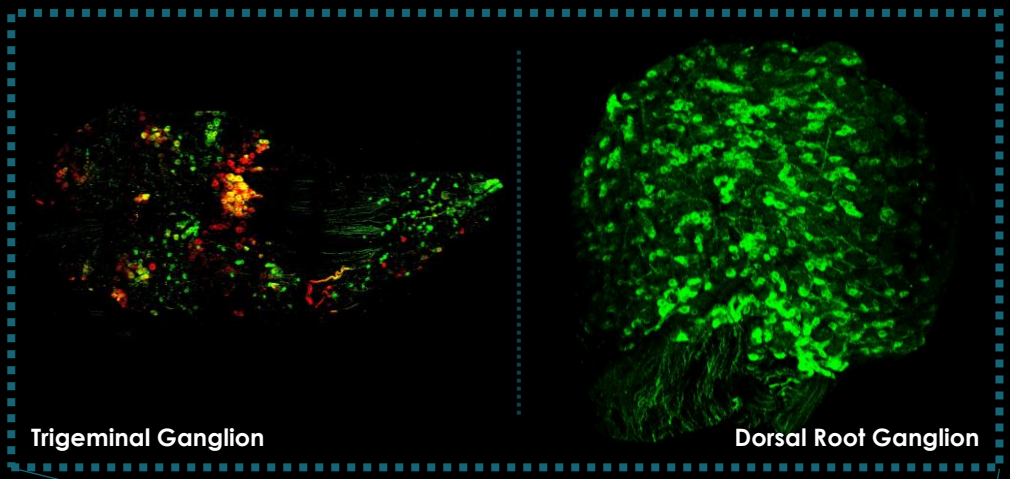

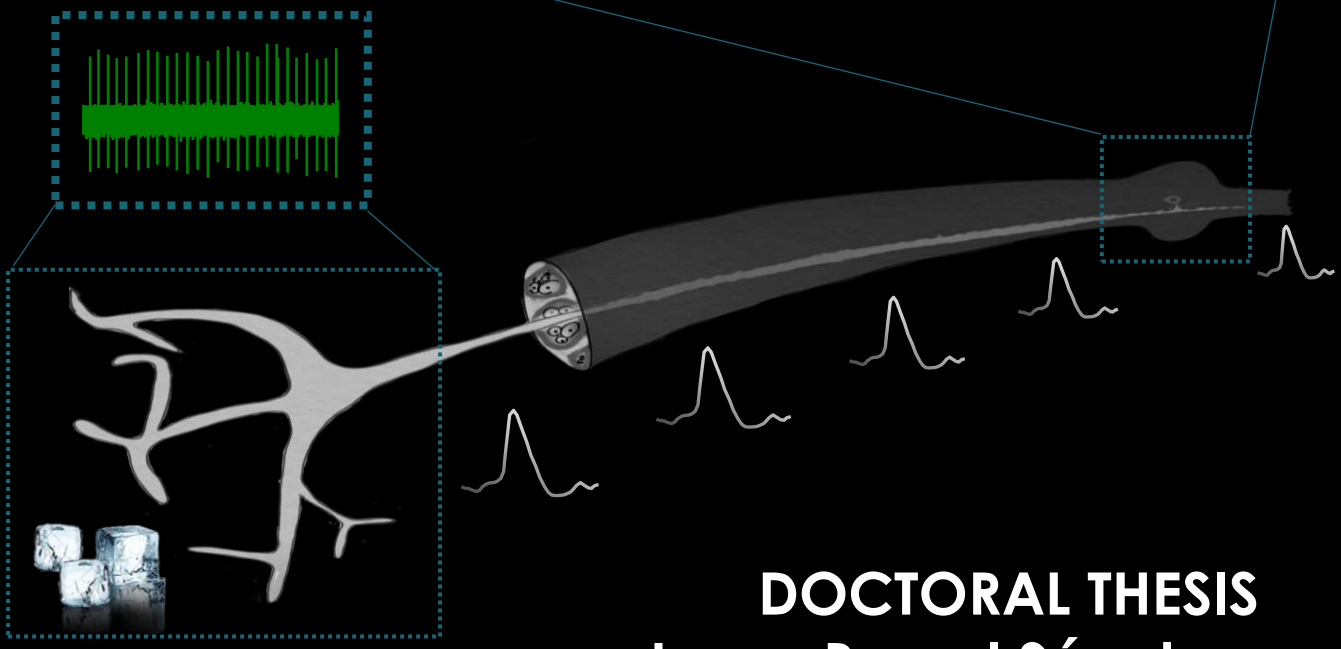

DOCTORAL THESIS

Laura Bernal Sánchez

Alcalá de Henares, 2020

Characterization of peripheral nociceptors during chronic secondary pain: experimental studies in mice

DOTORAL THESIS IN JOINT SUPERVISION WRITTEN BY

Laura Bernal

To obtain the degree of

DOCTOR OF PHYSIOLOGY

by the Universidad de Alcalá

- *International Doctorate Mention* -

(Doctorado en Señalización Celular)

and

DOCTOR OF HUMAN BIOLOGY

by the Friedrich-Alexander-Universität Erlangen-Nürnberg

(IZKF Research Training Group)

Alcalá de Henares, 2020

Supervisors: **Dr. Carolina Roza Fernández de Caleya** (Universidad de Alcalá)

Dr. Katharina Zimmermann (Friedrich-Alexander-Universität Erlangen-Nürnberg)

Laura Bernal was supported by a Scholarship from the Ministerio de Educación, Cultura y Deporte (Formación de Profesorado Universitario Scholarship, FPU15/02262 and Ayudas a la movilidad predoctoral EST17/00833), a contract from IZKF, and the Universidad de Alcalá (Ayudas a la movilidad de personal investigador en formación 2019). The work included in this thesis was supported by grants from Ministerio de Economia y Competitividad (BFU2012-37905 and SAF2016-77585-R), Universidad de Alcalá (CCG2014/BIO-020), IZKF Project E14, the Pfleger Foundation, and the German Research Council (DFG ZI 1172/3-1 and ZI 1172/4-1).

"Failure is simply the opportunity to begin again,

this time more intelligently"

Henry Ford

"[…] Well, what do we do about that? We treat these patients in a rather crude fashion at this point in time. We treat them with symptom-modifying drugs -- painkillers --which are, frankly, not very effective for this kind of pain. We take nerves that are noisy and active that should be quiet, and we put them to sleep with local anesthetics. And most importantly, what we do is we use a rigorous, and often uncomfortable, process of physical therapy and occupational therapy to retrain the nerves in the nervous system to respond normally to the activities and sensory experiences that are part of everyday life. And we support all of that with an intensive psychotherapy program to address the despondency, despair and depression that always accompanies severe, chronic pain.

But the future is actually even brighter. The future holds the promise that new drugs will be developed that are not symptom-modifying drugs that simply mask the problem, as we have now, but that will be disease-modifying drugs that will actually go right to the root of the problem.

So I have hope that in the future, the prophetic words of George Carlin will be realize, who said, "My philosophy: No pain, no pain"."

Dr. Elliot Krane, The Mystery of Chronic Pain, 2011

Professor of anesthesiology, perioperative and pain medicine at the Stanford University

Acknowledgements

Desde que empecé mi carrera investigadora tengo que agradecer a mucha gente el haber estado ahí para mí, aunque aquí solo nombre a una pequeña parte de ellos. La relación con todos ellos ha traspasado las líneas de la investigación y el trabajo hasta llegar a límites personales.

Debo comenzar con aquella persona que me descubrió lo que era la investigación, y me libró de unas prácticas aburridas en un laboratorio clínico. Desde ese momento, comenzamos una aventura que ha durado casi 8 años (8!!). Carol, gracias por dejarme entrar de tu laboratorio y usar tus pinzas, y tambiénpor haberme formado como científica y como persona. Chin Chin por todas las enseñanzas durante estos años, y todas las oportunidades que gracias a ti he conseguido. Todo esto hace que las broncas y regañinas se olviden.

Pese a llevar tantos años en el laboratorio he tenido mis idas y venidas. Una de las grandes oportunidades que he tenido ha sido poder vivir y trabajar en Alemania. Katharina, me recibiste con los brazos abiertos (y el set-up sin montar) y lo que he aprendido contigo me acompañará a lo largo de los años. De estos meses/años, me llevo además grandes amistades. Pamela, mi salvadora y compañera de viajes. Me aportaste mucho, y fuiste mi pilar fundamental. Filip, Christine, Zoltán, gracias.

Alfonso, sólo fueron tres meses que sirvieron para entablar amistad. Por compartir consejos y tu manera de hacer y ver la ciencia, y esas reuniones eternas que terminaban en el bar. Gracias por darme la oportunidad de ver cómo se trabaja allí y conocer a toda esa fantástica gente que formaba tu equipo.

Agradecer también a Many, que me permitió ver qué era eso de investigar en la empresa. Mis meses en Lilly fueron fantásticos y pude aprender mucho. He de decirte, enhorabuena por haber formado un grupo tan estupendo y con tan buen ambiente de trabajo. Muchas gracias Rita, Catherine, Francesca, Ruud, John, y a otros tantos.

Gracias a los del otro lado del pasillo por charlas durante estos años. También tuve la suerte de conocer a otros que pasaron por aquí, Elsa, Irene e Ismel, gracias.

Desde bien pequeña mi familia siempre ha estado ahí, apoyándome incluso cuándo no sabían muy bien que era un doctorado y de si iba o no a trabajar. Mil gracias por todo. Por último, un millón de gracias a mi compañero de vida, Carlos. Sin entender muy bien por qué mi trabajo era como era, has estado ahí en todo momento. Apoyando todas mis decisiones y viajes, aunque no siempre fuera lo mejor para ti.

Mucha más gente ha estado en mi vida estos años, pero no quiero extenderme demasiado, para todos ellos este último GRACIAS.

INDEX

List of Publications I
Meeting Attendances IV
Abbreviations VII

SUMMARY IX

ABSTRACT X

RESUMEN XI

ZUSAMMENFASSUNG XII

INTRODUCTION 1

Chronic pain 2

The nociceptive system 3

Peripheral nociceptors 7

Transduction in peripheral nociceptors 10

Primary afferents in orofacial pain 13

Primary afferents in neuropathic pain 17

Ion channels involved in membrane excitability 19

Hyperpolarization-activated cyclic nucleotide-gated channels 19

Kv7 potassium channels 20

RATIONALE AND GOALS 23

Section I 24

Section II 24

RESULTS 25

SECTION I: CHAPTER 1 26

SECTION II: CHAPTER 1 34

SECTION II: CHAPTER 2 47

DISCUSSION 62

CONCLUSIONS 65

Specific conclusions from Section I 66

Specific conclusions from Section II 66

BIBLIOGRAPHY 67

List of Publications

Publications directly related to this Thesis

Aklesso Kadala, Pamela Sotelo-Hitschfeld, Ziad Ahmad, Philipp Tripal, Benjamin Schmid, Alexander Mueller, **Laura Bernal**, Zoltan Winter, Sebastian Brauchi, Ulrich Lohbauer, Karl Messlinger, Jochen Lennerz, Katharina Zimmermann. *Fluorescent labelling and 2-photon imaging of mouse tooth pulp nociceptors*. **Journal of Dental Research**. 2018 Apr;97(4):460-466. doi: 10.1177/0022034517740577.

Impact Factor: 5.125 (2/90 Dentistry, Oral Surgery & Medicine)

Cites: 2

Laura Bernal, Carolina Roza. *Hyperpolarization-activated channels shape temporal patterns of ectopic spontaneous discharge in C-nociceptors after peripheral nerve injury*. **Eur J Pain**. 22(8), pp. 1377-1387. doi: 10.1002/ejp.1226

Impact Factor: 3.188 (10/31 Anesthesiology; 69/199 Clinical Neurology; 116/267 Neuroscience)

Cites: 6

Laura Bernal, Jose A. Lopez-Garcia and Carolina Roza. *Spontaneous activity in C-fibres after partial damage to the saphenous nerve in mice: effects of retigabine*. **Eur J Pain**. 2016 Sep;20(8):1335-45. doi: 10.1002/ejp.858.

Impact Factor: 3.019 (10/31 Anesthesiology; 69/194 Clinical Neurology; 120/259 Neuroscience)

Cites: 5

Other publications

Laura Bernal, Elsa Cisneros, Carolina Roza. *Expression of the regeneration-associated gen pSTAT3 and functional changes in uninjured nociceptors after peripheral nerve damage in mice.* Under preparation.

Laura Bernal*, Pamela Sotelo-Hitschfeld*, Christine König, Viktor Sinica, Amanda Wyatt, Zoltan Winter, Alexander Hein, Filip Touska, Susanne Reinhardt, Aaron Tragl, Ricardo Kusuda, Philipp Wartenberg, Allen Sclaroff, John D. Pfeifer, Fabien Ectors, Andreas Dahl, Marc Freichel, Viktorie Vlachova, Sebastian Brauchi, Carolina Roza, David E. Clapham, Ulrich Boehm, Jochen K. Lennerz and Katharina Zimmermann. *Odontoblast TRPC5 Channels Signal Cold Pain in Teeth.* Submitted to Science (13.07.2020).

Laura Bernal, Elsa Cisneros, Nuria García-Magro, Carolina Roza. *Immunostaining in whole-mount lipid-cleared peripheral nerves and dorsal root ganglia after neuropathy in mice.* Scientific Reports. 2019 Jun 10;9(1):8374. doi: 10.1038/s41598-019-44897-7.

Laura Bernal. *Insights into Voltage-Gated Sodium Channel 1.7 Contribution to Paclitaxel-induced Neuropathy.* Journal of Neuroscience 2018 Jul 4;38(27):6025-6027. doi: 10.1523/JNEUROSCI.0692-18.2018.

Aida Castellanos, Alba Andrés, **Laura Bernal**, Gerard Callejo, Nuria Comes, Arcadi Gual, Jonathan P. Giblin, Carolina Roza, Xavier Gasull. *Pyrethroids inhibit K2P channels and activate sensory neurons: basis of insecticide-induced paraesthesias.* Pain. 2018 Jan; 159(1):92-105 doi: 10.1097/j.pain.0000000000001068.

Alvarado-Vázquez A*, **Bernal L.*,** Paige CA, Grosick RL, Moracho Vilrriales C, Ferreira DW, Ulecia-Morón C, Romero-Sandoval EA. *Macrophage-specific nanotechnology-driven CD163 overexpression in human macrophages results in an M2 phenotype under inflammatory conditions*. Immunobiology. 2017 Aug;222(8-9):900-912. doi: 10.1016/j.imbio.2017.05.011.

Laura Bernal*, Abigail Alvarado-Vázquez*, David Wilson Ferreira, Candler A. Paige, Cristina Ulecia-Morón, Bailey Hill, Marina Caesar, E. Alfonso Romero-Sandoval. *Evaluation of a nanotechnology-based approach to induce gene-expression in human THP-1 macrophages under inflammatory conditions.* Immunobiology. 2017 Feb;222(2):399-408 doi: 10.1016/j.imbio.2016.08.010.

*equal contribution

Meeting Attendances

L. Bernal, E. Cisneros, C. Roza. *Expression of pSTAT3 after peripheral nerve damage: injured and non-injured afferents profile in neuropathic pain models*. Presented as a poster at Neuroscience 2019, October 19-23, 2019. Chicago, USA

Laura Bernal, Pamela Sotelo-Hitschfeld, Katharina Zimmermann, Carolina Roza. *Hipersensibilidad dental: estudios experimentales en ratón*. Oral presentation gave to IV Congress in Cell Signaling. March 20-22, 2019. Alcalá de Henares, Spain.

L. Bernal, E. Cisneros, N. García-Magro, P. Sotelo-Hitschfeld, C. Roza. *Immunostaining of whole-mount lipid-cleared dorsal root ganglia from mice after retrograde tracing from experimental neuromas*. Presented as a poster at 17th World Congress on Pain, September 12-16, 2018. Boston, USA.

P. Sotelo-Hitschfeld, **L. Bernal**, R. Kuzuda, S. Reinhardt, M. Lesche, C. Roza, S. Brauchi, A. Dahl, K. Zimmermann. *Transcriptomic characterization of mouse trigeminal sensory neurons originating from cornea, dura and molar teeth.* Presented as a poster at 17th World Congress on Pain, September 12-16, 2018. Boston, USA.

Laura Bernal, Carolina Roza. *Inmunohistoquímica en ganglios transparentes tras marcaje retrógrado de neuromas experimentales en ratón*. Oral presentation gave to III Congress in Cell Signaling. March 20-22, 2018. Alcalá de Henares, Spain.

Aida Castellanos, Alba Andrés, **Laura Bernal**, Gerard Callejo, Nuria Comes, Arcadi Gual, Jonathan P. Giblin, Carolina Roza, Xavier Gasull. *Pyrethroids inhibit K2P channels and activate sensory neurons: basis of insecticide-induced paraesthesias.* Presented as poster at Neuroscience 2017. November 11-15, 2017. Washington DC, USA.

Laura Bernal, Carolina Roza. *Nuevas dianas terapéuticas en el tratamiento de dolor neuropático de origen periférico.* Oral presentation gave to II Congress in Cell Signaling. March 14-16, 2017. Alcalá de Henares, Spain.

L. Bernal, P. Sotelo-Hitschfeld, C. Roza, K. Zimmermann. *Characterizing cold sensitivity in mouse tooth pulp nociceptors using a novel ex vivo jaw-alveolar nerve preparation and retrograde fluorescent labeling.* Presented as a poster at the 16th World Congress on Pain, September 26-30, 2016. Yokohama, Japan.

Laura Bernal, Aklesso Kadala, Ziad Ahmad, Alexander Mueller, Karl Messlinger, Katharina Zimmermann. *Advanced retrograde fluorescence labelling of dental primary afferent neurons innervating rat and mouse maxillary molars.* Presented as a poster at the 16th World Congress on Pain, September 26-30, 2016. Yokohama, Japan.

C. Roza, E. Cisneros, **L. Bernal**, J. Lopez-Garcia. *Kv7.2 channels in neuropathic pain: axonal transport and functional implications.* Presented as a poster at the 16th World Congress on Pain, September 26-30, 2016, Yokohama, Japan.

Laura Bernal, Carolina Roza, Katharina Zimmermann. *An in-vitro mouse jaw nerve preparation to study cold sensitivity in dental primary afferents.* Presented as poster in the IZKF-Symposium 2016 "Translational Medicine". June 16-17 2016. Kloster Banz, Germany.

A. Alvarado, **L. Bernal**, D. Ferreira, C. Paige, A. Romero-Sandoval. *Increase of anti-inflammatory cytokines in human macrophages that overexpress CD163 under different pro-inflammatory conditions.* Presented as a poster at the 2016 Scientific Meeting of the American Pain Society, May 11-14, 2016, Austin, TX, USA.

Abbreviations

ACC - anterior cingulate cortex

AP – action potential

ASIC – acid-sensing ion channel

BNST - bed nucleus stria terminalis

cAMP - cyclic adenosine monophosphate

CGRP - calcitonin gene-related peptide

C-MC – C-mechanocold fibre

C-MH – C-mechanoheat fibre

CNS- central nervous system

CV – conduction velocity

DiI – 1,1'-Dioctadecyl-3,3,3',3'-Tetramethylindocarbocyanine perchlorate

DM - dura mater

DPANs- dental primary afferent neurons

DRG – dorsal root ganglia

EGFPf – enhanced green fluorescent protein

FG – fluoro-gold

GPCR – G protein-coupled receptors

HCN – hyperpolarization-activated cyclic nucleotide-gated channel

HRP – horseradish peroxidase

IB4 - isolectin B4 from Griffonia simplicifolia B4

ICD-11 – 11st International Classification of Diseases

IL – interleukin

ISI – interspike interval

Kv7, KCNQ - voltage-gated potassium channels subfamily KQT

LTMR - low-threshold mechanoreceptors

MrgprD - Mas-related G-protein coupled receptor member D

NAc - nucleus accumbens

Nav – sodium voltage-gated channel

NEFH - neurofilament heavy

NGF - nerve growth factor

PAG - periaqueductal gray

PBS – phosphabe-buffered saline

PFA – paraformaldehyde

PFC - prefrontal cortex

PGE2 – prostaglandin E2

RET - glial-derived neurotrophic factor family ligand receptor

RF – receptive field

RVM - rostroventral medulla

S1 - primary somatosensory cortex

S2 - secondary somatosensory cortex

SD – standard deviation

SIF – synthetic interstitial fluid

SP – substance P

SST – somatostatin

TG – trigeminal ganglia

TNF - tumor necrosis factor

TrkA - tyrosine kinase receptor A

TRP - transient receptor potential

TRPA1 - transient receptor potential ankyrin 1

TRPC5 - transient receptor potential canonical 5 channel

TRPM8 - transient receptor potential melastatin 8

TRPV1 - transient receptor potential vanilloid 1

SUMMARY

ABSTRACT

Chronic Pain is one main cause of human suffering and disability, affecting 20% of the global population. However, we still lack effective treatment. Among the different forms of chronic pain, orofacial and neuropathic pain are of special interest in our research groups.

As orofacial pain is concerned, dental pain is unique, because stimulation of teeth only produces pain as feeling, with cold as the most prominent stimuli to evoke this sensation. There are several ion channels of the transient receptor potential (TRP) family (mainly TRPM8, TRPA1) that, at least in cutaneous nociceptors with their cell bodies in the dorsal root ganglia, participate in cold transduction. However, fewer studies have involved primary afferents innervating the teeth, in which cell bodies are located in the trigeminal ganglia together with cell bodies of neurons innervating other facial organs and structures. We optimized a method to specifically study primary afferent nociceptors innervating the tooth pulp of the mouse by retrograde labelling and found expression of different TRP channels in dental primary afferent neurons. Its combination with other methodologies will be the basis for futures studies on dental chronic pain and cold transduction mechanisms.

Within the entity of neuropathic pain, spontaneous pain is the main symptom reported by patients, which has been linked to spontaneous discharges in peripheral nociceptors. However, as most of the previous studies have focused on the evaluation of stimulus-induced symptoms, the underlying causes of spontaneous activity remain unclear. We used a mouse model of partial damage of a peripheral nerve and showed a high incidence of spontaneous nociceptors firing action potentials at constant rates. Using pharmacological tools, we demonstrated the contribution of hyperpolarization-activated cyclic nucleotide-gated (HCN) channels and a member of the voltage-gated potassium channel subfamily KQT (Kv7) to ectopic spontaneous activity in peripheral nociceptors. Our results suggest HCN and Kv7 channels as peripheral targets to treat neuropathic pain.

RESUMEN

La cronificación del dolor es la mayor causa de sufrimiento e incapaz humana, afectando al 20 % de la población mundial. Sin embargo, todavía carece de tratamiento eficaz. De las diferentes formas de dolor crónico que existen, el dolor orofacial y el dolor neuropático son de especial interés en nuestros grupos de investigación.

Dentro del dolor orofacial, el dolor dental es especial ya que cualquier estimualción en el diente produce sólo dolor, siendo el frío el estímulo más efectivo para evocar esta sensación. Hay diferentes moléculas de la familia de receptores de potencial transitorio (TRP por sus siglas en inglés, principalmente TRPM8 y TRPA1) que, en nociceptores cutáneos con cuerpos celulares en ganglios de la raíz dorsal, participan en la transducción al frío. Sin embargo, existe menos información referente a aferencias primarias que inervan los dientes, cuyos cuerpos celulares se encuentran en el ganglio trigémino, junto con cuerpos celulares de neuronas que inervan otras estructuras. Optimizamos un método que permite estudiar especificamente aferencias primarias que inervan la pulpa dental de ratón, utilizando el marcaje retrógrado. Así, estudiamos la expresión de diferentes canales TRP en neuronas inervando la pulpa dental. La combinación de estos estudios con otras metodologías es la base para futuros estudios en dolor dental y los mecanimos de transducción de estímulos de frío.

Dentro del dolor neuropático, el dolor espontáneo es el principal síntoma reportado por los pacientes, y el cuál ha sido ligado a descargas espontáneas en nociceptores periféricos. Sin embargo, la mayoría de los estudios previos se han enfocado en evaluar los síntomas evocados, motivo por el cual las causas subyacentes al dolor espontáneo siguen sin resolverse. Utilizamos un modelo de daño parcial a un nervio periférico que muestra una alta incidencia de nociceptores espontáneos con frecuencias estables. Utilizando farmacología, demostramos la contribución de canales con compuerta de nucleótidos cíclicos activado por hiperpolarización (HCN) y canales de potasio activados por voltaje de la subfamilia KQT (Kv) en la generación de actividad espontánea ectópica en nociceptores periféricos. Esto sugiere que estos canales serían dianas periféricas para el tratamiento del dolor neuropático.

ZUSAMMENFASSUNG

Chronische Schmerzen sind eine der Hauptursachen für menschliches Leid und Behinderung und betrifft 20% der Weltbevölkerung. Bisher fehlt es immer noch an wirksamen Behandlungsstrategien. Unter den verschiedenen Formen chronischer Schmerzen sind orofaziale und neuropathische Schmerzen in unseren Forschungsgruppen von besonderem Interesse.

Was orofaziale Schmerzen angeht, so sind Zahnschmerzen einzigartig, da die Stimulation der Zähne nur Schmerzen als Gefühl hervorruft, wobei Kälte den wohl bekanntesten Reiz darstellt, um diese Empfindung hervorzurufen. Es gibt mehrere Ionenkanäle der Transient Rezeptor Potential (TRP) -Familie (hauptsächlich TRPM8, TRPA1), die zumindest in kutanen Nozizeptoren, deren Zellkörper in den Hinterwurzelganglien liegen, an der Kältetransduktion beteiligt sind. In einer geringeren Anzahl an Studien wurden auch primäre Afferenzen der Zähne untersucht, wobei sich deren Zellkörper in den Trigeminalganglien befinden. Sie liegen dort in direkter Nachbarschaft von Zellkörpern, die andere Organe des Kopfes und die Gesichtshaut sensorisch innervieren. Wir haben eine Methode optimiert, um primär afferente Nozizeptoren, die die Zahnpulpa der Maus innervieren, durch retrograde Markierung molarer Oberkieferzähne spezifisch zu erkennen und zu untersuchen. In diesen Neuronen haben wir die Expression verschiedener TRP-Kanäle dokumentiert. Die Kombination dieser Markierungstechnik mit anderen funktionellen Methoden wird die Grundlage für zukünftige Studien zu chronischen Zahnschmerzen und Kältetransduktionsmechanismen bilden.

Innerhalb der Einheit der neuropathischen Schmerzen sind spontane Schmerzen das Hauptsymptom, über das Patienten berichten und es wurde mit spontanen Entladungen von peripheren Nozizeptoren in Verbindung gebracht. Da sich die meisten früheren Studien jedoch auf die Untersuchung von stimulusinduzierten Effekten konzentriert haben, bleiben die zugrunde liegenden Ursachen für spontane Aktivität in Nozizeptoren unklar. Wir verwendeten ein Mausmodell der teilweisen Schädigung eines peripheren Nervs und zeigten eine hohe Inzidenz von spontanen Nozizeptoren, die Aktionspotentiale mit konstanten Impulsraten abfeuern. Mit pharmakologischen Hilfsmitteln konnten wir die Beteiligung von hyperpolarisations-aktivierten zyklischen Nucleotid-gesteuerten (HCN) Kanälen und spannungsgesteuerten Kaliumkanälen der KQT Unterfamilie (Kv7) zur ektopischen spontanen Aktivität in peripheren Nozizeptoren demonstrieren. Unsere Ergebnisse legen

nahe, dass HCN- und Kv7-Kanäle zu effizienten peripheren Zielstrukturen bei der Behandlung von neuropathischen Schmerzen werden könnten.

INTRODUCTION

Chronic pain

The International Association for the Study of Pain (IASP) defines pain as "an unpleasant sensory and emotional experience associated with actual or potential tissue damage or described in terms of such damage". Whilst physiological pain acts as an early-warming protective system, chronification of pain is the main cause of human suffering and disability and one of the main reasons for patients to seek medical care (Goldberg & McGee, 2011; Mäntyselkä et al., 2001).

Chronic pain is defined as pain that lasts or recurs longer than 3 months (Treede et al., 2019). A large-scale survey in 2006, described that 20% of the Europeans (~95 million people) suffer from chronic pain, and 34% of the patients reported severe pain (Breivik et al., 2006; Pain Alliance Survey 2018). The lack of adequate treatment leads to a decreased quality of life, reduced productivity, the appearance of psychiatric symptoms and illness (i.e. depression, insomnia, anxiety) and increased risk for suicide (see Goldberg & McGee, 2011 for a review).

First-line pharmacological treatment includes acetaminophen and non-steroidal anti-inflammatory drugs, but also antidepressants, anticonvulsants, muscle-relaxant and opioids. Side effects include sedation, nausea, tolerance and addiction and opioid overdose being an extended problem in the US; besides, these medications might even promote the chronification of pain (see Bigal & Lipton, 2009 for a review). Unfortunately, a high number of patients are unresponsive to any of these treatments and the alternatives include ketamine infusions and spinal cord, transcranial or deep brain stimulation, which effects are still limited (Cohen et al., 2018; Farrell et al., 2018). Altogether, there is a medical need to search for new pharmacological targets.

Due to the high prevalence and disability rates, since 2018 chronic pain has been included as a disease in its own right in the International Classification of Diseases (ICD-11, https://icd.who.int/browse11/l-m/en) which eases diagnosis and pain management for clinicians (Treede et al., 2019). The ICD-11 recognizes **chronic primary pain** as pain with has an unknown origin, such as fibromyalgia or irritable bowel syndrome. When pain manifests as a symptom of another disease but lasts the resolution of the disorder, it is called **chronic secondary pain**. Neuropathic pain and chronic secondary orofacial pain are different categories among chronic secondary pain and are the areas of research of the laboratories where I have performed the experiments contained in the present thesis.

The nociceptive system

As a general feature, chronic pain conditions are the result of pathological processing throughout the **nociceptive system**.

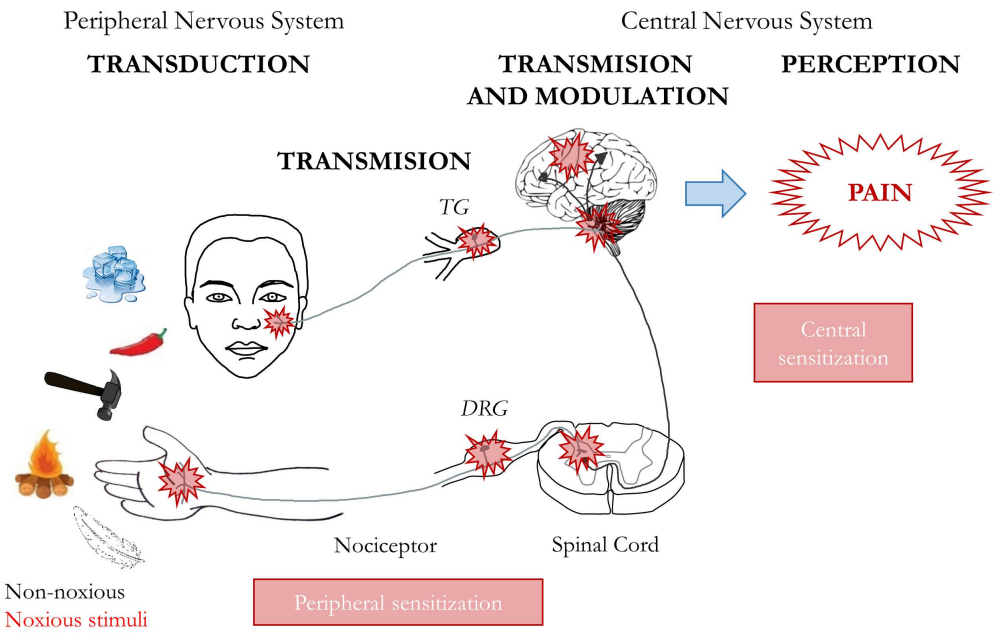

Figure 1. Detection of noxious stimuli occurs at the peripheral endings of nociceptors, which generate action potentials that propagate along the axon. The electrical signals reach the central nervous system, where they are integrated. In chronic pain conditions, there are alterations in the nociceptive processing at the level of the peripheral nociceptor, spinal cord and supraspinal structures (marked as red stars), which leads to peripheral and central sensitization and finally, to abnormal pain sensations. In this scenario, even non-noxious stimuli such as pleasant cooling or a light stroke of the skin with a feather, can evoke pain. TG: trigeminal ganglia; DRG: dorsal root ganglia.

The first element in the nociceptive system is the so-called *primary afferent nociceptor*, a specialized receptor able to detect stimuli that are usually perceived as painful (see below *Peripheral nociceptors*). Briefly, nociceptors are pseudounipolar neurons that have their soma in the trigeminal ganglia -TG- (sensory information from the head) or dorsal root ganglia -DRG- (from the trunk and limbs). The peripheral branch innervates skin, viscera, joints, muscles, etc, whilst the central projection ends in the central nervous system.

Primary afferents from the trunk and the limbs travel in 31 spinal nerves and enter the spinal cord through the dorsal roots. The afferents terminate in different laminae of the spinal cord

according to their physiological role, where they synapse with second-order neurons (Light & Perl, 1979; Rexed, 1952; Todd, 2002; Todd, 2010). Myelinated (Aδ-) nociceptors mainly terminate in lamina I and II, but might arborize up to lamina V. Unmyelinated C-nociceptors, thermoreceptors and some fibres responding to substances that evoke itch, terminate in lamina I and II. Myelinated (Aβ-, Aδ-) low-threshold mechanoreceptors (LTMRs) arborize in the spinal cord and end in the deep laminae of the dorsal horn (from lamina II to V), while unmyelinated LTMRs terminate in lamina II. In certain forms of chronic pain, LTMRs might be involved in touch-evoked pain (Campbell et al., 1988; Seal et al., 2009).

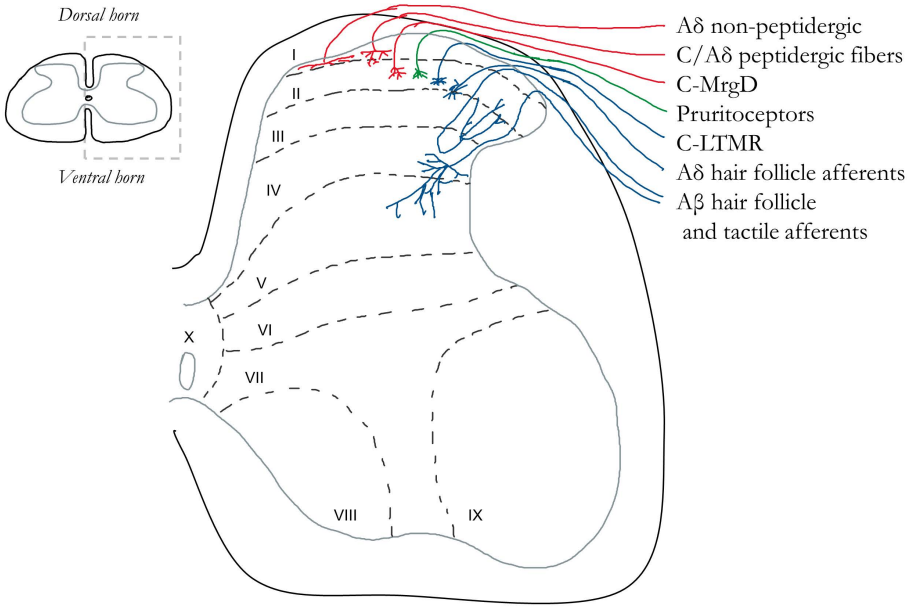

Figure 2. Central projections of primary afferents with cell bodies within the dorsal root ganglia. Central projections from different classes of primary afferents innervating the skin (Todd et al., 2018). MrgD: mas-related G protein-coupled receptor D; LTMR: low-threshold mechanoreceptor.

Sensory information from the face travels mainly through the three branches of the trigeminal nerve (ophthalmic -V_1-, maxillary -V_2- and mandibular nerves -V_3-) and terminates in the spinal trigeminal nucleus. This nucleus is divided into three subnuclei: *pars oralis*, *pars interpolaris* and *pars caudalis*. Nociceptive trigeminal afferents (mainly unmyelinated, but some myelinated Aδ-fibres) from the skin terminate in the *pars caudalis*, which also receives thermal sensations (Pajot et al., 2000; Sessle, 2000). Here, primary afferents enter topographically organized in an onion-skin distribution, so that upper face regions are represented ventrally and lower face regions, dorsally (see Figure 3, (Shigenaga et al., 1986). The subnucleus

interpolaris is associated with dental pain. Both the subnucleus *interpolaris* and *oralis* are associated with discriminative touch (myelinated LTMRs, (Sessle, 2000).

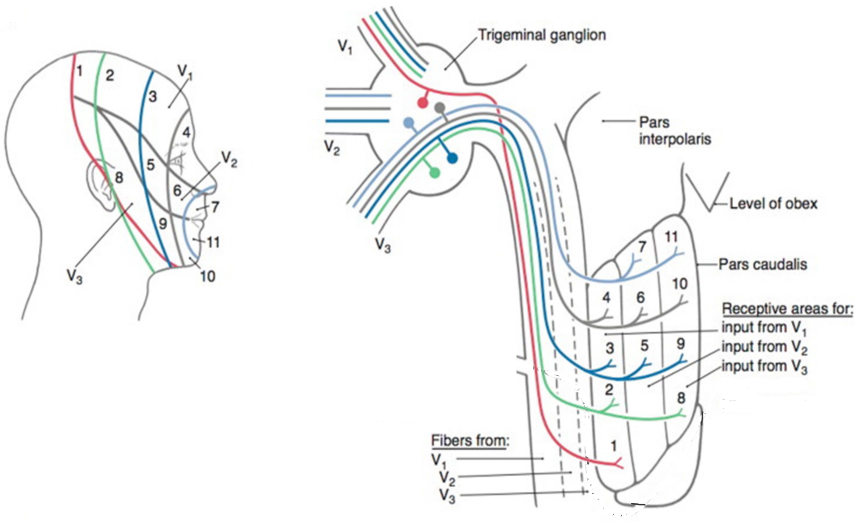

Figure 3. Central projections of primary afferents with cell bodies within the trigeminal ganglia. Central projections from primary afferents innervating the face end in the *pars caudalis* of the spinal trigeminal nucleus with an onion-skin pattern. Afferents associated with dental pain enter the *pars interpolaris*. Obtained from (Fillmore & Seifert, 2015).

Second-order neurons located in the spinal cord and the spinal trigeminal nucleus send their information to different nuclei in the brain by two main pathways (see Figure 4). The *spinothalamic-cortical pathway* processes the discriminative aspects of pain and the *spinoparabrachial-limbic pathway* is principally involved in processing the affective and motivational aspects of pain (Gauriau & Bernard, 2002). Furthermore, there are also descending inhibitory and facilitatory pathways that originate in the brainstem and cortical regions, and terminate diffusely within the spinal dorsal horn and trigeminal nuclei (see Figure 4, (Reynolds, 1969; Zhuo & Gebhart, 1997).

Altogether, pain perception is a complex process that involves a large network of areas and pathways, of which the individual functional contributions are still poorly understood.

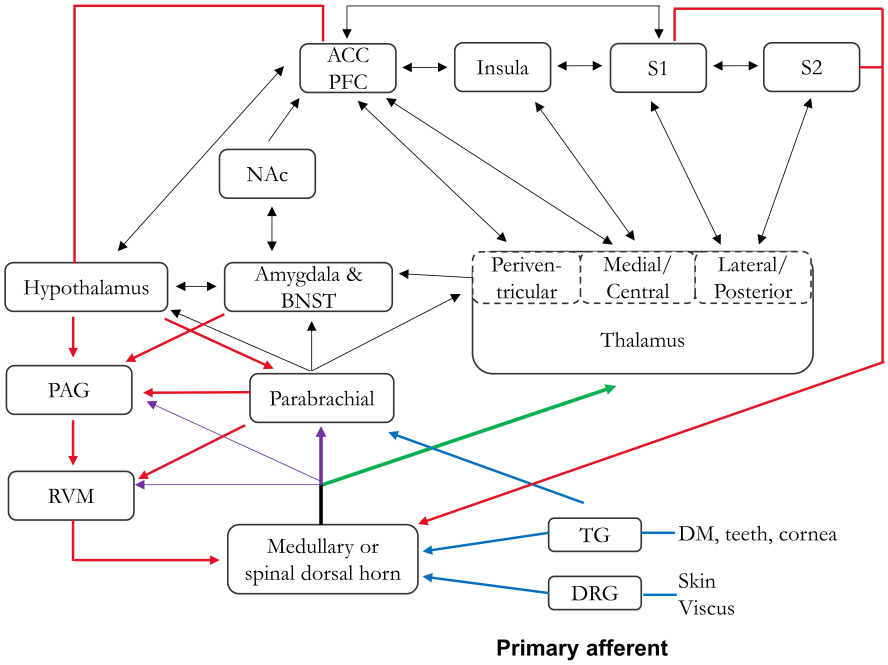

Figure 4. Diagram of neural pain pathways. Noxious information sensed by the primary afferents (blue) is processed by the spinothalamic-cortical pathway (discriminative aspects of pain, green) and the spinoparabrachial-limbic pathway (affective-motivational aspects of pain, purple). There are also descending modulatory pathways (red). ACC: anterior cingulate cortex; PFC: prefrontal cortex; S1: primary somatosensory cortex; S2: secondary somatosensory cortex; NAc: nucleus accumbens; BNST: bed nucleus stria terminalis; PAG: periaqueductal gray; RVM: rostroventral medulla; TG: trigeminal ganglion; DRG: dorsal root ganglion; DM: dura mater. Modified from (Todd et al., 2018).

During chronic pain, functional changes on different levels of the nociceptive system have been identified. At the peripheral level, nociceptive neurons reduce their activation threshold and increase sensory signalling (*peripheral sensitization*). For example, microneurography recordings from patients with phantom limb pain demonstrated ectopic spontaneous activity in the nerve stump (Nyström & Hagbarth, 1981). Furthermore, peripheral nerve block with lidocaine alleviated pain resulting from different neuropathies in humans (Galer et al., 1999; Gracely et al., 1992; Haroutounian et al., 2014; Khaliq et al., 2013; Wijayasinghe et al., 2016).

All these results suggest an important role of the primary afferents in chronic pain. This sustained hyperexcitability from peripheral nociceptors provokes "central sensitization" that leads to an increased function of neurons and circuits within the CNS (see Woolf, 2011 for a review).

Peripheral nociceptors

Most of the current knowledge of peripheral nociceptors comes from studies in rodents. Although peripheral nociceptors in rodents have smaller cell diameters compared to humans, the distribution of small and large neurons and neurochemical markers are similar (Josephson et al., 2001; Ray et al., 2018; Rostock et al., 2018).

Nociceptors are classified according to the size of their cellular bodies or somas. Small-diameter neurons (< 30 μm) are unmyelinated **C-fibres** with slow conduction velocity (<1 m/s) or thinly myelinated **Aδ-fibres** with fast conduction velocity (1-14 m/s) (Lawson, 2002; Lawson & Waddell, 1991; McCarthy & Lawson, 1990). The receptive field of Aδ-fibres is small and provides accurate localization of the site of the noxious stimulus in comparison with C-fibres which are associated with large receptive fields and less precise localization of pain. C-fibres comprise about 70-80% of the fibres in a nerve (Schmalbruch, 1986). Large-diameter neurons (>30 μm) are myelinated **Aβ-fibres** with ultrafast conduction velocity (14-40 m/s). Although they mainly carry information from touch mechanoreceptors, a small proportion are nociceptors (Burgess & Perl, 1967; Nagi et al., 2019).

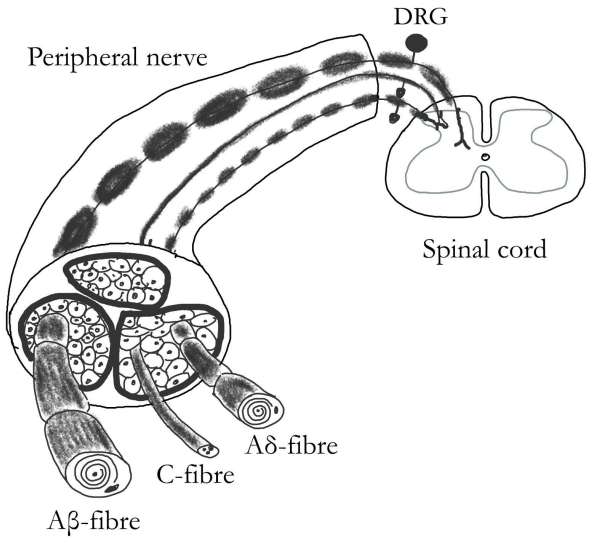

Figure 5. Types of sensory fibres according to their conduction velocity. There are slowly conducting unmyelinated C-fibres, fast conduction thinly myelinated Aδ-fibres, and ultra-fast conducting myelinated Aβ-fibres.

All primary afferent fibres use glutamate as their main excitatory neurotransmitter, but small-diameter nociceptors are usually classed according to the presence or absence of neuropeptides as excitatory neurotransmitters.

Peptidergic nociceptors contain mainly substance P (SP) and calcitonin gene-related peptide (CGRP) (Hökfelt et al., 1975; Ljungdahl et al., 1978; Wiesenfeld-Hallin et al., 1984). Activation of peptidergic nociceptors produces antidromic activation of their peripheral branches, which releases neuropeptides and initiates *neurogenic inflammation* (Bayliss, 1901). CGRP produces vasodilatation, whereas SP increases permeability and plasma extravasation, leading to a local inflammatory response (Edvinsson et al., 1987; Saria, 1984). Peptidergic nociceptors also express tyrosine kinase receptor A (trkA), the receptor for nerve growth factor (NGF) (Averill et al., 1995; Lawson et al., 2019). The binding of NGF to trkA produces upregulation of neuropeptides and modulates the function of different ion channels (such as voltage-gated potassium channels, sodium channels and transient receptor potential channels), contributing to chronic pain conditions (Fang et al., 2005; Gould et al., 2000; Jia et al., 2008; Zhang et al., 2005).

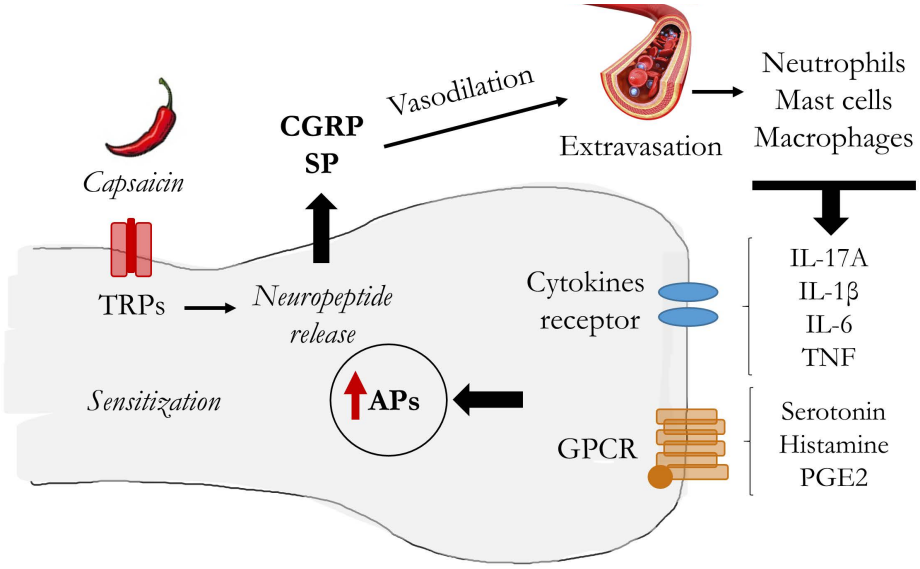

Figure 6. Neurogenic inflammation and the axon reflex. Activation of peripheral peptidergic nociceptors by tissue injury or chemicals (e.g. capsaicin) produces the release of neuropeptides from their peripheral endings, which lead to vasodilation and extravasation of immune cells. Molecules released by immune cells bind and activate nociceptors, altering the function of nerve terminals and leading to increased firing of action potentials. This mechanism contributes to peripheral sensitization. TRP: transient receptor potential; CGRP: calcitonin-gene related peptide; SP: substance P; IL: interleukin; TNF: tumour necrosis factor; PGE: prostaglandin; GPCR: G-protein coupled receptor; AP: action potential.

On the other hand, the so-called **non-peptidergic** C-nociceptors, lack these neuropeptides but can be differentiated as they bind the isolectin B4 from *Griffonia simplicifolia* B4 (IB4) (Nagy & Hunt, 1982; Silverman & Kruger, 1988a, 1988b; Stucky & Lewin, 1999). Most of the non-peptidergic neurons express the glial-derived neurotrophic factor family ligand receptor Ret and the Mas-related G-protein coupled receptor member D (MrgprD) (Franck et al., 2011; Zylka et al., 2005). Some of them also express purinergic receptors such as the P2X purinoceptor 3 (Lawson, Fang and Djouhri, 2019). Conditional ablation of MrgprD in mouse nociceptors showed that these neurons contribute to the physiological perception of mechanical pain (Cavanaugh et al., 2009). Some studies have suggested that IB4+ C-fibres would contribute to the affective component of pain, as they project to limbic regions (Basbaum & Bráz, 2009).

Recent studies using RNA sequencing (RNAseq) analysis have identified up to 10 subclasses of sensory neurons (Li et al., 2018; Li et al., 2016; Usoskin et al., 2015), including 4 subtypes of unmyelinated nociceptors and 1 group of myelinated nociceptors (see Figure 7) (Goswami et al., 2014; Thakur et al., 2014; Usoskin et al., 2015). These results pointed out the high heterogeneity of nociceptive neurons, most of which share molecular features that complicate their study.

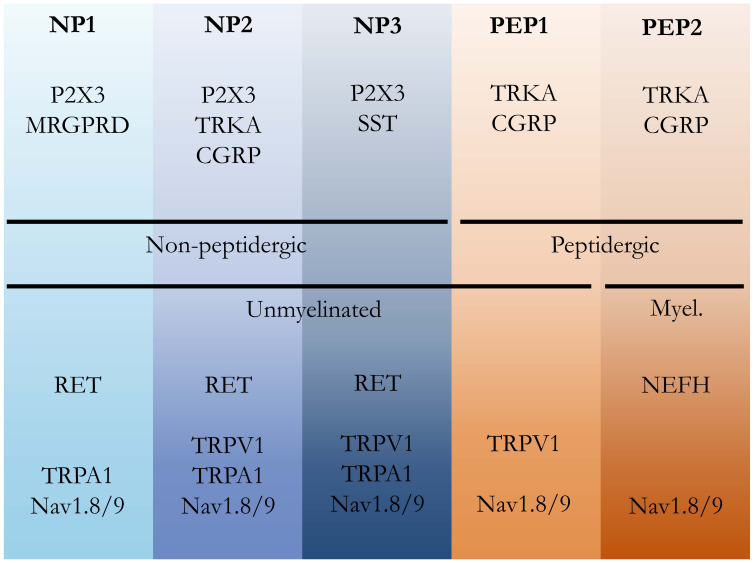

Figure 7. Transcriptomic profile of nociceptors. RNAseq analysis has provided evidence of 3 groups of non-peptidergic (NP1-3) neurons and 2 groups of peptidergic neurons (PEP1-2). P2X3: purinergic receptor; MRGPRD: Mas-related G-protein coupled receptor member D; TRKA: tyrosine kinase receptor A; RET: glial-derived neurotrophic factor family ligand-receptor; TRPA: transient receptor potential ankyrin; TRPV: transient receptor potential vanilloid; Nav: sodium voltage-gated channel; SST: somatostatin; CGRP: calcitonin gene-related peptide; NEFH: neurofilament heavy. (Modified from *Usoskin et al., 2015*).

Transduction in peripheral nociceptors

According to the respective adequate stimuli, nociceptors can be divided into mechanical, chemical, thermal, polymodal and silent nociceptors. The term polymodal refers to the ability to respond to several types of physical stimuli, while silent refers to the lack of response to any of the above-mentioned stimuli in physiological conditions. Most of the nociceptive C-fibres are polymodal, whilst Aδ-nociceptors mainly carry mechanical and/or thermal noxious information (Cain et al., 2001; Emery et al., 2016; Raja et al., 1988; Schmidt et al., 1995).

The proteins responsible for detecting a specific type of energy are termed *transduction molecules*. The first description of mechanosensitive channels appeared in 2010 with the proteins Piezo1 and Piezo2 (Coste et al., 2010). Although it has been suggested that Piezo2 is required for mechanosensitivity in sensitized nociceptors, the role of these channels in mechanical nociception is unclear (Murthy et al., 2018; Prato et al., 2017; Zhang et al., 2019). Acid-sensing ion channels (ASICs) respond to protons and mediate acid-induced nociception (see Wemmie et al., 2013 for a review). Most of the knowledge of transduction mechanisms refers to temperature, mediated by different members of the transient receptor potential (TRP) channel family (Figure 8).

The TRP superfamily is remarkably diverse, participating in a variety of transduction processes. All of them allow the entry of Na^+ and Ca^{2+} into the cell, leading to action potential generation. Most of these channels are expressed in both DRGs and TGs from rodents and humans (Facer et al., 2007; Manteniotis et al., 2013; Ray et al., 2018; Rostock et al., 2018).

Transient receptor potential vanilloid 1 (TRPV1) was the first mammalian thermo-channel characterized, ten years after the identification of the first trp locus encoding the *Drosophila* TRP, which functions as phototransducer (Montell & Rubin, 1989). Vampire bats adapted the TRPV1 gene to sense infrared radiation (Gracheva et al., 2011). In the mammalian skin and mucous membranes, TRPV1 is widely expressed among small-diameter peptidergic nociceptors, in which the molecule acts as a noxious heat sensor. This channel is also named the capsaicin receptor, due to its sensitivity to the active substance in chilli peppers (Caterina et al., 2000; Caterina et al., 1997; Cavanaugh et al., 2009). TRPV1 is widely recognized as a marker molecule of nociceptors.

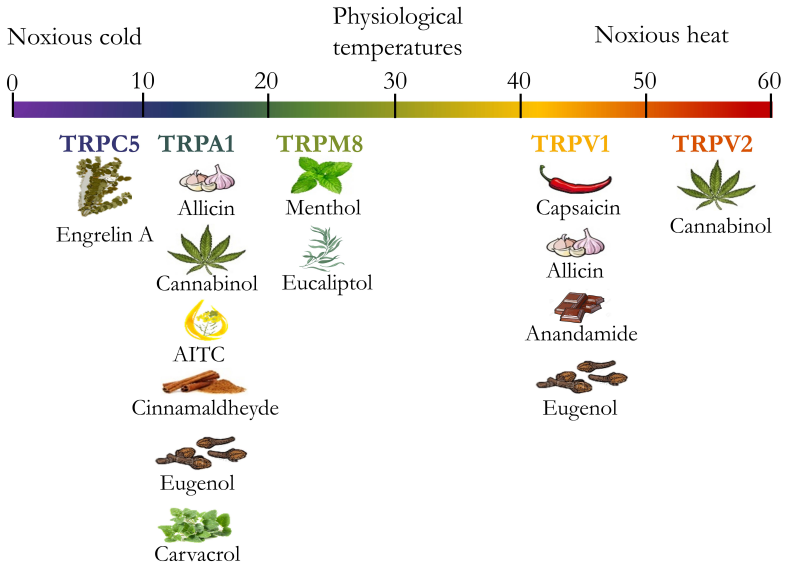

Figure 8. Representation of thermo-sensitive TRP channels expressed in sensory neurons. TRPM8 and TRPV1 respond to cold and heat, respectively. Furthermore, TRPA1 and TRPC5 respond to noxious cold (<17 ºC), and TRPV3 to noxious heat (>52 ºC). Below each channel, there are natural compounds (and a drawn of their origin) that activate them.

The main transduction molecule for the detection of environmental cold in mammals is **transient receptor potential melastatin 8 (TRPM8)**, because knockout mice showed reduced avoidance of innocuous cold temperature in the range of 27 and 15°C depending on the behavioural assay (Bautista et al., 2007; Colburn et al., 2007; Dhaka et al., 2007; Touska et al., 2016). TRPM8, also termed the menthol receptor, due to its sensitivity to various cooling agents (McKemy, 2007; Peier et al., 2002), seems also involved in the transduction of noxious cold temperatures, however its function overlaps with other ion channels and is less clearly resolved (see Viana, 2016 for a review). Neither peptidergic nor non-peptidergic mouse DRG nociceptors express TRPM8, and, it also does not colocalize with TRPV1 (Dhaka et al., 2008; Jankowski et al., 2017). In TGs, TRPM8 is barely co-expressed with TRPV1 and CGRP (Abe et al., 2005).

Transient receptor potential ankyrin 1 (TRPA1) is recognized as noxious cold sensor (Karashima et al., 2009; Story et al., 2003). Although its role in physiological cold pain was controversially discussed for a long time due to diverging results from different species and expression system (reviewed by Viana, 2016), it is clear that human TRPA1 is a cold transducer and intrinsically cold sensitive (Moparthi et al., 2014). In mice, synergy of TRPA1 and TRPM8 seems to confer the avoidance to cool and damaging cold, because mice

deficient in both channels have a slowed avoidance behaviour in the entire range of temperature from 25 to 5°C, a behaviour which is not observed in the single knockouts (Winter et al., 2017). However, this channel also contributes to the detection of painful heat (Vandewauw et al., 2018), akin to its role as an infrared sensor in snakes (Gracheva et al., 2010). TRPA1 is expressed in non-peptidergic nociceptors and highly co-expressed with TRPV1 (Barabas et al., 2012; Kobayashi et al., 2005). The channel is activated by several compounds, including pungent irritants and spices, like cinnamon, garlic, ginger, horseradish, menthol, and mustard oil and proalgesic agents like bradykinin (Jordt et al., 2004; Karashima et al., 2007; Takahashi & Mori, 2011).

The most recent TRP channel to be included in the list of mammalian cold sensors was the **transient receptor potential canonical 5 channel (TRPC5)** (Zimmermann et al., 2011), although its role as a cold sensor in physiological and pathological conditions remains unresolved and probably happens through adaptation of TRPM8.

Primary afferents in orofacial pain

Most of the studies regarding transduction mechanisms have been performed in cutaneous nociceptors with cell bodies in the DRGs, but it is usual to observe differences among nociceptive populations innervating different tissues. For example, meningeal nociceptors are excited by lower intensities of mechanical stimuli than cutaneous nociceptors (Levy & Strassman, 2002; Schlegel et al., 2004).

In general terms, orofacial pain refers to pain felt in the mouth, jaws and the face, but in several cases result from caries and dentin hypersensitivity (see West et al., 2013 for a review). Dental sensitivity is unique as, in contrast to other structures, stimulation of the teeth only produces pain (Jyväsjärvi & Kniffki, 1987). Intense thermal (heat or cold) stimulation applied on the intact tooth produces pain, which is used in the clinic to assess the vitality of the dental pulp (Jyväsjärvi & Kniffki, 1987; Närhi et al., 1992; Trowbridge, 1985). The most effective stimulus to produce pain is cold, which evokes pain in 85% of patients after removal of the enamel (Chidchuangchai et al., 2007). Furthermore, 75% of people with dentin hypersensitivity refer to pain after cold stimulation (Karim & Gillam, 2013; Miglani et al., 2010; West et al., 2013). This suggests that teeth are the most cold-sensitive structures in humans, hence nociceptors innervating the teeth may present a functional adaptation to cold. Although some studies have used microneurography to elucidate oral sensitivity in humans only one of these studies evaluated the response to cold directly applied to the teeth and showed ~75% of the dental primary afferents responding to cold (Iwata et al., 1991).

Teeth consist mainly of dentin (produced by odontoblasts) and the dental pulp (see Figure 9). Each tooth is protected by enamel, which covers the exposed surface and cementum, which covers the non-exposed root. The periodontal ligament connects the tooth root with the alveolar bone, which is covered with gingiva and the mucous membranes of the mouth. The axons of the primary afferents innervating the teeth are located in the dental pulp (Närhi, 1990). The nerves enter the dental pulp through the root tooth and radiate towards the coronal pulp to form the plexus of Raschkow. Most of the axons within the dental pulp are unmyelinated (70-90%), and some of them thinly myelinated (Fried et al., 1989; Johnsen & Johns, 1978; Paik et al., 2009; Walton & Nair, 1995). However, retrograde labelling of dental primary afferent with Fluorogold showed that most of the cell bodies in rats correspond to large myelinated fibres (Fried et al. 1989). Hence, it has been proposed that the teeth are innervated by myelinated neurons that disengage from their sheath upon arrival to the dental pulp and emerge as unmyelinated free nerve endings into the odontoblast layer and the

surrounding tubules of the predentin and dentin (Byers, 1985; Cadden et al., 1983; Trowbridge, 1985). Accordingly, some unmyelinated axons in the dental pulp showed immunoreactivity to myelinated nerves markers (Henry et al., 2012; Paik et al., 2010).

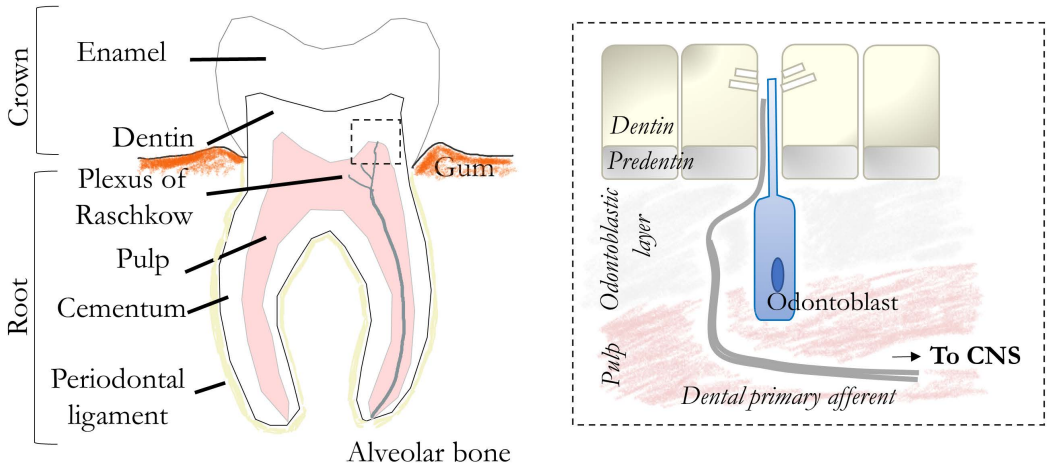

Figure 9. Tooth structure. The visible part of the teeth is the crown which is covered with enamel. The lower part represents the tooth root and is covered with a thinner layer of cementum which is anchored via the periodontal ligament in the alveolar bone. Inside of the hard substances is the pulp tissue. Peripheral nerve endings are located within the dental pulp and irradiate forming the plexus of Raschkow until they reach the odontoblastic layer. The odontoblastic layer is in the outer surface of the dental pulp and presents the cell bodies of the odontoblasts, which produce dentin and preserve the dentinal fluid that fills the dentinal tubules which harbour the odontoblast processes.

While transduction mechanisms from cutaneous nociceptors have been revealed in large detail as they are more easily accessible to experimental techniques, teeth nociceptors are not directly exposed to the external stimuli and the transduction mechanisms are therefore more difficult to investigate. Three different mechanisms for the origin of the pain messages in teeth have been proposed: 1) neural theory, in which the nerve endings become directly activated by external stimuli; 2) the hydrodynamic theory, wherein dentinal fluid movements within the dentinal tubules are detected by nerve endings; and 3) the odontoblast transducer theory, where odontoblasts themselves serve as pain transducers (see Chung et al., 2013 for a review). These theories are represented in Figure 10.

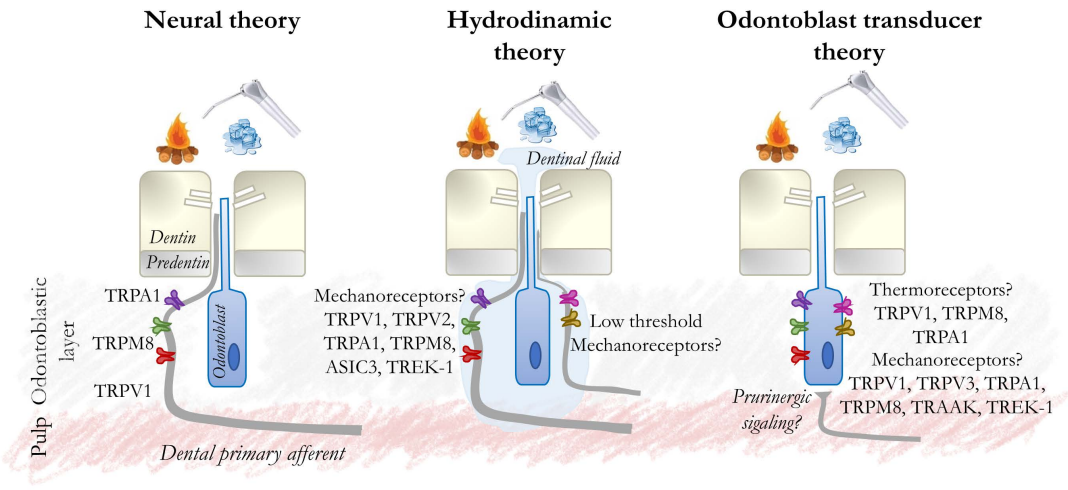

Figure 10. Three main hypotheses to explain tooth hypersensitivity. In the neural theory, transducers are in the nerve endings. The hydrodynamic theory suggests that movements of the dentinal fluid activate mechanoreceptors located in both neurons and odontoblasts. The odontoblast transducer theory proposed that noxious stimuli in the tooth activate transducers that are directly located in the odontoblasts, then the signal reaches the primary afferent, e.g. through paracrine signalling processes involving small molecule neurotransmitters such as ATP. Modified from (Chung et al., 2013).

Several ion channels have been reported to be expressed in dental primary afferents and odontoblasts of rodents and men (see Solé-Magdalena et al., 2018 for a review). Among them, TRP channels are believed to participate in the transduction mechanisms. For example different thermal transducers (TRPV1, TRPA1 and TRPM8) have been identified by calcium imaging, immunohistochemistry and PCR in odontoblasts from rodents (Okumura et al., 2005; Sato et al., 2013; Tsumura et al., 2013). Similarly, dental primary afferent neurons (DPANs) express TRPV1, TRPA1 and TRPM8 (Kim et al., 2011; Park et al., 2006). In humans, odontoblasts express TRPV1, TRPA1 and TRPM8 at protein and mRNA levels (Egbuniwe et al., 2014; El Karim et al., 2011), while TRPA1 was also expressed in numerous axons branching in the dental pulp (Kim et al., 2012). These channels could also contribute to pathological pain, as upregulation of TRPA1 has been observed in trigeminal ganglia innervating injured teeth in rodents (Haas et al., 2011) and painful dental pulp in humans (Kim et al., 2012).

Most of the functional studies regarding dental primary afferents have been done in dissociated mixed TG neurons *in vitro* using fluorometric assays (i.e. calcium imaging) and they have shown a proportion of neurons responding to cold stimulation (Madrid et al., 2006, 2009; Thut et al., 2003). However, it is important to consider that the TG contains neurons

innervating not only the skin but very diverse structures such as the teeth, the cornea, and the dura mater. Only a few studies have used retrograde labelling to study the expression of different proteins in identified DPANs in mice (Michot et al., 2018), but there is no information about the viability of these cells, something fundamental as the dye used for retrograde labelling (Fluorogold) has been described as neurotoxic (Naumann et al., 2000).

Primary afferents in neuropathic pain

Neuropathic pain is caused by direct damage to the somatosensory nervous system at the peripheral (peripheral neuropathy) or central level (central neuropathy). Up to 7-10 % of the population presents neuropathic pain, and the annual cost per patient in terms of medical treatment and work force is extremely high (~10,000 €) (Liedgens et al., 2016; Van Hecke et al., 2014). Neuropathic pain has different aetiologies, i.e. secondary to diabetes or to infection with herpes zoster virus, but most commonly arises from trauma/compression to nerve tissues (i.e. carpal tunnel syndrome, trigeminal neuralgia). A traumatic injury (transection) to a peripheral nerve, produces the formation of a neuroma (disorganized structure of axons, fibroblasts and Schwann cells) at the proximal end of the transected nerve (Ramón Y Cajal et al., 2012). Despite the different aetiology, patients share a series of common symptoms, so it is postulated that treatment should be based on the sensory profile instead of the aetiology (Forstenpointner et al., 2018; Truini et al., 2013; Vollert et al., 2017). This explains the need to understand the pathophysiological mechanisms that underlie each of the positive symptoms.

Allodynia is defined as pain due to a stimulus that does not normally provoke pain, whilst **hyperalgesia** is defined as increased pain sensitivity to a stimulus that normally provokes pain. Both mechanical and thermal allodynia/hyperalgesia have been described in patients, and there are plenty of animal models evaluating and quantifying them. **Spontaneous pain** is among the most frequently reported symptoms by patients (51-90%), but only a few animal studies have focussed on it (Attal, 2019; Bouhassira et al., 2005; Bouhassira & Attal, 2018; Truini, 2017).

Spontaneous pain appears in the daily life of patients and is described as pain without an apparent cause. Usually, spontaneous pain is referred to as "burning" (or "hot"), and "shooting" (or "electrical shocks", "paroxysmal pain"). Stimulation of C-fibres in healthy volunteers evokes a burning pain sensation (Ochoa, 2010), so it is believed that abnormal spontaneous activity in C-fibres underlies ongoing burning pain. In accordance, microneurography studies in patients with painful neuropathy have shown a direct relationship between spontaneous pain and spontaneous firing in C-fibres (Kleggetveit et al., 2012; Serra et al., 2012). Electric shock-like pain in patients with postherpetic neuralgia or carpal tunnel syndrome has been associated with the aberrant activity of non-nociceptive Aβ-fibres (Truini et al., 2008, 2009). Focal demyelination of Aβ-fibres might induce high-

frequency bursts of action potentials in these fibres, interpreted by the CNS as electric shock-like pain.

Various animal models of neuropathic pain described the development of spontaneous activity in different types of peripheral nerve fibres (Ali et al., 1999; Amir et al., 2005; Burchiel, 1984; Study & Kral, 1996; Wu et al., 2001; Wu et al., 2002). Supposedly, nerve damage provokes the development of ectopic spontaneous and/or evoked discharges in both axotomized and neighbouring intact fibres, which occurs in both A- and C-fibres (Ali et al., 1999; Li et al., 2000; Michaelis et al., 2000; Wu et al., 2001, Bernal et al. 2016, Bernal & Roza 2018).

As neuronal excitability depends on the presence of different ion channels regulating membrane potential threshold, hyperexcitability may be explained by altered expression of ion channels in peripheral nerves.

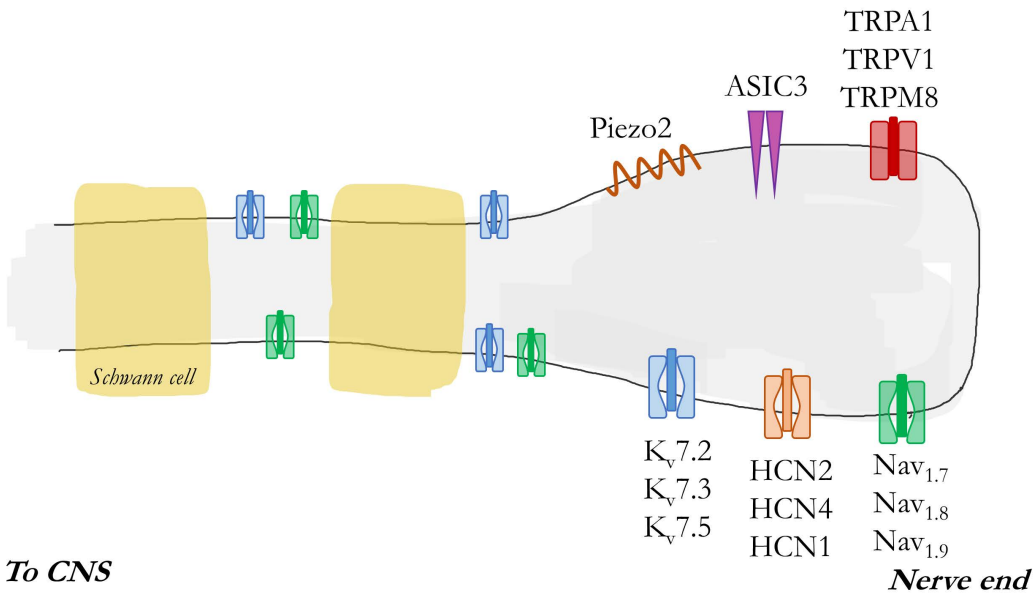

Figure 11. Types of ion channels and transduction molecules located in the cell membrane of a nociceptor. In the peripheral nerve endings, there are different transduction molecules (Piezo2, ASIC3) and ion channels (e.g. K_v7.2/3/5, HCN, Na_v1.7-9). In chronic pain conditions, there is an up or down-regulation of these transduction molecules and ion channels that change the membrane excitability, leading to a hyperexcitable state. K_V: voltage-gated potassium channels, HCN: hyperpolarization-activated cyclic nucleotide-gated channels, Na_V: voltage-gated sodium channels.

Ion channels involved in membrane excitability

There are several pieces of evidence on the contribution of voltage-gated sodium channels (Na_V) to neuropathic pain (Devor, Govrin-Lippmann and Angelides, 1993; Matzner & Devor, 1994; Roza et al., 2004). Most recently, evidence pointed out the contribution of hyperpolarization-activated cyclic nucleotide-gated (HCN) and voltage-gated potassium subfamily members KQT (K_V7) channels to spontaneous pain. These channels are reviewed in detail below.

Hyperpolarization-activated cyclic nucleotide-gated channels

HCN channels are cation channels permeable to K^+ and Na^+ that open at voltages near the resting membrane potential and are responsible for the I_h current. There are four isoforms (HCN 1-4) with different activation kinetics and sensitivity to cyclic nucleotides, such as cyclic adenosine monophosphate (cAMP). cAMP binds to the intracellular cyclic nucleotide-binding domain (CNBD) located at C-terminal and shifts the conductance voltage curve towards positive voltages (see Figure 12). Subtypes HCN2 and HCN4 are very sensitive HCN1 is less sensitive to cAMP, and HCN3 is insensitive to cyclic nucleotides (Chen et al., 2001). HCN channels are expressed mainly in the heart and the nervous system and are referred to as 'pacemakers' as they underlie pacemaker activity in the sinoatrial node (Santoro et al., 2000; Seifert et al., 1999). Within the nervous system, they are vital for normal neuronal excitability and become important in pathological states such as pain or epilepsy (Emery et al., 2011; Jung et al., 2007).

Although there is evidence of expression of different HCN subunits in nociceptors, their contribution to pain is not fully understood. In small-diameter nociceptors, HCN2 is highly expressed with lower expression of HCN4 (Momin et al., 2008). A smaller subgroup expresses HCN1 (Chaplan et al., 2003; Momin et al., 2008). Studies in mice demonstrated that HCN2 deletion in nociceptors did not alter the pain threshold but precluded the development of heat hyperalgesia after inflammation and nerve injury (Emery et al., 2011). Knockout mice for HCN1 showed less cold allodynia than wild-type littermates in neuropathic pain (Momin et al., 2008). Pharmacological block of HCN channels with ZD-7288 decreased mechanical hyperalgesia in neuropathic pain models (Chaplan et al., 2003; Jiang et al., 2008; Luo et al., 2007; Tsantoulas et al., 2017; Young et al., 2014). Furthermore, block of HCN channels reduced spontaneous activity in myelinated A-fibres (Chaplan et al., 2003; Jiang et al., 2008). Using electrophysiology, western blot and immunohistochemistry,

we and others have shown up-regulation of functional I_h currents in peripheral nerves after nerve injury (Chaplan et al., 2003; Jiang et al., 2008; Mazo et al., 2013).

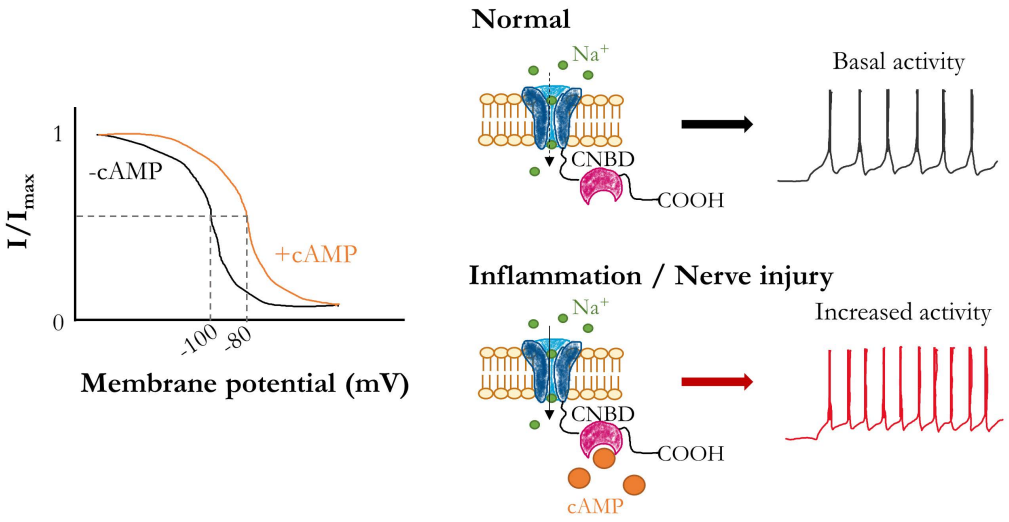

Figure 12. Activity of HCN channels in physiological conditions and pathological states. During inflammation or nerve injury there is an increase in cAMP concentration, leading to hyperactivity of HCN channels. Modified from Emery et al. (2012).

Several HCN blockers are available, such as ZD-7288 or ivabradine, but these drugs inhibit all HCN isoforms with the same potency. As a result, when applied systemically these compounds have powerful side-effects on the rhythmic activity of the heart, limiting their usefulness for non-cardiac indications such as pain. For this reason, it is important, first, to understand the role of each isoform on pain and then, develop isoform-specific compounds devoid of side effects.

Kv7 potassium channels

Kv7 potassium channels comprise five subunits (Kv7.1-7.5, encoded by KCNQ1-KCNQ5 genes) and form heteromultimers that underlie the M-currents (I_M). When the cell membrane potential depolarizes, these channels open and allow passive flow of K^+ ions along the gradient, out of the cell, which contributes to the repolarization in direction of the resting membrane potential of neurons (Delmas & Brown, 2005; Du et al., 2018; Du & Gamper, 2013; Huang & Trussell, 2011). The inhibition of the channel leads to increased excitability in central and peripheral neurons (Wulff et al., 2009). Figure 13 illustrates the effects of Kv7

channel modulation. Several years ago, it was reported that KCNQ gene mutations lead to peripheral nerve hyperexcitability (Wuttke et al., 2007).

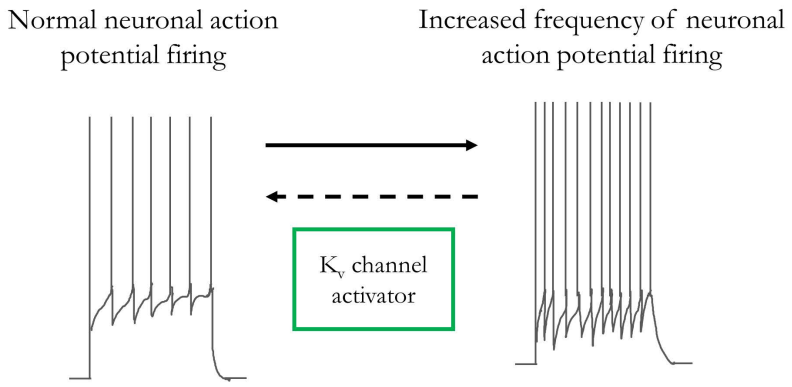

Figure 13. Potassium channels activity in physiological and pathological conditions. Changes in the ability of K_v channels to generate action potentials leads to neurological disfunction. Increases in the frequency of firing lead to pathological states of hyperexcitability (e.g. pain, seizures, anxiety), in which K_v channels activator restore normal firing. Modified from (Wulff et al., 2009).

Several studies in rodents have revealed expression of Kv7.2, Kv7.3 and Kv7.5 in DRGs, with Kv7.2 as the higher expressed in nociceptors (Passmore et al., 2012; Rose et al., 2011). The contribution of these channels to the development of pain has been widely verified. For example, inhibition of Kv7channels by intraplantar injection of XE991, a potent and selective Kv7 channel blocker, induces moderate pain in rats (Linley et al., 2008). Previous studies from our laboratory have shown increased expression of Kv7.2 in nerve-end neuromas of mice (Roza et al., 2011). Furthermore, retigabine (a Kv7 channel opener) reduced neuropathic pain symptoms (Blackburn-Munro & Jensen, 2003; Djouhri et al., 2019), maybe due to its ability to abolish ectopic activity (Roza & Lopez-García, 2008).

In the last decades, the focus on Kv7 as a pharmacological target for different pathologies has increased. Nowadays, the World Intellectual Property Organization lists more than a hundred patents related to Kv7 channel openers. Among those, retigabine belongs to the triaminopyridine family and is a non-selective Kv7 channel opener that targets all except for the Kv7.1 subunit (Tatulian et al., 2001). For several years retigabine was clinically approved as antiepileptic drug and for the treatment of other neurologic conditions (i.e. tinnitus, migraine, and neuropathic pain). However, in 2017, its use was clinically restricted to adjuvant therapy due to the high risk of skin discolouration, retinal pigmentation, urinary retention,

sedation and changes in heart parameters (Daniluk et al., 2016). Nevertheless, retigabine remains a useful research tool in animal pain models and Kv7 channels are interesting targets for novel analgesic treatments.

RATIONALE AND GOALS

The **global objective** of this thesis focusses on the study of primary afferent nociceptors in chronic pain conditions. The thesis has been divided into two sections and the specific objectives are explained in detail below.

Section I

Orofacial pain is frequently related to cold stimulation of the teeth. However, there is little information with respect to the transduction mechanisms in this system, as studies performed in TG neurons of mice have not properly identified neurons with peripheral terminals in the teeth, probably due to anatomical and technical restrictions. In order to identify changes during chronic pain, it is mandatory to understand first cold transduction mechanisms in physiological conditions.

Therefore, we aimed to overcome the difficulties and allow for the identification of TG neurons with terminals in the teeth by retrograde labelling from the dental pulp of mice. We then examined the expression of TRPM8 in dental primary afferent neurons and evaluated the viability of retro-labelled dental neurons by calcium imaging.

Section II

Spontaneous pain, the main symptom reported by patients with neuropathic pain, is caused by spontaneous activity in peripheral nociceptors. As spontaneous pain is refractory to treatments, it is important to identify new pharmacological targets.

Therefore, using experimental models of peripheral neuropathy in mice, we aimed to characterize the effect of pharmacological modulation of HCN and Kv7 channels on spontaneous activity in peripheral nociceptors.

RESULTS

SECTION I: CHAPTER 1

Fluorescent labeling and 2-Photon imaging of mouse tooth pulp nociceptors

Journal of Dental Research
1–7

DOI: 10.1177/0022034517740577
journals.sagepub.com/home/jdr

Fluorescent Labeling and 2-Photon Imaging of Mouse Tooth Pulp Nociceptors

A. Kadala[1*], P. Sotelo-Hitschfeld[1,2*], Z. Ahmad[1], P. Tripal[3], B. Schmid[3], A. Mueller[1], L. Bernal[1], Z. Winter[1], S. Brauchi[2], U. Lohbauer[4], K. Messlinger[5], J.K. Lennerz[6], and K. Zimmermann[1]

Abstract

Retrograde fluorescent labeling of dental primary afferent neurons (DPANs) has been described in rats through crystalline fluorescent DiI, while in the mouse, this technique was achieved with only Fluoro-Gold, a neurotoxic fluorescent dye with membrane penetration characteristics superior to the carbocyanine dyes. We reevaluated this technique in the rat with the aim to transfer it to the mouse because comprehensive physiologic studies require access to the mouse as a model organism. Using conventional immunohistochemistry, we assessed in rats and mice the speed of axonal dye transport from the application site to the trigeminal ganglion, the numbers of stained DPANs, and the fluorescence intensity via 1) conventional crystalline DiI and 2) a novel DiI formulation with improved penetration properties and staining efficiency. A 3-dimensional reconstruction of an entire trigeminal ganglion with 2-photon laser scanning fluorescence microscopy permitted visualization of DPANs in all 3 divisions of the trigeminal nerve. We quantified DPANs in mice expressing the farnesylated enhanced green fluorescent protein (EGFPf) from the transient receptor potential cation channel subfamily M member 8 (TRPM8$^{EGFPf/+}$) locus in the 3 branches. We also evaluated the viability of the labeled DPANs in dissociated trigeminal ganglion cultures using calcium microfluorometry, and we assessed the sensitivity to capsaicin, an agonist of the TRPV1 receptor. Reproducible DiI labeling of DPANs in the mouse is an important tool 1) to investigate the molecular and functional specialization of DPANs within the trigeminal nociceptive system and 2) to recognize exclusive molecular characteristics that differentiate nociception in the trigeminal system from that in the somatic system. A versatile tool to enhance our understanding of the molecular composition and characteristics of DPANs will be essential for the development of mechanism-based therapeutic approaches for dentine hypersensitivity and inflammatory tooth pain.

Keywords: TRPM8, TRPV1, retrograde labeling, dental primary afferent, carbocyanine dye, Fluoro-Gold

Introduction

Recent RNA sequencing efforts have revealed substantial diversity of functionally distinct neuron subtypes in the primary sensory system. Based on their unique transcriptional fingerprint, 11 types can be distinguished and serve mechanoreception, proprioception, thermosensation, itch, and nociception (Usoskin et al. 2015). Briefly, via single-cell sampling in combination with sequencing and grouping of related expression profiles, cell types can be classified in an unbiased fashion. The resulting catalog of somatic sensation unveiled a previously unknown level of complexity devoid of morphologic and functional information. Linking sensory subtype classification to functional and organ-specific information can be achieved only by direct and unambiguous labeling of neuronal subpopulations. This goal is commonly achieved by retrograde labeling with lipophilic carbocyanine dyes, which label sensory neuron cell bodies by retrograde transport when applied to locally restricted sites of innervation. The dye intercalates into nerve terminal membranes or at sites of axonal discontinuation; it is transported to the soma by axoplasmic transport; and it does not measurably interfere with cell viability and physiologic parameters (Honig and Hume 1986, 1989).

[1]Klinik für Anästhesiologie, Universitätsklinikum Erlangen, Friedrich-Alexander Universität Erlangen-Nürnberg, Erlangen, Germany
[2]Instituto de Fisiología, Facultad de Medicina, Escuela de Graduados, Facultad de Ciencias, Universidad Austral de Chile, Valdivia, Chile
[3]Optical Imaging Centre Erlangen, Friedrich-Alexander Universität Erlangen-Nürnberg, Erlangen, Germany
[4]Klinik für Zahnerhaltung und Parodontologie, Universitätsklinikum Erlangen, Friedrich-Alexander Universität Erlangen-Nürnberg, Erlangen, Germany
[5]Institut für Physiologie und Pathophysiologie, Friedrich-Alexander Universität Erlangen-Nürnberg, Erlangen, Germany
[6]Center for Integrated Diagnostics, Massachusetts General Hospital, Harvard Medical School, Boston, USA
*Authors contributing equally to this article.

A supplemental appendix to this article is available online.

Corresponding Authors:
K. Zimmermann, Universitätsklinikum Erlangen, Friedrich-Alexander Universität Erlangen-Nürnberg, Klinik für Anästhesiologie, Krankenhausstraße 12, 91054 Erlangen, Germany.
Email: katharina.zimmermann@fau.de
J.K. Lennerz, Center for Integrated Diagnostics, Department of Pathology, Massachusetts General Hospital, Harvard Medical School, 55 Fruit Street, Boston, MA 02114, USA.
Email: jlennerz@partners.org

In contrast to Fluoro-Gold (FG), carbocyanine dyes allow long-term staining of tissue (Honig and Hume 1986) and have emissions at variable wavelengths to allow double-labeling strategies. Other advantages of carbocyanines are that 1) they do not transfer from labeled to unlabeled cells (unless membranes are disrupted), 2) their emission wavelengths are independent of tissue pH, and 3) unlike FG, they are not neurotoxic (Naumann et al. 2000).

While the methodological basis for retrograde labeling has been established for decades (Honig and Hume 1986), the labeling of molar teeth and dental primary afferent neurons (DPANs) with crystalline DiI have been described only for rats (Eckert et al. 1997; Kim et al. 2011). In the mouse, molars can hold less dye, and fewer molars can be accessed. Here, we aimed to optimize this technique to enable use in the mouse and permit access to transgenic animal models for functional studies without side effects on physiologic function. We characterized the speed of axonal dye transport to the trigeminal ganglion, the numbers of stained DPANs, and the fluorescence intensity by using conventional crystalline DiI and NeuroTrace, a novel DiI formulation with improved membrane uptake and superior staining efficiency. We describe how to achieve reliable DiI labeling of DPANs in the mouse, and we illustrate our findings with results from cryosections, 2-photon excitation microscopy, and calcium microfluorimetry in live cultures of trigeminal ganglion (TG) neurons.

Methods

Animals

A total of 19 Wistar rats (40 to 81 d) and 14 C57BL/6J mice (61 to 121 d) of both sexes were included in the study. One TRPM8$^{EGFPf/+}$ mouse expressing the farnesylated enhanced green fluorescent protein (EGFPf) from the TRPM8 locus, (Dhaka et al. 2008) was used and genotyped as previously described (Vetter et al. 2013). Mice and rats were housed in an in-house open cage facility in a 12-h light-dark cycle according to the European Parliament Council (directive 2007/526/EG). The animal ethics committee and the local district government approved the protocol for in vivo surgical interventions. All experiments were conducted in accordance with the guidelines and regulations of animal care of the European Parliament Council (directive 2010/63EU). The study conforms to the ARRIVE (Animal Research: Reporting of In Vivo Experiments) guidelines.

Maxillary Molar Surgery

The anesthesia was induced with sevoflurane (Abbot) and maintained with 90 mg/kg of ketamine (Ketavet; Pharmacia) and 6 mg/kg of xylazine (Rompun 2%; Bayer). Carprofen (4 mg/kg, Rimadyl; Pfizer) and enrofloxacin (7.5 mg/kg, Baytril 5%; Bayer) were applied postoperatively after 12 h and every 24 h for the following 48 to 120 h. The anesthetized animal was in supine position, and the mouth was spread open, with the head kept in position by retractors and eventually rubber bands held by magnetic fixators. Molars were drilled vertically under microscope control until reaching the dentin-pulp border. Pulp bleeding, injury, and contamination of the periodontal tissue must be avoided. DiI (1,1′-dioctadecyl-3,3,3′3′-tetramethylindocarbo-cyanine perchlorate) and NeuroTrace DiI were from Molecular Probes. Molar holes were filled with the maximal amount of dye and occluded with adhesive and resin-based composite. Both were subsequently applied onto the intact enamel around the cavity and need to be light cured with a halogen 470-nm light source (750 mW/cm^2; Translux CL) for 15 and 20 s, respectively. The surgical procedure took 40 min. An appendix with extended surgical procedures is available in the online version of this article.

Collection of TGs and Confocal Microscopy

Fourteen mice and 19 rats were euthanized with 50 mg/kg of thiopental and perfused with 4% fresh paraformaldehyde (PFA) in phosphate-buffered saline (PBS) at the respective time points after dye application. Following fixation, the animal was decapitated, the skull opened, and the brain removed. Both TGs were detached from the skull base, with intact branches and dura mater surrounding the ganglia. Ganglia were stored for 4 h in PFA 4% at 4 °C, washed twice for 30 min in PBS, transferred to 30% sucrose in PBS, and stored at 4 °C overnight. The TGs were frozen on dry ice with Tissue-Tek OCT Compound (Sakura) and cut into 14-µm longitudinal sections with a cryostat (Leica CM3050S; Leica Biosytems). The sections were stained with DAPI and mounted onto poly-L-lysine-coated glass slides with glycerin-free mounting fluid (Fluoromount; Sigma-Aldrich) and cover slips. The sections were micrographed after mounting to prevent dissemination of dye through ruptured membranes.

The immunofluorescent images were acquired with a confocal laser scanning microscope (LSM 710; Carl Zeiss MicroImaging), ZEN 2010 software (Carl Zeiss MicroImaging), and ImageJ 1.48. DiI was examined with a rhodamine filter (λ = 561 nm), and an FITC filter (493 to 555 nm) was used to recognize lipofuscin autofluorescence and to map the overall structure of the section. Images were taken with a 20× objective (0.8 numerical aperture). Images from adjacent sections were compared. The fluorescence level (corrected total cell fluorescence) was calculated with the following formula: integrated density of the selected cell – (area of the selected cell × mean fluorescence of the background readings).

Parameters were extracted from regions of interest edging labeled cells and background areas.

Two-Photon Microscopy and 3-dimensional Reconstruction

The TRPM8$^{EGFPf/+}$ mouse was euthanized by cervical dislocation 5 d postsurgery and decapitated. The skull was opened, the brain removed, and the skull base preparation exposed to 4% PFA overnight. The TG was removed with intact branches and mounted in 1.0% low-melting agarose in a plastic-bottomed culture dish. Image stacks were acquired with a Zeiss LSM 880 NLO equipped with a 680- to 1,300-nm tunable and fixed 1,040-nm 2-photon laser from Newport Spectra-Physics and a

20× W-Plan Apochromat objective lens. Fluorophores were excited at 1,040 nm (DiI) and 920 nm (EGFPf), and fluorophore emissions were detected with nondescanned GaAsP detectors at 575 to 610 nm (DiI) and 500 to 550 nm (EGFPf). To achieve 3-dimensional reconstruction of the ganglion, 646 Z-slices with 650-nm distance were acquired. Fiji ImageJ was used to process the data and the Cell Counter plug-in for ImageJ to quantify the cells.

Cell Cultures and Calcium Microfluorimetry

Four mice were euthanized by cervical dislocation 5 d postsurgery, and TGs were removed with intact branches. Ganglia were transferred in sterile DMEM (Thermo Fisher Scientific) and cut into small pieces. DMEM was subsequently replaced with combined dispase (Gibco; purchased from Thermo Fisher Scientific) and collagenase (Sigma-Aldrich) in TNB medium, and the ganglia were incubated at 37 °C and 5% CO_2 for 45 min. The cell suspension was then washed with DMEM and TNB 100 medium, supplemented with TNB 100 lipid–protein complex (Biochrom), 100 µg/mL of streptomycin/penicillin (Thermo Fisher Scientific), and 1nM nerve growth factor 7S (Alomone Labs). Cell clusters were triturated in TNB to achieve a cell suspension, and 100 µL of suspension was applied per 1 poly-D-lysine-coated FluoroDish (World Precision Instruments). Dishes were incubated in 1 mL of TNB for 15 to 18 h at 37 °C and 5% CO_2, and after 12 to 18 h in culture, neurons were loaded with Fura-2^{AM} (Invitrogen). Fura-2^{AM} was dissolved in extracellular solution (ECS) containing 145mM NaCl, 5mM KCl, 1mM $MgCl_2$, 1.25mM $CaCl_2$, 10mM Hepes, and 10mM glucose; at pH 7.4, the cells were incubated for 30 min and then washed for 15 min in ECS. An automated fast solution changer designed by V. Vellani (CV Scientific) was used to superfuse the cells with ECS, capsaicin (3 µM), and KCl (145 mM). Capsaicin sensitivity was considered for an increase in the calcium response, measured as an area under the curve (AUC) increase >15% over the AUC of the baseline. For baseline and capsaicin response, 120-s time frames were included. The AUC was calculated with the following formula, with x representing the time and f the amplitude:

$$AUC = \int f(x)dx.$$

In vivo calcium imaging experiments were made with an Olympus IX83 inverted microscope and an Olympus UApoN340 20x water immersion objective. Fura-2^{AM}-loaded cells (3 µm supplemented with 0.02% pluronic dissolved in ECS) were excited with a xenon lamp (Lambda DG-4; Sutter Instrument) at 340 and 380 nm and the emission examined at 510 nm. An ORCA-Flash 4.0 LT digital camera (C11440; Hamamatsu Photonics) was used for image acquisition at a rate of 1/s. DiI was excited at 556 to 590 nm and examined at 602 to 664 nm.

Data Analysis and Statistics

Data in figures are presented as mean ± SEM. Values in text are given as mean ± SD. Unpaired Student's t tests and 1-way analysis of variance were calculated for statistical analysis with Statistica 7.1 (Stat Soft). Differences with P values <0.05 were regarded as statistically significant.

Results

Mouse maxillary bone and molars are less than a quarter of the size as those in the rat, and the molars can hold only a fraction of the dye harbored in rat molars. Using crystal DiI in the mouse maxillary molars, we never succeeded in applying sufficient dye quantities to achieve a fluorescence intensity to allow reliable distinction of DPANs from the background. In addition, the third maxillary molar in the mouse is inaccessible. These constraints argue for labeling of fewer mouse DPANs with higher overall intensities. We revisited the rat to evaluate axonal dye diffusion and fluorescence levels to optimize these parameters.

We evaluated the amount of stained DPANs in the trigeminal ganglion after 48, 72, 96, 120, and 168 h of axonal dye transport for DiI crystal and a new DiI gel called NeuroTrace. The average number of labeled neurons in the TG increased, with longer diffusion times for both formulations. Most DPANs were found after 120 h (Fig. 1A): Crystal DiI stained 44 ± 11 (n = 2 ganglia, 2 rats), 62 ± 66 (n = 4 ganglia, 3 rats), 49 ± 67 (n = 4 ganglia, 2 rats) and 78 ± 34 (n = 3 ganglia, 2 rats) after 48, 72, 96, and 120 h, respectively. In contrast, NeuroTrace labeled 18 ± 17 (n = 3 ganglia, 3 rats), 19 ± 12 (n = 2 ganglia, 1 rat), 19 ± 3 (n = 2 ganglia, 2 rats), and 56 ± 14 (n = 3 ganglia, 3 rats) after 48, 72, 96, and 120 h, respectively. Using paste, we also assessed the number of DPANs after 168 h and found 61 ± 11 DPANs (n = 2 ganglia, 2 rats, not illustrated); presumably, 120 h represents the most efficient time frame. Both approaches yielded similar, not statistically different, results. Nevertheless, staining with NeuroTrace appeared more reliable, as it produced a smaller SD of the sampling distribution (Fig. 1A).

To quantify differences in fluorescence intensity, we assessed corrected total cell fluorescence and found that fluorescence obtained with NeuroTrace was statistically (Fig. 1B) and visibly (Fig. 1C, D) more intense at almost all diffusion times and that it accumulated over time, reaching a peak at 120 h (Fig. 1B).

In the mouse, NeuroTrace successfully stained DPANs, and the average number of neurons increased with time similar to that of the rat (Fig. 2A): NeuroTrace labeled 8 ± 2 (n = 4 ganglia, 4 mice), 12 ± 8 (n = 2 ganglia, 2 mice) 23 ± 10 (n = 5 ganglia, 5 mice) and 31 ± 21 (n = 4 ganglia, 3 mice) after 48, 72, 96 and 120 h, respectively. Numbers of labeled DPANs per ganglion ranged between 1 and 52, with 6 ganglia having no labeled DPANs. Because mouse molars contain less fluorescent material, the fluorescence intensity remained lower but sufficient to allow an unambiguous distinction from background (Fig. 2B, C). Size distribution histograms of the cross-sectional area show similar size distributions in rats and mice, and the largest proportion of DPANs were small-diameter nociceptors (Fig. 2D).

Our quantitative assessment of immunofluorescent detection focused on the maxillomandibular area. To study the

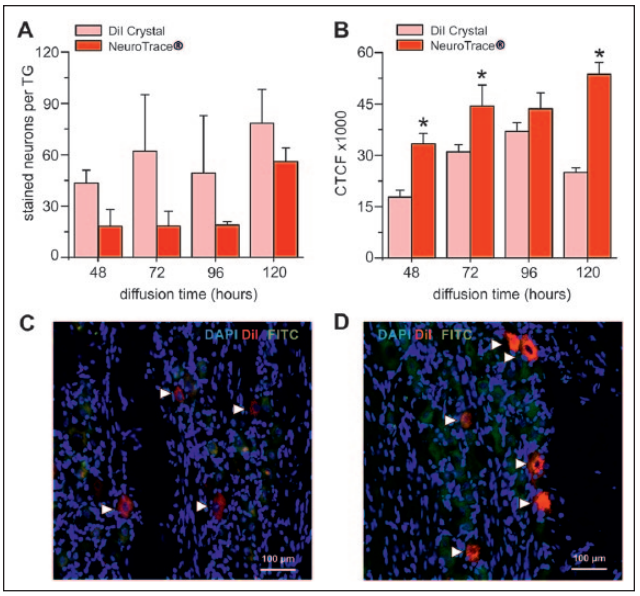

Figure 1. Retrograde labeling characteristics of rat maxillary dental primary afferent neurons (DPANs) with crystalline DiI and NeuroTrace DiI, a new DiI paste composed of an inert water-resistant gel with improved membrane penetration properties. (**A**) Mean ± SEM number of cells stained per trigeminal ganglion (TG) as a function of the DiI diffusion time (23 ganglia were included from 19 rats). Dye diffusion time of 5 d provided the highest amount of fluorescent cells in ganglia for both crystal and paste. The reproducibility was superior with the paste, resulting in a smaller SEM. (**B**) Fluorescence intensity of labeled trigeminal neurons as a function of the DiI diffusion time for paste (red) and crystal (light red). The fluorescence intensity was determined as corrected total cell fluorescence (CTCF) and calculated as described in Methods. NeuroTrace DiI paste stained the neurons with a higher fluorescence intensity, which resulted in a better distinction from background than crystal dye at nearly all time points (*$P < 0.05$, *t* test). (**C, D**) Confocal photomicrographs of cryosections of TG with DPANs labeled with (C) crystal or (D) NeuroTrace DiI tissue-labeling paste (labeled cells marked with arrowheads).

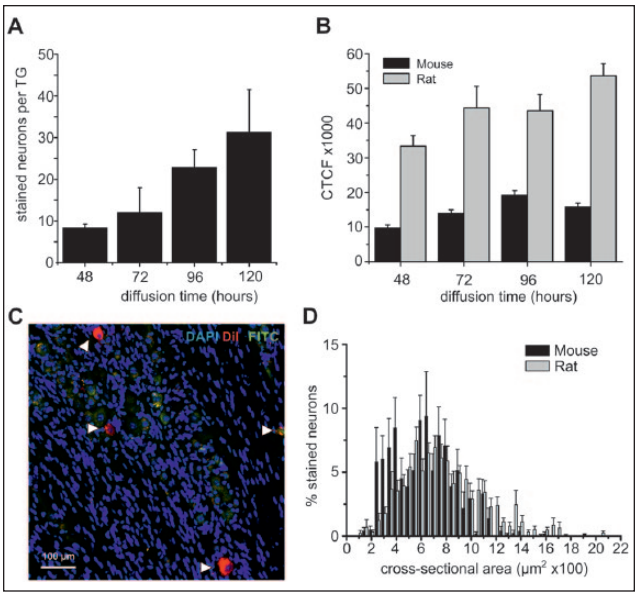

Figure 2. Retrograde labeling of mouse maxillary dental primary afferent neurons (DPANs) with NeuroTrace DiI paste. (**A**) The mean ± SEM number of cells stained per trigeminal ganglion (TG) as a function of the DiI diffusion time (15 ganglia were included from 14 mice) is lower in the mouse because only 2 instead of 3 molars can be accessed for labeling. (**B**) The fluorescence intensity is significantly lower in mouse DPANs as compared with the rat, irrespective of the diffusion time (*$P < 0.01$, *t* test) because the mouse molars contain less fluorescent material. The fluorescence intensity was determined as corrected total cell fluorescence (CTCF) and calculated as described in Methods. (**C**) Confocal photomicrograph of a cryosection of a mouse TG with DPANs stained with NeuroTrace DiI tissue-labeling paste (arrowheads). (**D**) Size distribution of labeled DPANs in bins per 50 µm^2 and determined as cross-sectional area for mouse (black) and rat (red). Tooth pulp afferents are a highly enriched population of small diameter nociceptors.

spatial distribution of maxillary DPANs, we reconstructed an entire mouse TG from image stacks obtained with a 2-photon microscope. Figure 3 illustrates DPANs in a TRPM8$^{EGFPf/+}$ TG. We identified a total of 176 DPANs and mapped the distribution in the 3 subregions of the TG. Briefly, more than half of the DPANs ($n = 100$, 57%) are located in V3, the mandibular division; 38% ($n = 67$) are contained in V2, the maxillary division; and the remaining 5% ($n = 9$) are spread throughout the ophthalmic division. Remarkably, the largest cluster of DPANs is aggregated in the anterior part of the mandibular division, and it contains the majority—that is, two-thirds of the TRPM8-containing DPANs (Fig. 3D, E).

Last but not least, we tested whether the staining of mouse DPANs with DiI was also appropriate for functional assessment, using in vivo calcium imaging with the ratiometric calcium dye Fura-2^{AM}. In dissociated TG cultures, fluorescent DPANs were well discernable (Fig. 4A–C). DiI-labeled cells were subjected to stimulation with 3µM capsaicin in ECS. Subsequently, high-potassium solution was applied to differentiate neurons from glia (Fig. 4D). The increase in intracellular calcium of the DPANs was not different from the nonlabeled adjacent neurons (Fig. 4E; $P = 0.4$, *t* test)

Discussion

Retrograde labeling of tooth pulp afferents is a key method to investigate the properties of tooth nociceptors. Yet, this method has been predominantly used in the rat through crystal DiI (Taddese et al. 1995; Eckert et al. 1997; Chaudhary et al. 2001; Park et al. 2006; Kim et al. 2011; Vang et al. 2012). In the mouse, so far only FG was employed successfully and applied with pulp access to the 2 front maxillary molars (Lin et al. 2015) or to the dentinal surface of 1 molar (Chung et al. 2011, 2012). In contrast to the carbocyanine dyes (Honig and Hume 1989), FG is neurotoxic (Naumann et al. 2000), but it outmatches DiI in its brighter and longer-lasting fluorescence and its greater uptake by axonal membranes (Schmued and Fallon 1986), which makes it similar to NeuroTrace and may explain why both, in contrast to crystal DiI, allowed successful mouse DPAN staining despite the anatomic limitations.

An unexpected finding was the occurrence of the majority of maxillary molar DPANs in the mandibular and also, to a

minor extent, the ophthalmic parts of the reconstructed TG. One earlier study utilized horseradish peroxidase (HRP) deposited in cat canine dental pulp, and it found that innervating neurons were indeed occasionally located in the mandibular and ophthalmic areas (Anderson and Rosing 1977); yet, another study described separate locations for cell bodies innervating lower and upper cat canines in the mandibular and maxillary divisions (Arvidsson 1975). For cat and monkey, a somatotopic organization of the trigeminal ganglion, foremost for tactile information, is in good agreement with earlier physiologic and anatomic studies (Kerr and Lysak 1964; Beaudreau and Jerge 1968; Lende and Poulos 1970). For the rat, chromatolytic changes following trigeminal nerve branch transection showed that dental afferent innervation follows a predominant mediolateral but no dorsoventral somatotopic pattern (Mazza and Dixon 1972; Gregg and Dixon 1973). Our large cluster of DPANs identified in the anterior part of the mandibular division, with some continuation in the maxillary division, is in accordance with this finding. Although species differences may account for a progressive reduction of somatotopy in rodents, the concept of vertebrate jaw development provides an additional convincing explanation for the distribution of the DPANs. In the craniofacial developmental program, the upper jaw develops as a composite structure, and the ophthalmic nerve is not segregated (Higashiyama and Kuratani 2014). The rostral part of the upper jaw is derived from the premandibular domain, which receives innervation from ophthalmic nerve branches, while the posterior part arises from the mandibular arch, innervated by the maxillomandibular component (Higashiyama and Kuratani 2014).

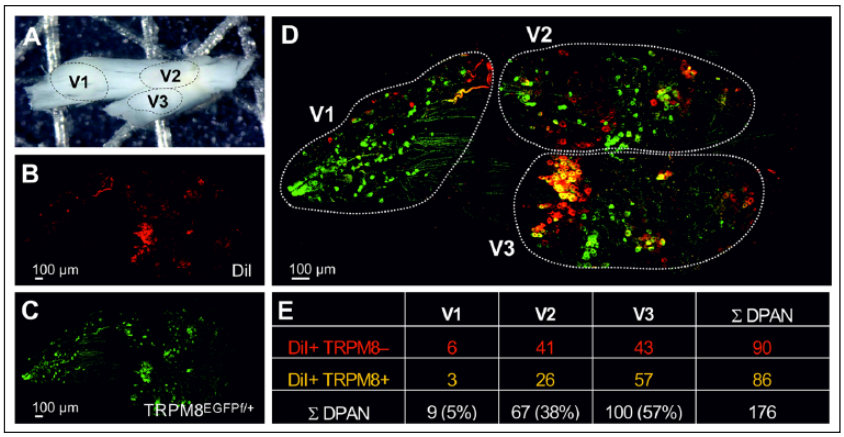

E	V1	V2	V3	Σ DPAN
DiI+ TRPM8–	6	41	43	90
DiI+ TRPM8+	3	26	57	86
Σ DPAN	9 (5%)	67 (38%)	100 (57%)	176

Figure 3. Spatial distribution of the dental primary afferent neurons (DPANs) of the first 2 maxillary molars in the 3 sections of the trigeminal ganglion of a TRPM8$^{EGFPf/+}$ mouse. The DPANs were visualized from a 3-dimensional reconstruction of image stacks obtained with a 2-photon laser scanning microscope. (**A**) Transmitted light photomicrograph of the trigeminal ganglion highlighting the ophthalmic (V1), maxillary (V2), and mandibular (V3) sections. (**B–D**) Two-photon laser scanning microscope images of the trigeminal ganglion showing the retrograde-labeled DPANs in red (B), TRPM8 in farnesylated enhanced green fluorescent protein (EGFPf; C), and a merged view of both images (D). The sections were identified following (Boada 2013). (**E**) Quantification of DPANs with and without TRPM8 in 3 sections of the trigeminal ganglion. An appendix with a 3-dimensional view is available online.

Immunohistochemistry yielded a large variability of DPAN cell counts among individual experiments but also in comparison with the 3-dimensional reconstruction. Technical shortcomings—including inhomogeneous distribution of different dye quantities and, hypothetically, some leak through the root apical foramen—may contribute to the observation; previous labeling studies based on HRP transport also saw substantial variation in DPAN counts, but this concerned the overall amount of cells harbored in 1 TG, which is why these are most likely highly individual parameters. In 2 studies, the total cell number of 1 rat TG ranged between 23,258 and 46,713 (Aldskogius and Arvidsson 1978) and 40,910 to 62,030 (Gregg and Dixon 1973); in the latter study, cell bodies associated with maxillary or mandibular molar innervation accounted for ~1% of TG cells, as quantified by chromatolysis after root apex transection (Gregg and Dixon 1973). Comparable with our experiments—in which we observed a 50% failure rate (i.e., 14 mice with labeled DPANs in at least 1 ganglion were included,

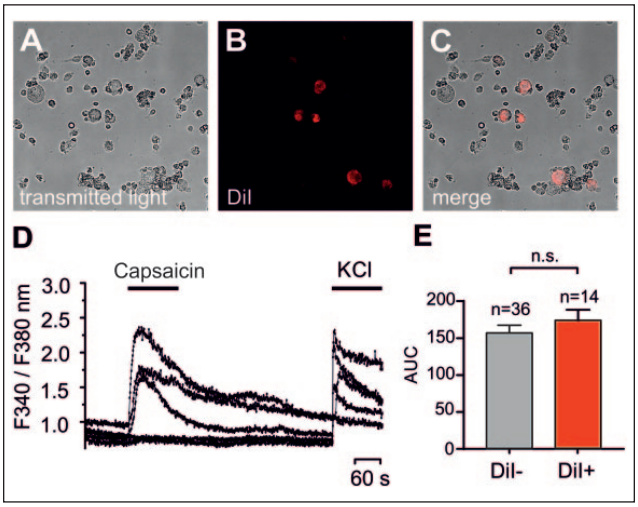

Figure 4. Capsaicin sensitivity of mouse DiI-labeled maxillary dental primary afferent neurons (DPANs) in TG cultures. (**A–C**) Photomicrographs of mouse TG neurons in cell culture with DiI in red discerning the DPANs. (**D**) Representative calcium transient of capsaicin-sensitive and capsaicin-insensitive (3 µM) DPANs depicted as ratio. Potassium chloride (KCl, 145 mM) was applied to identify neurons. (**E**) The increase in intracellular calcium in response to capsaicin (3 µM) is not different in presence or absence of DiI. Data are from 4 male C57BL/6J mice, and ganglia from 2 mice were used for each culture. Values are presented as mean ± SEM.

but in another 14 animals, the surgery yielded no labeled DPANs)—a work with HRP in the cat reported a rate of 30% failed experiments, with no labeling after HRP exposure (Arvidsson 1975). Nevertheless, with the high level of manual and technical skills required for this particular surgery in the mouse, we consider a 50% success rate a reproducible approach

for DPAN visualization, especially because the number of dropouts decreased noticeably with practice and experience. In this study, the number of cells with HRP granula was between 5 and 136 per tooth—quite similar to the variability in our hands. Another HRP study estimated 163 cells to innervate 1 feline canine tooth (Anderson and Rosing 1977) and a third one, as much as 199 cells (Pearl et al. 1977). Two previous studies with DiI in the rat found that 1) 30 to 50 DPANs are labeled, albeit counted in dissociated TG cultures and after crystal DiI exposure of all maxillary molar pulps (Taddese et al. 1995; Eckert et al. 1997) and 2) about 136 ± 58 were counted from immunohistochemical analysis in the rat following HRP labeling (Sugimoto et al. 1988). In a further study, where 1 rat mandibular molar was exposed to HRP, the counted cells ranged from 142 to 288 (Aker 1987). Our 2-photon reconstruction, which we regard as the most accurate method to date, identified 176 DPANs from 2 mouse maxillary molars.

Our model is appropriate for morphologic studies using immunohistochemistry and functional studies of single cultured neurons, such as patch clamp, calcium microfluorimetry, and polymerase chain reaction (Taddese et al. 1995; Cook et al. 1997; Chung et al. 2011; Kim et al. 2011; Vang et al. 2012). The model does rely on the fact that only dental primary afferents appear labeled. Although the tooth constitutes a natural barrier, dye leakage and dissemination via the root or disintegrated mucosal and periodontal tissue represent a realistic concern, and the periodontal ligament in particular has abundant sensory innervation (Arvidsson 1975). In our hands, application of dye to bleeding pulp resulted in few or no labeled cells; similarly, application to uninjured pharyngeal mucosa yielded no staining. Under microscope control, dye leakage and injury to the adjacent periodontal ligament/tissue can be excluded. Our control experiments are supported by previous findings that DiI in the bloodstream does not contribute to labeling and that only axons with disintegrated membrane serve to uptake dye (Eckert et al. 1997). Nevertheless, a dissemination of dye through the root apical foramen into periodontal tissue cannot be controlled for but should matter only in case of injury; even then, it is highly likely that uptake of the dye in dental pulp and root nerves occurs in these cases as well.

In rats, DiI labeling allowed patch clamp recordings and led to recognition of the majority of dental primary afferents as nociceptors with capsaicin sensitivity and a characteristic hump in the action potential shape (Kim et al. 2011). Immunofluorescence identified nociceptors as IB4 binding and verified expression of TRPV1 and specific ligand-gated ion channels for ATP ($P2X_2$, $P2X_3$). Based on reverse transcription polymerase chain reaction, TRPM8, TRPA1, and the nociceptor-specific sodium channel subtype $Na_V1.8$ (Cook et al. 1997; Kim et al. 2011; Vang et al. 2012) were detected. In our reconstruction from a C57BL/6J mouse, we found that 49% of the DPANs expressed TRPM8. In contrast, in rat TGs, single-cell reverse transcription polymerase chain reaction identified mRNA from TRPM8 in 35% of the DPANs. The difference may be due to alterations under culture conditions or may be species dependent (Kim et al. 2011). Mainly nociceptors and only a few Aβ-like DPANs were identified by staining with the neurofilament 200 marker in the rat (Vang et al. 2012), which also matches the size distribution histogram established in our study for both species.

In summary, our study provides first-time evidence that specific retrograde labeling from mouse dental afferents is possible with carbocyanine dyes. We regard the possibility of retrograde labeling of dental afferents in mice as an enabling technology. In particular, future studies can now combine the strength of transgenic mouse models and single-cell transcriptomics with morphology and functional characterization of neuronal subpopulations. Such integrative studies are necessary to recognize the mechanistic basis of how tooth pain segregates from trigeminal, somatic, and visceral pain and to support the development of therapeutic approaches for dentine hypersensitivity and tooth pain.

Author Contributions

A. Kadala, P. Sotelo-Hitschfeld, contributed to conception, design, data acquisition, analysis, and interpretation, drafted and critically revised the manuscript; Z. Ahmad, A. Mueller, L. Bernal, Z. Winter, contributed to data acquisition, critically revised the manuscript; P. Tripal, B. Schmid, contributed to conception, design, data acquisition, and analysis, critically revised the manuscript; S. Brauchi, contributed to data interpretation, critically revised the manuscript; U. Lohbauer, contributed to conception and design, critically revised the manuscript; K. Messlinger, J. Lennerz, contributed to conception, design, and data interpretation, critically revised the manuscript; K. Zimmermann, contributed to conception, design, data analysis, and interpretation, drafted and critically revised the manuscript. All authors gave final approval and agree to be accountable for all aspects of the work.

Acknowledgments

Part of the present work was performed in fulfillment of the requirements for obtaining the degree dentariae medicinae doctoris (Dr. med. dent.). The authors thank Birgit Vogler and Jana Schramm for expert technical assistance. This study was funded by IZKF Project E14, the Pfleger Foundation, and the German Research Council (DFG ZI 1172/3-1 and ZI 1172/4-1). P.S.H. acknowledges support from CONICYT (21140372) and MECESUP (AUS 1203) fellowships. The authors declare no potential conflicts of interest with respect to the authorship and/or publication of this article.

References

Aker FD. 1987. Innervation of rat molar teeth: II. A quantitative analysis of primary sensory neurons innervating a mandibular molar tooth. Anat Rec. 219(2):186–192.

Aldskogius H, Arvidsson J. 1978. Nerve cell degeneration and death in the trigeminal ganglion of the adult rat following peripheral nerve transection. J Neurocytol. 7(2):229–250.

Anderson KV, Rosing HS. 1977. Location of feline trigeminal ganglion cells innervating maxillary canine teeth: a horseradish peroxidase analysis. Exp Neurol. 57(1):302–306.

Arvidsson J. 1975. Location of cat trigeminal ganglion cells innervating dental pulp of upper and lower canines studied by retrograde transport of horseradish peroxidase. Brain Res. 99(1):135–139.

Beaudreau DE, Jerge CR. 1968. Somatotopic representation in the gasserian ganglion of tactile peripheral fields in the cat. Arch Oral Biol. 13(3): 247–256.

Boada MD. 2013. Relationship between electrophysiological signature and defined sensory modality of trigeminal ganglion neurons in vivo. J Neurophysiol. 109(3):749–757.

Chaudhary P, Martenson ME, Baumann TK. 2001. Vanilloid receptor expression and capsaicin excitation of rat dental primary afferent neurons. J Dent Res. 80(6):1518–1523.

Chung MK, Jue SS, Dong X. 2012. Projection of non-peptidergic afferents to mouse tooth pulp. J Dent Res. 91(8):777–782.

Chung MK, Lee J, Duraes G, Ro JY. 2011. Lipopolysaccharide-induced pulpitis up-regulates TRPV1 in trigeminal ganglia. J Dent Res. 90(9):1103–1107.

Cook SP, Vulchanova L, Hargreaves KM, Elde R, McCleskey EW. 1997. Distinct ATP receptors on pain-sensing and stretch-sensing neurons. Nature. 387(6632):505–508.

Dhaka A, Earley TJ, Watson J, Patapoutian A. 2008. Visualizing cold spots: TRPM8-expressing sensory neurons and their projections. J Neurosci. 28(3):566–575.

Eckert SP, Taddese A, McCleskey EW. 1997. Isolation and culture of rat sensory neurons having distinct sensory modalities. J Neurosci Methods. 77(2):183–190.

Gregg JM, Dixon AD. 1973. Somatotopic organization of the trigeminal ganglion in the rat. Arch Oral Biol. 18(4):487–498.

Higashiyama H, Kuratani S. 2014. On the maxillary nerve. J Morphol. 275(1):17–38.

Honig MG, Hume RI. 1986. Fluorescent carbocyanine dyes allow living neurons of identified origin to be studied in long-term cultures. J Cell Biol. 103(1):171–187.

Honig MG, Hume RI. 1989. Dil and diO: versatile fluorescent dyes for neuronal labelling and pathway tracing. Trends Neurosci. 12(9):333–335, 340–341.

Kerr FW, Lysak WR. 1964. Somatotopic organization of trigeminal-ganglion neurones. Arch Neurol. 11:593–602.

Kim HY, Chung G, Jo HJ, Kim YS, Bae YC, Jung SJ, Kim JS, Oh SB. 2011. Characterization of dental nociceptive neurons. J Dent Res. 90(6):771–776.

Lende RA, Poulos DA. 1970. Functional localization in the trigeminal ganglion in the monkey. J Neurosurg. 32(3):336–343.

Lin JJ, Du Y, Cai WK, Kuang R, Chang T, Zhang Z, Yang YX, Sun C, Li ZY, Kuang F. 2015. Toll-like receptor 4 signaling in neurons of trigeminal ganglion contributes to nociception induced by acute pulpitis in rats. Sci Rep. 5:12549.

Mazza JP, Dixon AD. 1972. A histological study of chromatolytic cell groups in the trigeminal ganglion of the rat. Arch Oral Biol. 17(3):377–387.

Naumann T, Hartig W, Frotscher M. 2000. Retrograde tracing with Fluoro-Gold: different methods of tracer detection at the ultrastructural level and neurodegenerative changes of back-filled neurons in long-term studies. J Neurosci Methods. 103(1):11–21.

Park CK, Kim MS, Fang Z, Li HY, Jung SJ, Choi SY, Lee SJ, Park K, Kim JS, Oh SB. 2006. Functional expression of thermo-transient receptor potential channels in dental primary afferent neurons: implication for tooth pain. J Biol Chem. 281(25):17304–17311.

Pearl GS, Anderson KV, Rosing HS. 1977. Anatomic evidence revealing extensive transmedian innervation of feline canine teeth. Exp Neurol. 54(3):432–443.

Schmued LC, Fallon JH. 1986. Fluoro-Gold: a new fluorescent retrograde axonal tracer with numerous unique properties. Brain Res. 377(1):147–154.

Sugimoto T, Takemura M, Wakisaka S. 1988. Cell size analysis of primary neurons innervating the cornea and tooth pulp of the rat. Pain. 32(3): 375–381.

Taddese A, Nah SY, McCleskey EW. 1995. Selective opioid inhibition of small nociceptive neurons. Science. 270(5240):1366–1369.

Usoskin D, Furlan A, Islam S, Abdo H, Lonnerberg P, Lou D, Hjerling-Leffler J, Haeggstrom J, Kharchenko O, Kharchenko PV, et al. 2015. Unbiased classification of sensory neuron types by large-scale single-cell RNA sequencing. Nat Neurosci. 18(1):145–153.

Vang H, Chung G, Kim HY, Park SB, Jung SJ, Kim JS, Oh SB. 2012. Neurochemical properties of dental primary afferent neurons. Exp Neurobiol. 21(2):68–74.

Vetter I, Hein A, Sattler S, Hessler S, Touska F, Bressan E, Parra A, Hager U, Leffler A, Boukalova S, et al. 2013. Amplified cold transduction in native nociceptors by M-channel inhibition. J Neurosci. 33(42):16627–16641.

SECTION II: CHAPTER 1

Hyperpolarization-activated channels shape temporal patterns of ectopic spontaneous discharge in C-nociceptors after peripheral nerve injury

EJP
European Journal of Pain

ORIGINAL ARTICLE

Hyperpolarization-activated channels shape temporal patterns of ectopic spontaneous discharge in C-nociceptors after peripheral nerve injury

L. Bernal, C. Roza

Department of Biología de Sistemas, Universidad de Alcalá, Alcalá de Henares, Madrid, Spain

Correspondence
Carolina Roza
E-mail: carolina.roza@uah.es

Funding sources
This study was supported by the Spanish Government SAF2016-77585-R. LB was supported by a FPU Scholarship (Ministerio de Educacion, Cultura y Deporte, Spain).

Conflict of interest
None declared.

Accepted for publication
29 March 2018

doi:10.1002/ejp.1226

Abstract

Background: Neuropathic pain is thought to be mediated by aberrant impulses from sensitized primary afferents, and the temporal summation of the discharges might also influence nociceptive processing. Hyperpolarization-activated cyclic nucleotide-gated (HCN) channels (Ih current) generate rhythmic activity in neurons within the central nervous system and contribute to nociceptors excitability in neuropathic pain.
Methods: We searched for single fibres with ectopic spontaneous discharges from an *in vitro* preparation in mice containing a neuroma formed in a peripheral branch of the saphenous nerve together with the undamaged branches.
Results: Both damaged (axotomized) and undamaged fibres (putative intact) developed ectopic spontaneous activity with different temporal spike trains: Clock-like, Irregular or Bursts. The Ih current blocker, ZD7288, significantly suppressed ectopic spontaneous discharges in nociceptive fibres (3/5 Aδ- and 24/31 C-units and 1 nonclassified) by 64%. Additionally, ZD7288 changed the spike patterns of 5/7 Clock-like and 3/4 Burst units to Irregular. Exogenous cAMP produced a significant ~65% increase in the ectopic firing in 5 Irregular fibres, which was restored by ZD7288. In six additional fibres (three Clock-like and three Irregular), exogenous cAMP had no further effect, but co-application with ZD7288 decreased their discharge by half. These units showed significant higher levels of discharges than the cAMP-sensitive ones.
Conclusions: Our data suggest that HCN channels modulate ectopic spontaneous firing in C-nociceptors and shape their temporal patterns of discharge which will, ultimately, modify the nociceptive message received and processed by second-order neurons.
Significance: We show an involvement of HCN channels in the modulation of ectopic spontaneous discharges from C-nociceptors. This finding exposes a mechanism of nociceptive transmission enhancement and highlights the clinical relevance of peripheral HCN blockade for spontaneous pain relief during neuropathy.

1. Introduction

Spontaneous pain, the main symptom reported by patients with peripheral neuropathies (Truini et al., 2013; Vollert et al., 2017), seems to originate and prevail through aberrant spontaneous discharges fired by peripheral afferents (Baron et al., 2013; Meacham et al., 2017). The ectopic reorganization of different Nav and Kv channels renders hyperexcitable

membranes leading to abnormal firing (Campbell and Meyer, 2006; Devor, 2006). Among these entities, experimental evidences point to a fundamental role of the Ih current in this pathology. The Ih current, driven by *hyperpolarizing-activated cyclic nucleotide channels* or HCN channels, is increased in medium and large diameter size DRG and trigeminal neurons after nerve injury (Chaplan et al., 2003; Yao et al., 2003; Kitagawa et al., 2006). Pharmacological blockade of HCN channels decreases mechanical hyperalgesia in different neuropathic pain models (Chaplan et al., 2003; Luo et al., 2007; Jiang et al., 2008; Young et al., 2014; Tsantoulas et al., 2017) and reduces spontaneous activity in myelinated A-fibres after nerve damage when applied locally (Chaplan et al., 2003; Jiang et al., 2008).

Hyperpolarization-activated cyclic nucleotide-gated channels are referred to as 'pacemaker channels' as they underlie rhythmic activity within groups of excitable cells. Their activation favours the probability of subsequent AP firing shaping neuronal responsiveness and the temporal spike trains of the neuronal discharge (Lüthi and McCormick, 1998). Primary afferent fibres are quiescent unless stimulated, however, upon nerve damage they became spontaneous and may exhibit different temporal patterns of discharge (Tal and Eliav, 1996; Michaelis et al., 2000; Bernal et al., 2016). A redistribution of HCN channels after nerve damage would have a decisive influence on these spike trains. It has long been suggested that both the magnitude and the quality of pain sensation are encoded by the temporal summation of the nociceptive discharge (Koltzenburg and Handwerker, 1994; Cho et al., 2016) and that different responses before and after a nerve injury might be associated with the temporal patterns of spontaneous spikes (Sandkühler, 1996). However, the relevance of the temporal patterns of ectopic discharges in the nociceptive message has never been examined in depth before.

Microneurographic studies in neuropathic pain patients described the presence of spontaneously active C-fibres, which correlate with the presence of pain (Kleggetveit and Jørum, 2010; Kleggetveit et al., 2012; Serra et al., 2012). Although impulse barrage from sensitized afferents seems relevant during neuropathic pain (Pitcher and Henry, 2008; Haroutounian et al., 2014), the characterization of the effects of HCN channel peripheral blockade on ectopic C-fibres has not been attempted before. To address this question, we performed a series of experiments in a mice model of partial axotomy of the saphenous nerve, which renders ~20%–30% of the C-fibres spontaneously active when examined *in vitro*, exhibiting discharge rates suitable for pharmacological studies (Bernal et al., 2016). We examined the effect of the Ih blocker ZD7288 on spontaneously active fibres alone or in combination with an exogenous cAMP donor, which is a modulator of HCN excitability (Stieber et al., 2005) known to up-regulate in models of neuropathic pain (Tsantoulas et al., 2017).

2. Materials and methods

2.1 Animals

Adult outbred CD1 female mice (n = 36, body weight 26–55 g) were used. European Union and State legislation for the regulation of animal experiments was followed, and the local Animal Care Facility and Regional Government approved the experimental protocols (project licence: ES280050001165).

2.2 Spared saphenous nerve injury (SSNI)

Nerve-end neuromas were induced by section of one of the peripheral branches of the saphenous nerves in 28 mice as previously described (Bernal et al., 2016). Briefly, under deep anaesthesia with isoflurane (~3.5%–4% in pure O_2), the saphenous nerve was exposed at the mid-thigh level. One of the branches was dissected free and tightly ligated with 8-0 silk, and its distal end was inserted in a 2-mm-long silicone tube (0.44 mm internal diameter) to prevent lateral innervation of surrounding tissue. The incision was closed. Neuromas were created in both paws. Animals were housed in groups of four and inspected periodically for infections or abnormal behaviour. Mice had access to water and food *ad libitum*.

Most of the experiments were performed ~4 week after the surgery (median 27 days, range 15–57). Mice were killed by cervical dislocation, and the saphenous nerve with the neuroma attached to the skin flap was excised and pinned down to a Sylgard®-based recording chamber, corium side up. At the recording chamber, preparations were superfused with oxygenated synthetic interstitial fluid (SIF, see composition below) at a rate of 5 ml/min and maintained at 32 ± 1 °C by means of a Peltier device (Warner Instruments, Hamden, CT, USA). The silicon tube around the neuroma was removed, and the neuroma was placed into a glass suction electrode.

2.3 Electrical recordings and fibre characterization

The electrical activity from sensory fibres was recorded by means of suction microelectrodes engineered from

glass pipettes (20–30 μm external tip diameter) filled with SIF as previously described (Roza and Lopez-Garcia, 2008). The microelectrode tip was carefully placed in contact to the proximal end of the nerve trunk under visual guidance using a micromanipulator and after applying negative pressure. Experiments were run only when a single fibre was recorded or clearly differentiated from background discharges based on spike amplitude and shape.

The microelectrode was left for a minimum of 1 min to record spontaneous activity (which was defined as a discharge rate >0.03 Hz, 2 spikes/min). Then, controlled electrical pulses of variable duration and intensity (0.2–0.5 ms pulse width, maximum strength 1 mA) were delivered to the neuroma – via a glass suction electrode or *neuroma electrode* – or to the nerve trunk distal to the neuroma – with a bipolar tungsten electrode or *field electrode* (WPI, World Precision Instruments, Sarasota, FL, USA) – to identify the origin of the fibres and classified them as axotomized or putative intact fibres, respectively.

Mechanosensitivity was explored by gently touching the neuroma or the skin flap with a smooth-tipped glass rode (diameter = 0.5 mm). No attempts were made to establish mechanical thresholds in order to avoid mechanical sensitization. For those fibres presenting mechanical receptive fields in the skin, electrical stimulation was subsequently applied on the receptive field.

Thermal stimulation was only tested when recorded fibres presented spontaneous activity. Temperature increments up to ~45 °C or decrements down to ~15 °C were applied by means of a custom-designed manual thermal stimulator. Our device consisted of a small hollow metal cube (~ 9 mm^2 contact surface), which allowed circulation of hot or cold water. The stimuli were ramp-shaped, and the desired temperatures were reached in ~25 s. The probe/skin temperature was measured with a thermopar, which was fed to the computer via a temperature controller (Physitemp BAT-12, Physitemp Instruments, Clifton, NJ, USA).

Electrical signals were recorded by means of a Dagan EX4-400 amplifier (Dagan, Minneapolis, MS, USA), digitized at 20 KHz (Power 1401, CED, Cambridge Electronic Design, Cambridge, UK) and stored for offline analysis. Fibres were classified according to their conduction velocity into Aδ-units (CV > 1 < 16 m/s) or C-units (CV < 0.9 m/s) based on pilot experiments using whole nerve recordings, which showed a CV of 0.8 m/s for the C-fibre volley.

When a second preparation from the same animal was used (within the same day), it was stored in oxygenated SIF at 4 °C. There were no detectable differences in results between the first and second preparations studied.

2.4 Control experiments in intact fibres

In a separate series of experiments performed in eight mice, the saphenous nerve was dissected in continuity with the skin flap and placed in the recording chamber. Electrophysiological recordings and mechanical/thermal stimulation were performed following the same protocol described above for putative intact units.

2.5 Testing the effects of Ih current modulation on spontaneous activity

ZD7288 (4-ethylphenylamino-1,2-dimethyl-6-methylaminopyrimidinium chloride) has been shown to be a specific HCN channel blocker when used at low concentration in our experimental conditions (Mazo et al., 2013). We tested its effect in a proportion of fibres with ectopic spontaneous discharges. Following a baseline period of ~30 min in which the fibre exhibited stable firing, ZD7288 was superfused for 30 min to the whole preparation. To establish changes in spontaneous activity, the firing frequency was measured 5 min prior to ZD7288 – baseline – and compared with the firing frequency for the last 5 min just before washout. A reduction >35% in the mean instantaneous or peak frequencies of the discharge was considered as an effect. In an additional set of experiments, we aimed to evaluate the extent to which the effect of Ih blockade on ectopic spontaneous firing could be further modulated by cAMP. We tested the effects of the cAMP donor 8-bromoadenosine 3′,5′-cyclic monophosphate sodium salt (8-Br-cAMP) in a proportion of fibres with ectopic spontaneous discharges before or after ZD7288 superfusion. 8-Br-cAMP (100 μmol/L) was applied alone (before ZD7288), in combination with ZD7288 or after ZD7288 and left for 40 min. The firing frequency of the fibre was calculated during the last 5 min of perfusion. An increase/decrease of 35% in the mean frequency of discharge was considered an effect.

Finally, the effect of ZD7288 was tested in a proportion of cold-responsive fibres with ongoing discharges in skin-nerve preparations obtained from naïve mice.

2.6 Solutions

SIF composition was (mmol/L) as follows: 108 NaCl, 3.48 KCl, 0.7 $MgSO_4$, 26 $NaHCO_3$, 1.7 NaH_2PO_4,

1.53 $CaCl_2$, 9.6 sodium gluconate, 5.55 glucose and 7.6 sucrose.

Stock solutions of 10^{-2} mol/L ZD7288 (Tocris, Bristol, UK) and 10^{-3} mol/L 8-Br-cAMP (Sigma-Aldrich, St. Louis, MI, USA), prepared in ultrapure water, were stored in aliquots at −20°C. On the day of the experiment, the drugs were freshly diluted in SIF to their final concentrations: 10 μmol/L for ZD7288 and 100 μmol/L for 8-Br-cAMP.

2.7 Data analysis

Waveforms were analysed offline with Spike 2 software (CED, Cambridge Electronic Design). Mean frequency of spontaneous discharges was measured during an undisturbed 5-min period. Autocorrelogram histograms (ACHs) were plotted from the spikes recorded during that period of time, and contamination of the refractory period (2 ms) after spike sorting was assessed. Only data obtained from unequivocally classified units were further analysed. The pattern of spontaneous activity was established using the algorithm Gaussian Locking to a free Oscillator (GLO) that allows identification of regularity in the patterns of spontaneous discharges. Briefly, GLO analyses the instant frequency of individual spikes to characterize the regularity of the spike train. This is determined by the β1 and β2 values (for complete details, see Ref. (Bingmer et al., 2011)) and the ACH shape. Some of the neurons were characterized by the presence of firing grouped in bursts with different characteristics that were analysed by a customer algorithm called *Burst Analyser* (BAR). BAR is based on the interspike interval (ISI) obtained from the spike trains of individual neurons and detects the spikes that are fired within a burst. This algorithm allows a characterization of the spike train based on the proportion of spikes fired within a burst, the intraburst frequency and the number of spikes per burst. A fibre that shows at least half of its spikes in burst was classified as Burst. Fibres with simple spikes were classified as Clock-Like ($\beta1 < 0.35$ and ACH with at least two peaks) or Irregular (fibres that did not fit in any of the previous groups). For further characterization of the spike patterns, we assessed ISI distribution and interburst intervals – or interval between the first spikes of consecutive bursts – before and after ZD7288.

Statistical analyses were performed in GraphPad Prism 6.0 (GraphPad Software, San Diego, CA, USA) on the raw data using *t*-test or one-way ANOVA, followed by a post hoc test when appropriate. The level of statistical significance was set at $p < 0.05$. Values are quoted as mean ± standard error of the mean (SEM).

3. Results

The aim of this work was to understand the contribution of the *Ih* current in the development of ectopic spontaneous discharge and its role in shaping the different patterns of ectopic spontaneous discharges in C-fibre nociceptors after partial damage to the saphenous nerve. We searched for fibres present with ectopic spontaneous activity and examined the effect of ZD7288 alone or in combination with 8-Br-cAMP on 54 ectopic spontaneously active fibres (48 C-, 5 Aδ-fibres and 1 nonclassified) with inputs from the neuroma ($n = 8$) or the intact skin ($n = 46$).

3.1 Characteristics of nociceptors with ectopic spontaneous discharges

In the SSNI model, ectopic spontaneous discharges develop in axotomized C-fibres but also in C-fibres with mechanical inputs from the skin (distant from the neuroma), which were subsequently named 'putative intact' fibres – see Ref. (Bernal et al., 2016).

The general electrophysiological properties of axotomized fibres ($n = 8$) and putative intact fibres ($n = 46$) presented with ectopic spontaneous discharges are summarized in Table 1.

As shown in Fig. 1, visual inspection of the ectopic discharges unveils the presence of a variety of temporal patterns. Automatic classification, based on our algorithms and ISI distribution, defined three groups (see Fig. 1D). Most of the recorded units ($n = 38$) were classified as Irregular, as they presented an erratic firing pattern during the recording period (see Fig. 1C). Ten further fibres were classed as Clock-like as they presented regular discharges (see Fig. 1A). For analysis and representation purposes, the mean discharge frequency values are given for these two groups of units and are presented in Table 2. The remaining six fibres fired in burst and were classed as Burst (see Fig. 1B). Since bursts are clusters of action potentials separated by silent periods, peak frequencies and interburst intervals described better this temporal pattern of discharge (Bingmer et al., 2011). These values are given in Table 2.

3.2 Effects of Ih blockade on ectopic spontaneous discharges

ZD7288 was applied in a total of 37 fibres with different temporal patterns. The spontaneous activity was significantly reduced in most of the fibres tested

Table 1 Electrophysiological properties of fibres with ectopic spontaneous discharges.

Origin of the fibres	C-fibres	Aδ-fibres	Non-classified
Axotomized (n = 8)	6	2	
Conduction velocity (m/s)	0.51 ± 0.07	3.32 ± 1.46	
Mechanical stimulation of the neuroma	6 (100%)	2 (100%)	
Putative intacts (n = 46)	42	3	1
Conduction velocity (m/s)	0.49 ± 0.02	5.56 ± 2.12	
Without response to natural stimuli	3 (8%)	1 (33%)	
With responses to natural stimuli			
Mechanical	17 (40%)	2 (67%)	
Heat-Cold	1 {20 & 40 °C} (2%)		
Mechano-Heat	17 {41 °C} (40%)		
Mechano-Cold	2 {21 °C} (5%)		
Mechano-Heat-Cold	2 {25 & 42 °C} (5%)		1 {20 & 40 °C}

Numbers in brackets refers to thermal threshold and in parenthesis percentage of fibres.

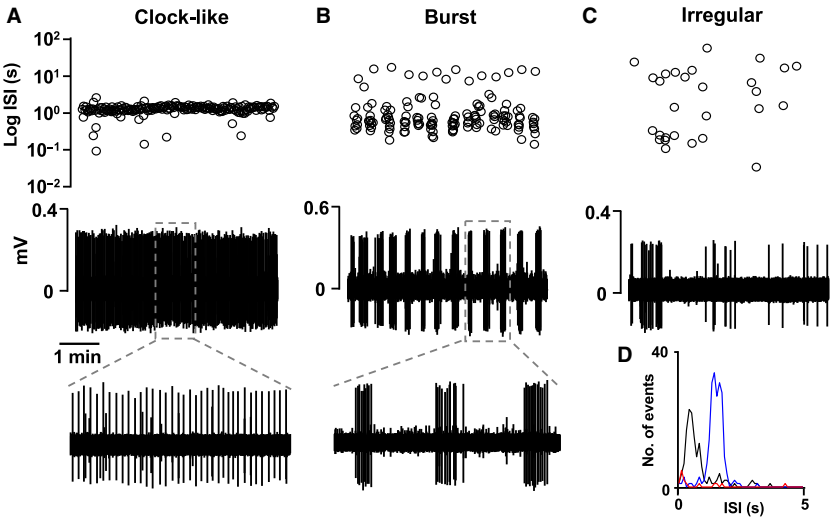

Figure 1 C-nociceptors exhibit different temporal patterns of spontaneous ectopic discharges after peripheral nerve damage. (A) shows the typical regular spike train of a Clock-like unit (C-mechano putative intact fibre, CV: 0.60 m/s, mean frequency: 0.65 Hz). Note that all spikes are fired at a similar interspike interval around 1 s. The inset expands a minute of the recorded trace to appreciate the regularity. (B) shows an example of a Burst unit (C-mechano-heat putative intact fibre, CV: 0.30 m/s, peak frequency 3.9 ± 0.39 Hz, interburst interval of 14.17 ± 0.96 s), which according to DER had 91% of the action potentials fired within a burst. The inset expands a minute of the recorded trace to appreciate individual bursts. (C) shows an example of an Irregular unit (C-mechano axotomized fibre, CV: 0.41 m/s with a mean firing rate of 0.10 Hz). The activity of the fibres is presented as the original recordings (mV) and as and ISI plot in a logarithmic y-scale (Log ISI). (D) ISI distribution for the CL (blue), Burst (black) and Irregular (red) fibres abovementioned.

(28/37) without affecting their conduction velocity (0.52 ± 0.03 vs. 0.52 ± 0.03 m/s, n = 15, p = 0.98). The effects were similar among the axotomized and putative intact population and also between the C- and Aδ-fibres. Hence, for clarity and readability proposes, the effects of ZD7288 are shown separately for each of these temporal patterns (see Fig. 2).

ZD7288 significantly reduced by 61% the mean discharge (from 0.40 ± 0.15 to 0.20 ± 0.10, n = 3/5 Aδ- and 14/21 C-fibres) of the Irregular units. For the Clock-like units, the mean discharge was reduced by 64% in the seven fibres tested (from 0.46 ± 0.07 to 0.15 ± 0.03, six C-fibres and one nonclassified). Moreover, ISI was significantly increased in all of them (from 2.29 ± 0.04 to 6.6 ± 0.34 s) and five of the units became irregular. The peak discharge of the Burst units was reduced in the presence of ZD7288 (from 12.47 ± 3.22 to 4.32 ± 3.11, n = 4 C-fibres), which, in addition, increased Interburst intervals in two of the units and impaired bursting in the remaining two (Fig. S1). Fig. 3 shows a representative example of the effect of ZD7288 in fibres with different patterns of discharge.

Table 2 Number units and their discharge frequency (in Hz) according to their temporal spike patterns.

	Axotomized		Putative intacts		
Spike-train patterns	C-fibres	A-fibres	C-fibres	A-fibres	Non-classified
Irregular (Inst. Fq.)	0.19 ± 0.04 (n = 5)	1.35 ± 1.24 (n = 2)	0.26 ± 0.05 (n = 28)	0.11 ± 0.04 (n = 3)	
Clock-like (Inst. Fq)	0.26 (n = 1)		0.60 ± 0.08* (n = 8)		0.37 (n = 1)
Burst (n = 6)					
Inst. Fq.			0.78 ± 0.16		
Peak Fq.			19.52 ± 8.03		
Intraburst Fq.			2.48 ± 0.53		
Interburst Fq.			0.16 ± 0.01		
Spikes/burst			12 ± 1.62		

Inst. Fq., instantaneous frequency.
*p < 0.05 Mann–Whitney test Clock-like versus Irregular.

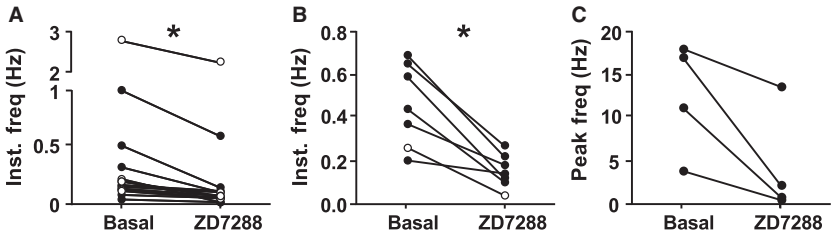

Figure 2 The graphs show the effect of ZD7288 (10 μmol/L) on the mean frequency of discharge for Irregular (A, n = 17), Clock-like (B, n = 7) and Burst (C, n = 4) fibres. White circles accounts for axotomized fibres, and black circles account for putative intact. *p < 0.05, Wilcoxon matched pairs.

In a separate series of control experiments, we probed for the presence of C-mechano-cold nociceptors (C-MC), which, although rare, might exhibit ongoing activity at physiological temperature (Zimmermann et al., 2009). A total of 50 fibres were recorded from naïve skin-nerve preparations (18 A∂- and 32 C-units, with mean conduction velocities of 3.66 ± 0.66 and 0.50 ± 0.03 m/s, respectively). Only three C-units that responded when the temperature of their receptive fields was lowered (mean threshold: 21 ± 2 °C) presented ongoing irregular discharges. The spontaneous firing of these C-MC fibres was unaltered in the presence of ZD7288 (from 0.36 ± 0.25 to 0.26 ± 0.15 Hz, p > 0.05, data not shown).

Together, these results demonstrate that functional HCN channels play a key role in the generation of the ectopic spontaneous discharges after axotomy, but their contribution in shaping the temporal patterns of discharge on pain fibres made them attractive elements to understand neural coding and peripheral discharge impact on central sensitization.

3.3 Ih modulation with 8-Br-cAMP had differential effects on ectopic spontaneous activity

To decipher which subunit could be involved in the development of ectopic spontaneous activity, we evaluated the impact of cAMP of the ectopic discharges using the permeable hydrolysis-resistant cAMP analog 8-bromoadenosine 3′,5′-cyclic monophosphate (8 Br-cAMP, 100 μmol/L) in 14 C-units with spontaneous activity and different temporal patterns.

In five Irregular units, 8-Br-cAMP increased the mean discharge by ~65% (from 0.12 ± 0.03 to 0.19 ± 0.04 Hz) and this effect was reversed by ZD7288 in all of them (to 0.12 ± 0.04 Hz). In the remaining nine fibres, 8-Br-cAMP was devoid of effect on mean instantaneous frequency. However, upon application of ZD7288, the ectopic firing was reduced by ~48% (from 0.54 ± 0.1 to 0.28 ± 0.06 Hz) in three Irregular and three Clock-like (for analysis and presentation purposes, the data of these two groups have been plotted together, see Fig. 4A). The remaining three units with irregular patterns were unaffected by any of the compounds and might represent a population of neurons, in which spontaneous discharges are independent of functional HCN, in accordance with the data presented above in point 3.2.

In a group of the units tested with ZD7288 (*see Results 3.2 above*), 8-Br-cAMP was co-applied immediately after to assess whether the described excitatory effects were mediated via HCN channels. In six units, the inhibition of the spontaneous activity by ZD7288 was maintained upon application of 8-Br-cAMP (100 μmol/L). The

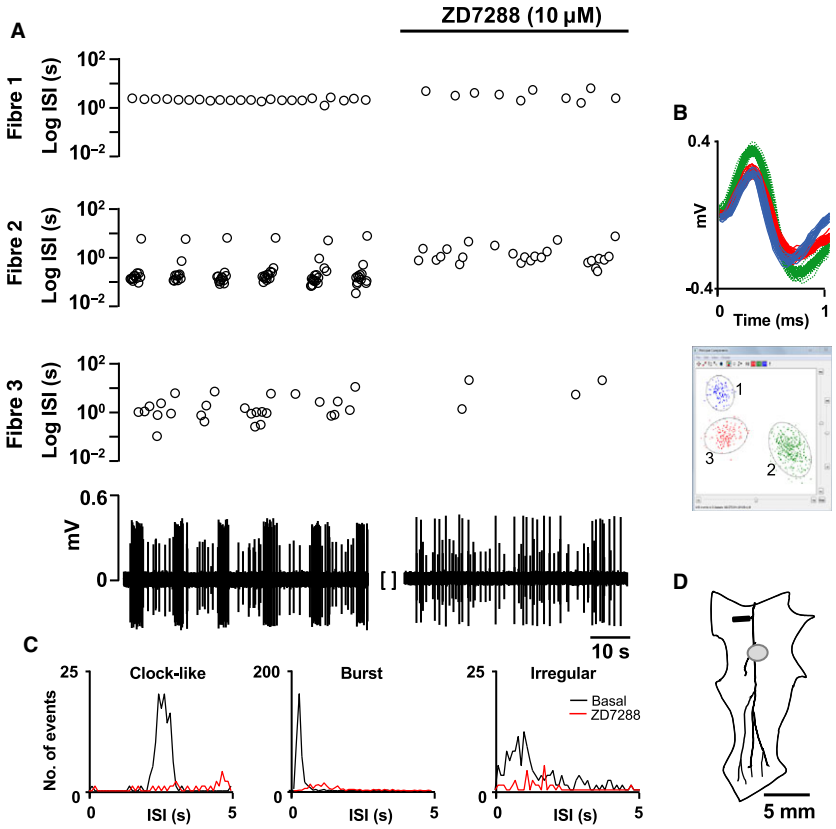

Figure 3 HCN channel blockade alters the firing pattern of sensitized C-nociceptors. (A) shows the recordings of spontaneous activity of three fibres recorded within the same filament before (left panel) and after application of ZD7288 (right panel). Fibre 1 is a nonclassified Clock-like unit (mean discharge frequency: 0.37 Hz). Fibre 2 is a C-mechano-heat Burst unit, which according to DER has 95% of the action potentials fired within a burst (peak frequency: 11.58 ± 1.12 Hz and interburst interval: 9.53 ± 0.37 s). Fibre 3 is a C-heat-cold Irregular unit (mean discharge frequency: 0.48 Hz). Note that ZD7288 reduced the discharges and changed the temporal patterns of fibres 1 and 2. The activity is presented as the original recordings (mV) and as ISI plot in a logarithmic *y*-scale (Log ISI). Gap [] represents a ~30-min interval. (B) The upper graph shows the template shapes of the sorted spikes plotted superimposed in a 5-min period (fibre 1: blue, fibre 2: green and fibre 3: red). The bottom panel shows the three clusters clearly differentiated upon using principal components analysis (PCA) in Spike 2. (C) ISI distribution before (black) and after ZD7288 (red). (D) Representation of the preparation with the mechanical receptive field of fibre 2 indicated by the grey circle. The black rectangle represents the neuroma.

effects were similar for the three Irregular and one Clock-like unit (0.38 ± 0.1 Hz control, 0.13 ± 0.04 ZD7288 and 0.1 ± 0.03 Hz ZD7288 + 8-Br-cAMP, $n = 4$, shown in Fig. 4B) and for the two Burst units which peak discharges dropped from 17.42 ± 0.5 to 7.92 ± 5.66 Hz with ZD2788 and to 4.23 ± 2.82 Hz with ZD7288 + 8-Br-cAMP (data not shown).

In terms of cAMP sensitivity and levels of spontaneous discharges, our data suggest the presence of, at least, two population of fibres, which might present a differential expression in their HCN subtype composition.

4. Discussion

In our study, we have shown that the blockade of HCN channels reduces ectopic spontaneous discharges in a large population of C-fibres innervating experimental neuromas as well as in neighbouring C-fibres innervating intact skin. We have also shown that HCN channels help to shape the temporal patterns of the ectopic spontaneous discharges, consequently adjusting the nociceptive processing of second-order neurons. The sensitivity to 8-Br-cAMP suggests differential expression and/or functionality of HCN channels at the site of damage.

4.1 Role of HCN in the development of ectopic spontaneous discharges

In our experiments, the pan-HCN blocker ZD7288 applied at 10 µmol/L significantly inhibited ectopic spontaneous discharges in a large percentage of the examined nociceptive fibres (3/5 Aδ- and 24/31 C-units). These results are in agreement with previous

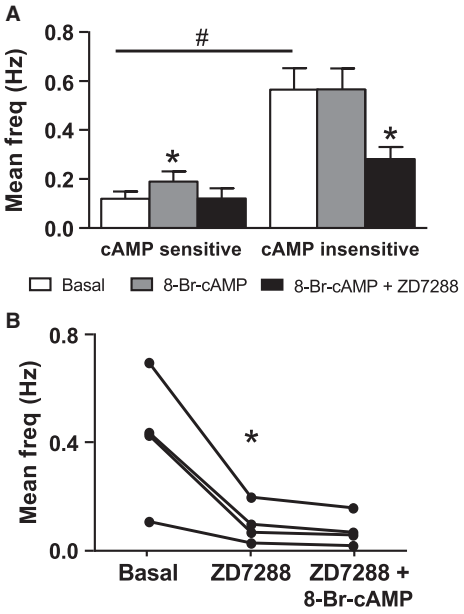

Figure 4 (A) Application of 8-Br-cAMP (100 μmol/L) revealed the presence of fibres with different sensitivity to exogenous cAMP which, in addition, was correlated with the basal levels of spontaneous discharges ($^{\#}p < 0.05$, Mann–Whitney test). Note that exogenous cAMP was unable to further excite the group of units with significantly higher rates of ectopic Clock-like or Irregular discharges ($n = 6$) but increased the discharge in those with lower rates ($n = 5$ Irregular units). Co-application of 8-Br-cAMP with ZD7288 (10 μmol/L) reduced the discharge firing to a similar degree (~55%) in both groups of fibres, reaching basal levels in the exogenous cAMP-sensitive group ($^{*}p < 0.05$, one-way ANOVA). (B) The effect of 8-Br-cAMP is likely HCN-specific as it was devoid of effect when HCN channels were previously blocked by ZD7288. The graph shows the inhibitory effect of ZD7288 on the mean frequency of discharge of four individual nociceptors (one Clock-like and three Irregular fibres, $^{*}p < 0.05$, One-way ANOVA).

data describing an inhibitory effect of locally administrated Z7288 on ectopic spontaneous discharges from myelinated A-fibres recorded *in vivo* after peripheral nerve damage or inflammation (Chaplan et al., 2003; Jiang et al., 2008). Similarly, single axotomized C-axons recorded *in vitro* exhibited a marked reduction in the conduction velocity evoked by repetitive electrical stimulation, which was largely dependent on up-regulation of functional Ih currents (Mazo et al., 2013). These observations point out an increased expression of functional HCN channels at the site of injury and/or along the peripheral nerve in both fast and slow conducting primary afferents (Chaplan et al., 2003; Jiang et al., 2008; Mazo et al., 2013; Young et al., 2014), which, based on our observations, is not restricted to the damaged neurons. These changes are likely to influence central processing. For example, a recent study in diabetic mice showed an increased c-fos expression in second-order neurons, which was reversed upon pharmacological blockade of peripheral HCN channels and by deleting HCN2 channels in small nociceptive neurons (Tsantoulas et al., 2017). This would suggest that ongoing activity from C-fibres is enough to trigger central sensitization. Here, we show for the first time the involvement of HCN channels in the development of ectopic spontaneous discharges in C-nociceptors. In the context of neuropathic pain, it is to note that spontaneously active C-fibres correlates with the presence of pain in patients (Kleggetveit and Jørum, 2010; Kleggetveit et al., 2012; Serra et al., 2012).

The conduction velocity of the fibres was unaltered, which suggests that the action of ZD7288 was devoid of unspecific effects on Nav channels (Wu et al., 2014). Furthermore, in similar experimental conditions, compound action potentials of A- and C-fibres recorded from intact nerves were unaffected by concentrations of 100 μmol/L ZD7288 (Mazo et al., 2013).

4.2 Role of HCN in neural coding in peripheral nociceptors

One of the most interesting observations in this report is the description of different patterns of discharge recorded extracellularly from C-nociceptors, comparable to those described in the spinal cord (Roza et al., 2016). Similar patterns of discharge have been already described in large myelinated fibres after axotomy (Tal and Eliav, 1996; Michaelis et al., 2000). Our data show for the first time that Ih currents play a role in shaping the temporal patterns of discharge in C-nociceptors, unequivocally altering the message received and processed at the spinal cord. Since 1926, the basic coding element of a neural code was established as the number of spikes fired in a fraction of time (Adrian and Zotterman, 1926a,b). However, it has long been accepted that a much more complex code arises when neurons are able to emit temporal patterns of spikes whose timing is reliable on a short timescale (Fellous et al., 2004). It is remarkable that spike patterns are conserved in homologous regions across species (Mochizuki et al., 2016), suggesting a key role of spike trains in neuronal coding. Unfortunately, data on the role of primary afferents' firing patterns in neural coding have been barely reported (Orio et al., 2012).

About ~20% of the C-fibres exhibited a pattern of regular discharges, which resembles pacemaker-like activity. Remarkably, by blocking HCN channels, the

regular pattern of pacemakers was modified to an irregular spiking mode. An attractive aspect of the Ih current is its widespread contribution to the generation of 'pacemaker' potentials in several nuclei of the CNS where it contributes to the generation of rhythmogenic behaviours of neural networks (Lüthi and McCormick, 1998). We proposed that the presence of Ih currents is also responsible for the rhythmic activity of the Clock-like C-nociceptors, which develops after nerve damage. The regular patterns of discharge from cold-sensitive corneal endings depend on the expression of functional Ih currents (Orio et al., 2012). Although the physiological relevance of these patterns is still unclear, in terms of coding, regular firing can be advantageous because downstream neurons achieve higher signal-to-noise ratio (i.e. regular firing would be more efficient than irregular firing in transmitting nociceptive message to the relay neurons in the spinal cord). For example, the percentage of dorsal horn neurons with Clock-like patterns and high rates of spontaneous discharge were significantly increased after peripheral nerve damage, a likely indicator of central sensitization (Roza et al., 2016).

A small proportion of the C-fibres (~12%) showed a pattern of ectopic spontaneous discharges in bursts of low intraburst frequency but peak discharges of ~20 Hz. We also observed that HCN blockade rendered some of those fibres nonbursty. Early studies already showed that a small proportion of spontaneous activity in forms of burst in Aβ-fibres after nerve injury were modified by ZD7288 (Jiang et al., 2008). In neural coding, a burst of action potentials increases the possibility of neurotransmitter release in comparison with single spike firing, i.e. favouring message propagation – see Ref. (Lisman, 2011) for a review. For example, burst patterns of activity can produce synaptic plasticity in hippocampal neurons (Huerta and Lisman, 1995). In our context, burst of activity from C-nociceptors would favour integration of nociceptive information by second-order neurons, hence potentiating central sensitization (Roza et al., 2016).

4.3 HCN subtypes involved in the generation of ectopic spontaneous discharges

The four members of the HCN family (HCN1 to HCN4) form homo- or heterotetramers yielding Ih current with different activation kinetics and sensitivity to cyclic nucleotides (Chen et al., 2001; Stieber et al., 2005). HCN1 and 2 are the dominant isoforms expressed in sensory neurons (Moosmang et al., 2001; Chaplan et al., 2003; Momin et al., 2008; Acosta et al., 2012), but it is generally accepted that HCN2 has a relevant role in the development of positive neuropathic pain symptoms, as HCN2 deletion from Nav1.8 expressing nociceptors completely precluded the development of mechanical and thermal hyperalgesia in experimental models of neuropathic pain (Emery et al., 2011; Young et al., 2014; Tsantoulas et al., 2017).

In the presence of cAMP, HCN2 subunit shifts towards more positive membrane potentials, whilst HCN1 remains unaltered (Stieber et al., 2005). The effect of the exogenous cAMP donor 8-Br-cAMP on the aberrant spontaneous activity in our experimental model revealed the presence of two types of units within those present with HCN channels (sensitive to ZD7288). Around 45% of them were sensitive to cAMP, in agreement with the expression of HCN2. In the remaining fibres, cAMP had no effect, which could be explained by the expression of functional HCN1. However, as this group of C-fibres showed significantly higher rates of discharge and included all of the Clock-like units, it could be possible that they present HCN2 channels already modulated by elevated levels of endogenous cAMP, as it has been described to occur after peripheral nerve damage (Allodi et al., 2012) and diabetic-induced neuropathy (Tsantoulas et al., 2017).

We believe that our results suggest the presence of different HCN subunits at the site of damage, which would influence differently the levels of spontaneous discharges but also adjust the temporal trains. For example, both HCN1 and HCN2 determine firing patterns from cold-sensitive endings in the cornea (Orio et al., 2009, 2012).

4.4 Role of HCN channels in neuropathic pain

As one of the characteristic symptoms in patients with peripheral neuropathies is the development of spontaneous pain (Vollert et al., 2017), blocking aberrant ongoing activity from irritable C-nociceptors should prevent the onset of neuropathic pain. The data presented here, together with previous observations (Chaplan et al., 2003; Jiang et al., 2008; Mazo et al., 2013; Young et al., 2014; Tsantoulas et al., 2017), support a peripheral accumulation of functional HCN channels at the site of injury, which contributes to generation of aberrant spontaneous discharges in axotomized and putative intact C-fibres. As Ih current also determines the specific temporal patterns of the ectopic discharges in nociceptors, peripheral blockade of HCN channels would also affect spike-time-dependent plasticity in second-order neurons (Caporale and Dan, 2008; Poo and Bi, 2016).

Altogether, Ih seems as a valuable peripheral target worth exploring for the clinical treatment of spontaneous pain of neuropathic origin. Moreover, studying HCN modulation would provide interesting tool to understand the neural coding in peripheral nociceptors. In this regard, the evaluation of potential analgesics should include an evaluation of the effects on the temporal spike patterns as well as effects on total discharge.

Acknowledgements

We are grateful to Dr. Ivan Rivera-Arconada for helpful discussions during experimental design and Dr. Ana Lopez-Guajardo for critical review of the manuscript and English revision.

Author's contributions

LB carried out electrophysiological recordings, data analysis and contributed in the design of the experiments and writing of the manuscript. CR carried out conception and design of the experiments, drafting and critical revising of the manuscript and participated in the electrophysiological recordings, analysis and interpretation of data. All authors read and approved the final manuscript.

References

Acosta, C., McMullan, S., Djouhri, L., Gao, L., Watkins, R., Berry, C., Dempsey, K., Lawson, S.N. (2012). HCN1 and HCN2 in Rat DRG Neurons: Levels in Nociceptors and Non-Nociceptors, NT3-Dependence and Influence of CFA-Induced Skin Inflammation on HCN2 and NT3 Expression. *PLoS ONE* 7, e50442-17.

Adrian, E.D., Zotterman, Y. (1926a). The impulses produced by sensory nerve endings: Part 3. Impulses set up by Touch and Pressure. *J Physiol* 61, 465–483.

Adrian, E.D., Zotterman, Y. (1926b). The impulses produced by sensory nerve-endings: Part II. The response of a Single End-Organ. *J Physiol* 61, 151–171.

Allodi, I., Udina, E., Navarro, X. (2012). Specificity of peripheral nerve regeneration: Interactions at the axon level. *Prog Neurobiol* 98, 16–37.

Baron, R., Hans, G., Dickenson, A.H. (2013). Peripheral input and its importance for central sensitization. *Ann Neurol* 74, 630–636.

Bernal, L., Lopez-Garcia, J.A., Roza, C. (2016). Spontaneous activity in C-fibres after partial damage to the saphenous nerve in mice: Effects of retigabine. *Eur J Pain* 20, 1335–1345.

Bingmer, M., Schiemann, J., Roeper, J., Schneider, G. (2011). Measuring burstiness and regularity in oscillatory spike trains. *J Neurosci Methods* 201, 426–437.

Campbell, J.N., Meyer, R.A. (2006). Mechanisms of neuropathic pain. *Neuron* 52, 77–92.

Caporale, N., Dan, Y. (2008). Spike Timing-Dependent Plasticity: A Hebbian Learning Rule. *Annu Rev Neurosci* 31, 25–46.

Chaplan, S.R., Guo, H.-Q., Lee, D.H., Luo, L., Liu, C. et al. (2003). Neuronal hyperpolarization-activated pacemaker channels drive neuropathic pain. *J Neurosci* 23, 1169–1178.

Chen, S., Wang, J., Siegelbaum, S.A. (2001). Properties of hyperpolarization-activated pacemaker current defined by coassembly of HCN1 and HCN2 subunits and basal modulation by cyclic nucleotide. *J Gen Physiol* 117, 491–504.

Cho, K., Jang, J.H., Kim, S.-P., Lee, S.H., Chung, S.-C., Kim, I.Y., Jang, D.P., Jung, S.J. (2016). Analysis of Nociceptive Information Encoded in the Temporal Discharge Patterns of Cutaneous C-Fibers. *Front Comput Neurosci* 10, 118.

Devor, M. (2006). Sodium Channels and Mechanisms of Neuropathic Pain. *J Pain* 7, S3–S12.

Emery, E.C., Young, G.T., Berrocoso, E.M., Chen, L., McNaughton, P.A. (2011). HCN2 Ion Channels Play a Central Role in Inflammatory and Neuropathic Pain. *Science* 333, 1462–1466.

Fellous, J.-M., Tiesinga, P.H.E., Thomas, P.J., Sejnowski, T.J. (2004). Discovering spike patterns in neuronal responses. *J Neurosci* 24, 2989–3001.

Haroutounian, S., Nikolajsen, L., Bendtsen, T.F., Finnerup, N.B., Kristensen, A.D., Hasselstrøm, J.B., Jensen, T.S. (2014). Primary afferent input critical for maintaining spontaneous pain in peripheral neuropathy. *Pain* 155, 1272–1279.

Huerta, P.T., Lisman, J.E. (1995). Bidirectional synaptic plasticity induced by a single burst during cholinergic theta oscillation in CA1 *in vitro*. *Neuron* 15, 1053–1063.

Jiang, Y.-Q., Xing, G.-G., Wang, S.-L., Tu, H.-Y., Chi, Y.-N. et al. (2008). Axonal accumulation of hyperpolarization-activated cyclic nucleotide-gated cation channels contributes to mechanical allodynia after peripheral nerve injury in rat. *Pain* 137, 495–506.

Kitagawa, J., Takeda, M., Suzuki, I., Kadoi, J., Tsuboi, Y. et al. (2006). Mechanisms involved in modulation of trigeminal primary afferent activity in rats with peripheral mononeuropathy. *Eur J Neurosci* 24, 1976–1986.

Kleggetveit, I.P., Jørum, E. (2010). Large and Small Fiber Dysfunction in Peripheral Nerve Injuries With or Without Spontaneous Pain. *J Pain* 11, 1305–1310.

Kleggetveit, I.P., Namer, B., Schmidt, R., Helås, T., Rückel, M., Ørstavik, K., Schmelz, M., Jørum, E. (2012). High spontaneous activity of C-nociceptors in painful polyneuropathy. *Pain* 153, 2040–2047.

Koltzenburg, M., Handwerker, H.O. (1994). Differential ability of human cutaneous nociceptors to signal mechanical pain and to produce vasodilatation. *J Neurosci* 14, 1756–1765.

Lisman, J.E. (2011). Bursts as a unit of neural information: Making unreliable synapses reliable. *Trends Neurosci* 20, 38–43.

Luo, L., Chang, L., Brown, S.M., Ao, H., Lee, D.H., Higuera, E.S., Dubin, A.E., Chaplan, S.R. (2007). Role of peripheral hyperpolarization-activated cyclic nucleotide-modulated channel pacemaker channels in acute and chronic pain models in the rat. *Neuroscience* 144, 1477–1485.

Lüthi, A., McCormick, D.A. (1998). Periodicity of thalamic synchronized oscillations: The role of Ca2 + -mediated upregulation of Ih. *Neuron* 20, 553–563.

Mazo, I., Rivera-Arconada, I., Roza, C. (2013). Axotomy-induced changes in activity-dependent slowing in peripheral nerve fibres: Role of hyperpolarization-activated/HCN channel current. *Eur J Pain* 17, 1281–1290.

Meacham, K., Shepherd, A., Mohapatra, D.P., Haroutounian, S. (2017). Neuropathic Pain: Central vs. Peripheral Mechanisms. *Curr Pain Headache Rep* 21, 28.

Michaelis, M., Liu, X., Jänig, W. (2000). Axotomized and intact muscle afferents but no skin afferents develop ongoing discharges of dorsal root ganglion origin after peripheral nerve lesion. *J Neurosci* 20, 2742–2748.

Mochizuki, Y., Onaga, T., Shimazaki, H., Shimokawa, T., Tsubo, Y. et al. (2016). Similarity in Neuronal Firing Regimes across Mammalian Species. *J Neurosci* 36, 5736–5747.

Momin, A., Cadiou, H., Mason, A., McNaughton, P.A. (2008). Role of the hyperpolarization-activated current Ih in somatosensory neurons. *J Physiol* 586, 5911–5929.

Moosmang, S., Stieber, J., Zong, X., Biel, M., Hofmann, F., Ludwig, A. (2001). Cellular expression and functional characterization of four hyperpolarization-activated pacemaker channels in cardiac and neuronal tissues. *Eur J Biochem* 268, 1646–1652.

Orio, P., Madrid, R., Peña, La, De, E., Parra, A. et al. (2009). Characteristics and physiological role of hyperpolarization activated currents in mouse cold thermoreceptors. *J Physiol* 587, 1961–1976.

Orio, P., Parra, A., Madrid, R., Gonzalez, O., Belmonte, C., Viana, F. (2012). Role of Ih in the firing pattern of mammalian cold thermoreceptor endings. *J Neurophysiol* 108, 3009–3023.

Pitcher, G.M., Henry, J.L. (2008). Governing role of primary afferent drive in increased excitation of spinal nociceptive neurons in a model of sciatic neuropathy. *Exp Neurol* 214, 219–228.

Poo, M.-M., Bi, G.-Q. (2016). Synaptic modification by correlated activity: Hebb's Postulate Revisited. *Neuron* 92, 591–596.

Roza, C., Lopez-Garcia, J.A. (2008). Retigabine, the specific KCNQ channel opener, blocks ectopic discharges in axotomized sensory fibres. *Pain* 138, 537–545.

Roza, C., Mazo, I., Rivera-Arconada, I., Cisneros, E., Alayón, I., Lopez-García, J.A. (2016). Analysis of spontaneous activity of superficial dorsal horn neurons *in vitro*: Neuropathy-induced changes. *Pflugers Arch Eur J Physiol* 468, 2017–2030.

Sandkühler, J. (1996). Neurobiology of spinal nociception: New concepts. In *Towards the Neurobiology of Chronic Pain*. Carli, G., Zimmerman, M., eds. (Amsterdam: Elsevier) 207–224.

Serra, J., Bostock, H., Solà, R., Aleu, J., García, E., Cokic, B., Navarro, X., Quiles, C. (2012). Microneurographic identification of spontaneous activity in C-nociceptors in neuropathic pain states in humans and rats. *Pain* 153, 42–55.

Stieber, J., Stöckl, G., Herrmann, S., Hassfurth, B., Hofmann, F. (2005). Functional expression of the human HCN3 channel. *J Biol Chem* 280, 34635–34643.

Tal, M., Eliav, E. (1996). Abnormal discharge originates at the site of nerve injury in experimental constriction neuropathy (CCI) in the rat. *Pain* 64, 511–518.

Truini, A., Garcia-Larrea, L., Cruccu, G. (2013). Reappraising neuropathic pain in humans—how symptoms help disclose mechanisms. *Nat Rev Neurol* 9, 572–582.

Tsantoulas, C., Laínez, S., Wong, S., Mehta, I., Vilar, B., McNaughton, P.A. (2017). Hyperpolarization-activated cyclic nucleotide-gated 2 (HCN2) ion channels drive pain in mouse models of diabetic neuropathy. *Sci Transl Med* 9, eaam6072.

Vollert, J., Maier, C., Attal, N., Bennett, D.L.H., Bouhassira, D. et al. (2017). Stratifying patients with peripheral neuropathic pain based on sensory profiles. *Pain* 158, 1446–1455.

Wu, X., Liao, L., Liu, X., Luo, F., Yang, T., Li, C. (2014). Is ZD7288 a selective blocker of hyperpolarization-activated cyclic nucleotide-gated channel currents? *Channels* 6, 438–442.

Yao, H., Donnelly, D.F., Ma, C., LaMotte, R.H. (2003). Upregulation of the hyperpolarization-activated cation current after chronic compression of the dorsal root ganglion. *J Neurosci* 23, 2069–2074.

Young, G.T., Emery, E.C., Mooney, E.R., Tsantoulas, C., McNaughton, P.A. (2014). Inflammatory and neuropathic pain are rapidly suppressed by peripheral block of hyperpolarisation-activated cyclic nucleotide-gated ion channels. *Pain* 155, 1708–1719.

Zimmermann, K., Hein, A., Hager, U., Kaczmarek, J.S., Turnquist, B.P., Clapham, D.E., Reeh, P.W. (2009). Phenotyping sensory nerve endings *in vitro* in the mouse. *Nat Protoc* 4, 174–196.

Supporting Information

Additional Supporting Information may be found online in the supporting information tab for this article:

Figure S1. Effect of ZD7288 (10 μmol/L) on the percentage of spikes in trains (A), number of trains (B), intra-burst mean frequency (C) and inter-burst interval (D) from the 4 burst fibres tested. Note in A and B that two fibres stopped firing in bursts and only their basal activity is represented in C and D.

figureS1

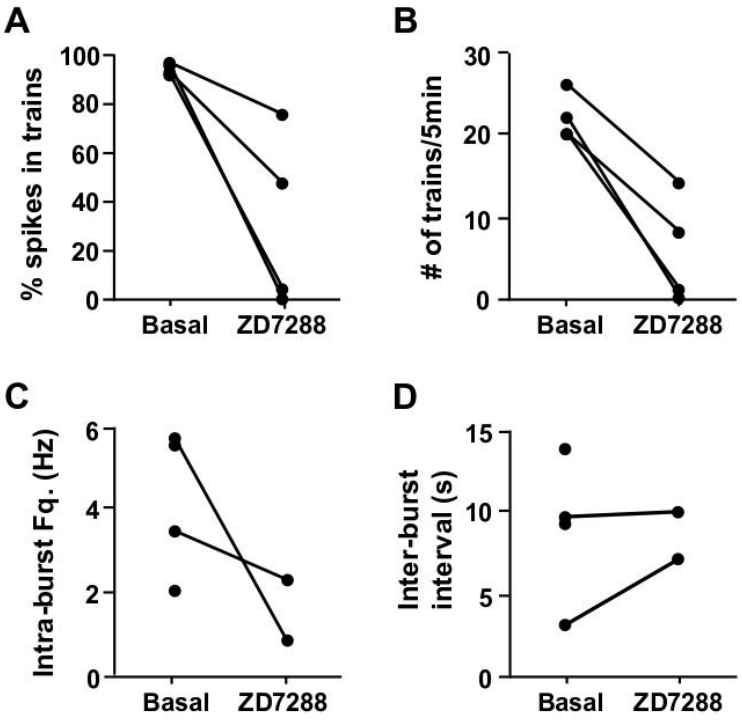

Supplementary figure 1. Effect of ZD7288 (10µM) on the percentage of spikes in trains (A), number of trains (B), intra-burst mean frequency (C) and inter-burst interval (D) from the 4 burst fibres tested. Note in A and B that two fibres stopped firing in bursts and only their basal activity is represented in C and D.

SECTION II: CHAPTER 2

Spontaneous activity in C-fibres after partial damage to the saphenous nerve in mice: Effects of retigabine

EJP
European Journal of Pain

ORIGINAL ARTICLE

Spontaneous activity in C-fibres after partial damage to the saphenous nerve in mice: Effects of retigabine

L. Bernal, J.A. Lopez-Garcia, C. Roza

Dpto. Biología de Sistemas, Edificio de Medicina Universidad de Alcalá, Alcalá de Henares, Madrid, Spain

Correspondence
Carolina Roza
E-mail: carolina.roza@uah.es

Funding sources
This study was supported by the Spanish Government (BFU 2012-37905) and Universidad de Alcalá (CCG2014/BIO-020).

Conflicts of interest
None declared.

Accepted for publication
17 December 2015

doi:10.1002/ejp.858

Abstract

Background: Spontaneous pain is the most devastating positive symptom in neuropathic pain patients. Recent data show a direct relationship between spontaneous discharges in C-fibres and spontaneous pain in neuropathic patients. Unfortunately, to date there is a lack of experimental animal models for drug testing.
Methods: We recorded afferent fibres from a new experimental model *in vitro*. The preparation contains a neuroma formed in a peripheral branch of the saphenous nerve together with the undamaged branches, which maintain intact terminals in a skin flap.
Results: Fibres with stable rates of ectopic spontaneous discharges were found among axotomized (5 A- and 18 C-fibres, mean discharge 0.48 ± 0.08 Hz) and 'putative intact' fibres (12 C-fibres, mean discharge 0.28 ± 0.08 Hz). A proportion (~9%) of axotomized fibres had mechanical receptive fields in the skin far beyond the site of injury. Collision experiments demonstrated that action potentials evoked from neuroma and skin travelled by the same fibre, indicating functional cross-talk between neuromatose and putative intact fibres. Retigabine, the specific Kv7 channel opener, depressed spontaneous discharges by 70% in 15/18 units tested. In contrast, responses to mechanical stimulation of the skin were unaltered by retigabine.
Conclusions: Partial damage to a peripheral nerve may increase the incidence of spontaneous activity in C-fibres. Retigabine reduced spontaneous activity but not stimulus-evoked activity, suggesting an important role for ion channels in the control of spontaneous pain and demonstrating the utility of the model for the testing of compounds in clinically relevant variables.
What does this study add?: Our *in vitro* experimental model of peripheral neuropathy allows for pharmacological characterization of spontaneously active fibres. Using this model, we show that retigabine inhibits aberrant spontaneous discharges without altering physiological responses in primary afferents.

1. Introduction

Chronic damage to a peripheral nerve commonly results in spontaneous pain and mechanical allodynia (Truini et al., 2013). These positive sensory symptoms are thought to be produced by ectopic activity originated at the site of injury and/or at the neuronal soma of both injured and their adjoining uninjured fibres. This persistent aberrant activity from the periphery triggers and maintains central sensitization (Campbell and Meyer, 2006). As most forms of neuropathic pain are refractory to analgesic treatments, there is an urgency to explore new targets for pain therapy.

Recent reports have established a direct relationship between the occurrence of spontaneous pain and the presence of C-fibres with spontaneous activity in neuropathic patients (Kleggetveit et al., 2012; Serra et al., 2012). Besides, most electrophysiological characterization of fibres recorded from different animal models includes a proportion of units with spontaneous discharges from both damaged and neighbouring intact branches (Wu et al., 2001; Gorodetskaya et al., 2003; Amir et al., 2005; Djouhri et al., 2006; Hulse et al., 2010). However, the low proportion of spontaneous C-fibres as well as their low and/or irregular firing frequency have precluded the possibility of performing proper pharmacological studies. For example, in our hands, different sets of data obtained from the saphenous nerve-end neuroma in mice generated small proportions of spontaneously active C-fibres (~5–10%) generally with firing rates below 0.01 Hz (Roza et al., 2003, 2006; Roza and Lopez-Garcia, 2008; Mazo et al., 2013).

Still, the peripheral input after nerve damage seems crucial in the maintenance of neuropathic pain. In experimental neuropathic rats, dorsal horn hyperexcitability was reversed by application of lidocaine along the peripheral damaged nerve (Pitcher and Henry, 2008). Consistently, a recent study showed that peripheral nerve block resulted in complete abolition of spontaneous pain in neuropathic patients (Haroutounian et al., 2014). The ectopic incorporation of Nav and Kv channels at the site of injury or at DRG cells has been proposed to underlie abnormal hyperexcitability following axonal damage (Campbell and Meyer, 2006; Devor, 2006); hence, targeting specifically molecules responsible for the hyperexcitability in the primary afferents may be a promising strategy for the treatment of neuropathic pain. For instance, the I_M current enhancer retigabine showed a strong inhibitory effect on ectopic discharges from neuromatose endings (Roza and Lopez-Garcia, 2008) and reduced excitability in unmyelinated fibres from human patients suffering from vascular disease or polyneuropathy (Lang et al., 2008).

In the clinic, partial nerve injuries are more frequently seen than complete denervation, and most of the knowledge about neuropathic pain arises from models of partial injury, particularly performed at the sciatic nerve (Toia et al., 2015). In this context, we have developed an *in vitro* model comprising of a skin-flap attached to the intact saphenous nerve except for one of its terminal branches, which had been previously sectioned to produce a neuroma. As motor integrity remains, bilateral manipulations can be performed in the same animal.

2. Materials and methods

2.1 Animals

Adult outbred CD1 female mice ($n = 27$, body weight 25–49 g) and breed at the University Animal House were used (the animals came from Harlan, Spain). European Union and State legislation for the regulation of animal experiments was followed. All experimental protocols were approved by the University of Alcala Committee on Animal Research and the Regional Government (project licence: CEI:2011/01/CEI01/20111209).

2.2 Creation of a neuroma by section of a branch of the saphenous nerve

Nerve-end neuromas were produced by total section of one of the peripheral branches of the saphenous nerve. The surgeries were performed under sterile precautions and deep anaesthesia with isoflurane (~3–3.5% in pure O_2). In the absence of withdrawal reflexes, a small incision was made in the skin at the level of the mid-thigh to expose the saphenous nerve. One of the peripheral branches was dissected free and tightly ligated with 8-0 nylon monofilament, and its distal end was inserted in a 1.5-mm-long polyethylene tube (0.44-mm internal diameter) to prevent lateral innervation of surrounding tissue. The neuromas were created in both paws, however, in ~5% of the paws, none of the peripheral branches could be clearly separated without damaging nearby branches and axotomy was discarded. The incision in the skin was closed with silk 5-0 sutures and Betadine® was topically applied. The total duration of the surgery was ~20 min per mouse, and the recovery from anaesthesia was completed in ~5 min. The animals were housed in groups of 4 and given access to food and water *ad libitum*. The animals were inspected periodically for infections, weight lost, abnormal behaviour or autotomy.

2.3 Surgical extraction and maintenance of the neuroma-skin flap

Experiments were performed 16–53 days after neuroma induction (mean 28 days). Mice were killed by cervical dislocation, and the saphenous nerve together with the neuroma and the skin flap were excised and pinned down to a Sylgard®-based

recording chamber, corium side up. The silicon tube around the neuroma was carefully removed and the neuroma was placed into a glass suction electrode which diameter was adjusted to produce minimal mechanical stimulation of the neuroma. At the recording chamber, preparations were superfused with oxygenated synthetic interstitial fluid (SIF, composition – in mmol/L: 108 NaCl, 3.48 KCl, 0.7 $MgSO_4$, 26 $NaHCO_3$, 1.7 NaH_2PO4, 1.53 $CaCl_2$, 9.6 sodium gluconate, 5.55 glucose and 7.6 sucrose) at a rate of 5 mL/min. Recording temperature was monitored and maintained at 32 ± 1 °C by means of a Peltier device (Warner Instruments, Hamden, CT, USA).

A second preparation from the same animal was stored in oxygenated SIF at 4 °C and used if required, in the same day. There were no detectable differences in results between the first and second preparations studied.

2.4 Electrophysiological procedures

The electrical activity from sensory fibres was recorded by means of suction microelectrodes obtained from glass pipettes (20–30 μm external tip diameter) filled with SIF as previously described (Roza and Lopez-Garcia, 2008). The microelectrode tip was carefully placed in contact to the proximal end of the nerve trunk under visual guidance by using a micromanipulator and after applying negative pressure, the electrode was left for a minimum of 1 min in order to record spontaneous activity (which was defined as a discharge rate >2 spikes/min). Experiments were run only when a single fibre was recorded or clearly differentiated from background discharges on the basis of spike amplitude and shape. Then, controlled electrical pulses of variable duration and intensity (0.2–0.5 ms pulse width, maximum strength 1 mA) were delivered to the neuroma via a suction electrode in order to identify the number of fibres present in the filament and to establish the origin of the spontaneously active units in the neuroma-skin flap preparation. Finally, the suction electrode was carefully removed from the neuroma, and mechanosensitivity was explored by gently touching the neuroma and the skin flap with a smooth-tipped glass rode (diameter = 0.5 mm). Repetitive insertion/extraction of the neuroma from the glass electrode had no effect on spontaneous activity, and this procedure confirmed that, if present, spontaneous activity was not an artefact induced by the stimulating electrode. If a mechanical response was evoked from the skin, electrical pulses of variable duration and intensity (0.5 ms, maximal strength up to 10 mA) were applied with a field electrode (a thin bipolar tungsten electrode; WPI, World Precision Instruments, Sarasota, FL, USA). Stimuli were applied at the most sensitive spot of the receptive field (RF) to identify the fibres on the basis of their conduction velocity (CV). No attempts were made to establish mechanical thresholds in order to avoid mechanical sensitization.

Thermal stimulation was tested only when the recorded fibres presented spontaneous activity. Increases up to ~45 °C (in ~60 s) or decreases down to 15 °C (in ~90 s) were applied by means of the Peltier device, affecting the whole preparation. Direct application on top of the neuroma of heated (~42 °C) or cooled (~15 °C) SIF by means of a syringe helped us to define whether the thermal responsiveness originated at the neuroma.

Electrical signals were recorded by means of a Dagan EX4-400 amplifier (Dagan, Minneapolis, MS, USA), digitized at 20 KHz (Power 1401, CED, Cambridge Electronic Design, Cambridge, UK), and stored for off-line analysis. Fibres were classified according to their conduction velocity into A-units (CV > 1 m/s) or C-units (CV < 0.8 m/s) on the basis of pilot experiments using whole nerve recordings, which showed a CV of 0.8 m/s for the C-fibre volley.

2.5 Collision techniques

Collision techniques were applied in a proportion of fibres with an electrical input from the neuroma that presented as well a mechanical RF in the peripheral skin. As the action potentials (AP) generated at one site propagates antidromically to other branches, when two AP initiation sites are activated simultaneously, collision occurs and only the AP from the shortest latency site reaches the recording electrode.

For this protocol, electrical suprathreshold pulses were simultaneously applied to the neuroma (site A, glass suction electrode) and the peripheral RF (site B, field electrode). When collision occurred only one spike was recorded; hence, the stimulation interval was increased until two spikes were recorded (collision avoided). This procedure was performed stimulating site A first (delay in B) and then site B first (delay in A). For one of the units, we used the marking technique: site A was stimulated electrically while site B was mechanically stimulated at a constant force with a gravity driven vFrey (Klein et al., 2006) positioned on a micromanipulator. When the electrically evoked impulse is slowed by a naturally

evoked burst of action potentials, the spikes belong to the same unit (Peng et al., 1999; Zimmermann et al., 2009).

2.6 Testing the effects of Retigabine on spontaneous activity and mechanical responses

The Kv7 channel opener N-2-amino-4-4-fluorobenzylamino phenylcarbamic acid ethylester (kindly donated by NeuroSearch, Ballerup, Denmark), retigabine, was dissolved in DMSO at 10^{-2} mol/L and stored in aliquots at −20 °C. Retigabine was diluted in SIF to their final concentration of 10 μmol/L immediately prior to use. The concentration was chosen according to previous reports to obtain near maximal effects while retaining a good selectivity (Passmore et al., 2003; Rivera-Arconada and Lopez-Garcia, 2006).

Retigabine was tested in a proportion of fibres with spontaneous activity. For those units with a mechanical RF in the skin, the effects of retigabine on mechano-responsiveness were also assessed. In order to reproduce mechanical stimulation in both intensity and location, gravity-driven vFrey probes were mounted on a micromanipulator and moved down until the probe tip (0.6 mm diameter) contacted perpendicularly the most sensitive spot of the RF. A probe, twice vFrey threshold, was applied for ~5 s three times at 5-min intervals to determine the stability of the response. Due to the tight experimental arrangements, it was not feasible to reach the RF of a few fibres in this way, and hence, mechanical responses were obtained by manual application of the vFrey or a glass rode. Then, retigabine was superfused for 30 min to the whole preparation, and the controlled mechanical stimuli were repeated at least twice in the presence of retigabine and again twice during wash-out. The magnitude of each mechanical response was quantified as the total number of spikes counted during the 5 s of the stimulation. Mean values of the repetitive responses were taken for statistical analysis and representation.

To establish changes in spontaneous activity, the mean firing frequency was measured in periods of 5 min. The baseline level (5 min prior to retigabine superfusion) was compared with the firing frequency just before washing out and ~30 min after that. For analysis and representation purposes, the maximum effect of retigabine within 30 min of perfusion and the maximum recovery within 30 min of drug wash out were taken.

2.7 Data analysis

Waveforms were analysed off-line with Spike 2 software (CED, Cambridge Electronic Design). Autocorrelograms were performed for each of the recorded fibres to assess the goodness of the spike sorting. Statistical analyses were performed in Graphpad Prism 6.0 (GraphPad Software, San Diego, CA, USA) on the raw data using Mann–Whitney, Wilcoxon Matched and one-way ANOVA, following by Dunn's *post hoc* test as appropriate. The level of statistical significance was set at $p < 0.05$. Values are quoted as mean ± standard error of the mean (SEM).

3. Results

A total of 27 mice were used in this study and none of the animals showed signs of autotomy, infection or unusual behaviour. A total of 100 fibres were fully characterized and studied in three sets of experiments as follows: 75, 5 and 16 units were used for Experiment #1, #2 and #3, respectively. Data obtained from the remaining 4 units were used for both Experiments #2 and #3.

3.1 Incidence of spontaneous activity in axotomized fibres

Experiment #1 aimed at evaluating the incidence of spontaneous activity in axotomized fibres after partial nerve damage of the saphenous nerve; hence, only fibres with electrical or mechanical inputs from the neuroma were fully characterized. Occasionally spontaneous fibres without inputs from the neuroma were also observed during this characterization, but no attempt was made to further evaluate those units as our focus of interest was the axotomized units.

We recorded a total of 75 units classified according to their CV as C- (0.33 ± 0.01 m/s, range: 0.12–0.64, $n = 60$) or A-fibres (CV: 2.60 ± 0.78 m/s, range 1.12–9.17 m/s, $n = 12$). The remaining 3 units were not electrically identified, but responded to mechanical stimulation of the neuroma.

Spontaneous activity at baseline temperature was present in 14/60 C-fibres (23%) and their properties are summarized in Table 1. Most of these units showed irregular ongoing discharges (mean frequency 0.35 ± 0.10 Hz; range, 0.1–1.23 Hz; $n = 11$). Fig. 1 shows an original example. The remaining three fibres fired in bursts (mean frequency 0.82 ± 0.14 Hz; range 0.63–1.09 Hz and mean intraburst frequency 1.78 ± 0.37 Hz), which contained between 8 and 40 spikes. Only one of the A-fibres (~8%) fired spontaneously at 2.5 Hz.

Thermal responsiveness was only evaluated in fibres with spontaneous activity and was present in 7/15 spontaneous fibres. Five of the units were polymodal nociceptors, 3 of which showed putative burst discharges at 32 °C (an original example is shown in Fig. 2). Moreover, one of the C-fibres was a heat nociceptor, and the remaining unit was the spontaneous A-fibre that behaved as a warm receptor, increasing their firing rate upon heating (between 35 and 40 °C) and silencing upon cooling below 20 °C. According to previous data from fibres innervating normal skin (Zimmermann et al., 2009), spontaneous activity in the units recorded here can be regarded as abnormal.

The presence of ectopic mechanosensitivity was assessed in all of the units. Twenty-six units (20 C-, 3 A-fibres and the 3 nonclassified units) responded to mechanical stimulation of the neuroma. A further group of 7 C-fibres (5 of which presented spontaneous discharges) apparently responded to mechanical stimulation of skin areas far apart from the neuroma, thus AP shapes evoked from both sites were conspicuously similar.

3.2 Axotomized fibres stimulated from the skin

Experiment #2 was designed to explore our preliminary observations regarding fibres activated from the neuroma as well as from the skin far beyond the site of injury. Hence, we searched for axotomized fibres with an additional input from the skin and used collision techniques to confirm or discard whether both inputs travelled within the same fibre (Peng et al., 1999).

We examined a total of 9 units (8-A and 1 C-fibre), all but one had mechanical RFs in the skin, the remaining unit was a mechano-insensitive axotomized A-fibre with a response to electrical stimulation of the skin. For 8 units, simultaneous electrical stimulation of the neuroma (site A) and the skin (site B) produced only one spike (evoked from the neuroma, according to its latency), indicating a positive collision and hence a functional interconnection. Increasing the interval between stimuli presentation eventually led to the recording of a second action potential (Supporting Information Fig. S1A for a representative example). We observed that the minimum interval to avoid collision was larger than the estimated according to CV and distance between A and B (Supporting Information Table S1). For the remaining unit, an Aδ D-hair, we used the marking technique. As this fibre type is extremely

Table 1 Properties of axotomized fibres with spontaneous activity.

Fibre type	C (n = 14)	A (n = 1)
CV (m/s)	0.32 ± 0.03	7.33
Without response to natural stimuli	4[b]	
With responses to natural stimulation of the neuroma		
Mechanical	4[b]	
Polymodal (MH)	3 (42–45 °C)[1a–2b]	
Polymodal (MC)	1 (25 °C)[a]	
Polymodal (MHC)	1 (21 °C & 41 °C)[a]	
Heat	1 (40 °C)[b]	1 (A warm; 35 °C)[b]

MH, mechano-heat; MC, mechano-cold; MHC, mechano-heat-cold.
Numbers in parenthesis refers to thermal thresholds.
[a]Spontaneous activity in burst.
[b]Irregular ongoing spontaneous activity.

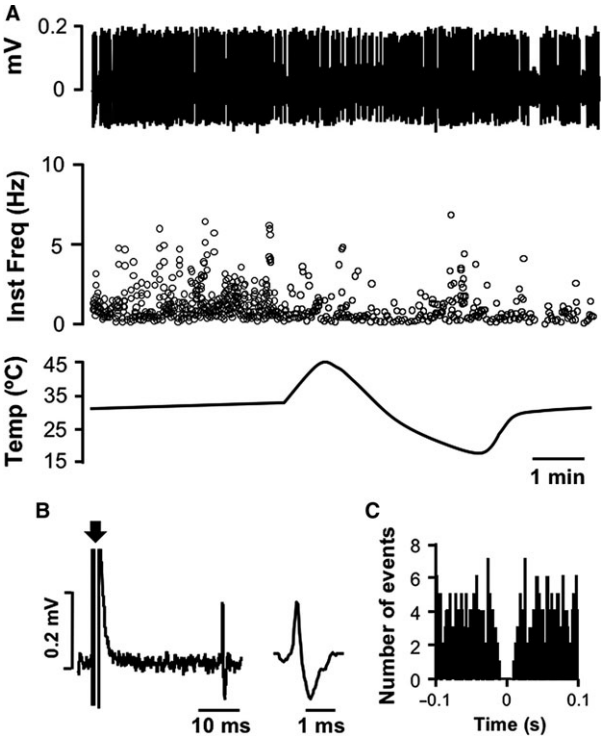

Figure 1 Representative example of an axotomized C-fibre with ongoing spontaneous activity (mean frequency, 0.78 Hz). (A) The upper panel shows the original recording which is represented as instantaneous frequency in the middle panel. The lower panel in (a) shows the simultaneous temperature change in the recording chamber. Note the absence of a clear response to heating and cooling. (B) Response to electrical stimulation of the neuroma indicates a latency of 32 ms (as the recording distance was 14 mm, the calculated CV of the unit was 0.4 ms). The inset shows the spike shape averaged from the spontaneous activity. The arrow indicates stimulus artefact. (C) The autocorrelogram histogram of the recorded unit shows the goodness of spike sorting.

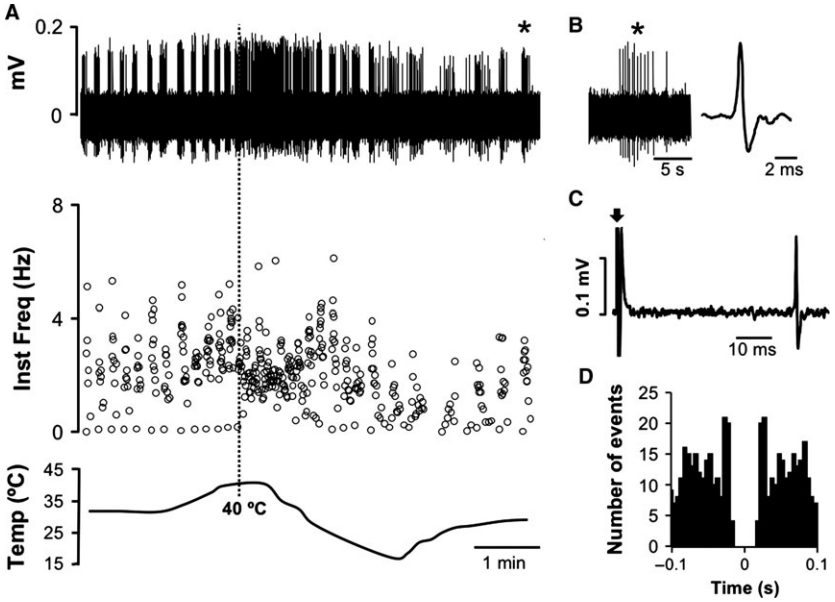

Figure 2 Representative example of an axotomized C-polymodal nociceptor with spontaneous activity in bursts (intraburst frequency, 2.29 Hz). (A) The upper panel shows the original recording which is represented as instantaneous frequency in the middle panel. The bottom graph shows simultaneous recording temperature. The heat threshold of the unit was ~40 °C. In (B), an expanded burst (*) and the spike shape averaged from the spontaneous activity is shown. (C) Response to electrical stimulation of the neuroma indicates a latency of 36.5 ms (as the recording distance was 11 mm, the calculated CV of the unit was 0.30 m/s). (D) The autocorrelogram of the recorded unit shows the goodness of spike sorting.

sensitivity to mechanical stimulation (Lechner and Lewin, 2013), the placement of the field electrode over the skin produced mechanical responses that contaminated responses to the electrical stimulus. In this case, mechanical stimulation of the skin produced a delay in the latency of the action potential induced by electrical stimulation of the neuroma (~4 ms). The RF distribution of the examined fibres (except for the Aδ D-Hair unit, as 1 mN vFrey, suprathreshold for these types of units, evoked a response regardless the stimulated spot along the whole skin) is shown in Supporting Information Fig. S1B.

Only in one case in which the spike shape of evoked responses from skin and neuroma was very similar, simultaneous stimulation of the neuroma and the skin evoked two spikes, indicating that responses came from two disconnected fibres (as no further data were obtained from these two units, they do not add to the total number of examined units).

According to the results obtained here, we infer that the 7 C-axotomized fibres described in 3.1 which were evoked by mechanical stimulation of the skin indicate the presence of a functional cross-talk between axotomized and intact fibres in ~9% of the axotomized units.

3.3 Pharmacological studies on spontaneously active units

3.3.1 Origin of the spontaneous fibres tested

For Experiment #3, we searched exclusively for fibres with spontaneous activity to test the feasibility of pharmacological experiments. We recruited 4 C- (mean CV 0.52 ± 0.1 m/s) and 4 A-fibres (mean CV 3.46 ± 1.1 m/s) with electrical inputs from the neuroma (axotomized units). Four of them (1 C- and 3 A-fibres) also presented a mechanical RF in the skin (verified by collision experiments), but did not respond to mechanical stimulation of the neuroma. Seven of the fibres showed ongoing discharges (mean frequency 0.43 ± 0.18 Hz) and a remaining C-fibre fired in bursts (mean frequency 0.52 Hz). Thermal responses were not tested.

In addition, we recorded from 12 spontaneously active C-fibres which were not evoked by stimulation of the neuroma but presented a mechanical RF in the skin. Ten of the units showed ongoing discharges (mean frequency 0.25 ± 0.09 Hz) and the remaining two units fired in bursts (mean frequency 0.48 ± 0.26 Hz, and mean intra-burst frequency 2.1 ± 0.4 Hz). Only three of these fibres responded to thermal stimulation (1 C-MH, 42 °C threshold

and 2 C-MC, with 17 and 20 °C thresholds). According to what has been previously described for fibres innervating normal skin (Zimmermann et al., 2009), spontaneous activity in these units is aberrant. These units were termed 'putative intacts'.

3.3.2 Effects of retigabine on spontaneous and evoked activity

The effects of bath application of retigabine (10 μmol/L) were tested in 6 axotomized (4C- and 2A-fibres) and 12 putative intact C-units. Retigabine reduced spontaneous discharges by ~70% in all atomized fibres and most of the putative intact fibres (9/12; Fig. 3 for an original example). Although retigabine appeared to have a stronger effect on axotomized fibres than on putative intacts (~80%, from 0.35 ± 0.11 Hz to 0.12 ± 0.07 Hz vs. ~63%, from 0.21 ± 0.07 to 0.08 ± 0.03 Hz, respectively), this difference did not reach statistical significance (Fig. 4A).

In six of those units (3 putative intact and 3 axotomized), the effects of retigabine on their mechanical responses were quantitatively evaluated (vFrey hair range 4–32 mN). For these 6 units, retigabine reduced significantly their spontaneous discharges but had no effect in their mechanical responses ($p < 0.05$, and $p = 0.25$, respectively, one-way-ANOVA; Fig. 3 for an original example and Fig. 4B). Similar results were obtained in five other units (3 putative intact and 2 axotomized) upon qualitative exploration of their mechanosensitivity with a glass rode.

4. Discussion

Here, we report data from a new *in vitro* model of a terminal branch axotomy which contains neuromatose endings together with fibres in neighbouring branches that have functional receptors in the skin flap.

Our model allows for stimulation of the neuroma as well as a putative intact skin flap while recording from a common saphenous nerve. Using this model, we found that ~23% of the axotomized C-fibres recorded showed ectopic spontaneous discharges. In addition, we also recorded a group of spontaneous fibres with a receptor field in the skin flap. Both injured and intact fibres presented stable rates of spontaneous activity and both showed a mean dis-

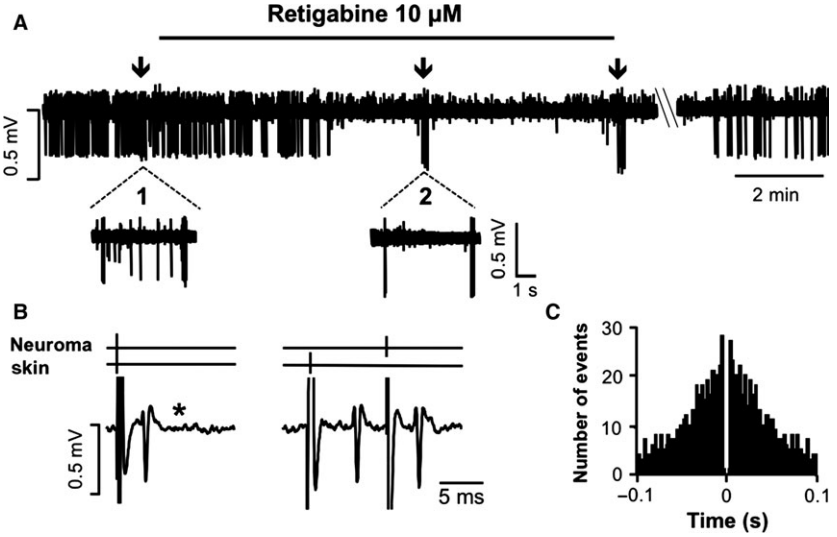

Figure 3 (A) Original recording from an axotomized A-fibre showing spontaneous ongoing activity and presenting a mechanical receptive field in the skin (1 mN threshold). Note that the spontaneous discharge (0.4 Hz) was completely abolished in the presence of retigabine. The arrows indicate the application of controlled mechanical stimuli to the RF in the skin (4 mN vFrey), and the insets in 1 and 2 show mechanical responses in detail before (1) and during perfusion of retigabine (2). The fibre had the typical pattern of a rapidly adapting mechanoreceptor responding with a burst of ~10 spikes upon application and removal of the vFrey (~75 and ~120 Hz, respectively, in three consecutive control responses and two more under retigabine). We believe that the few spikes fired at ~0.6 Hz within the time of application of the stimulus in 1 are a continuation of the ongoing activity and not evoked by the stimulus. Bars \\ in (A) indicate a 45-min interval. (B) Simultaneous electrical stimulation from the neuroma and the skin precluded the action potential from the skin. Collision was avoided with a 9-ms delay between stimuli. The CVs calculated from the neuroma and skin were 5 and 4.38 ms, respectively. (C) The autocorrelogram shows the goodness of spike sorting. The total recording time for this unit was 165 min. The mechanical RF of the unit is depicted in Supporting Information Fig. S1 (marked with *).

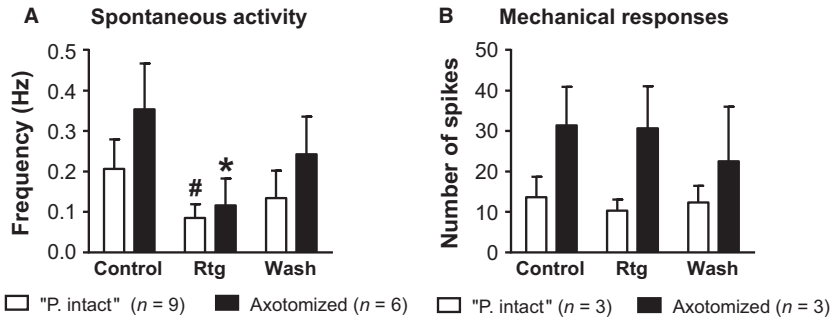

Figure 4 (A) Retigabine (10 μmol/L) significantly inhibited the spontaneous activity in 15/18 fibres tested (* and #, $p < 0.001$, one-way ANOVA). Graph in (B) shows the lack of effect of retigabine on mechanical responses of the skin flap.

charge rate of ~0.38 Hz, hence allowing for pharmacological characterization. Retigabine, the specific Kv7 opener, significantly depressed ectopic spontaneous discharges but preserved mechanical responses in the peripheral skin when present.

This study shows that the existence of mechanical responses in intact skin after peripheral nerve damage is not sufficient criteria to discriminate intact from axotomized fibres.

4.1 Increased incidence of spontaneous activity after partial damage of the saphenous nerve

An interesting issue arising from our data is the nature of the mechanisms underlying the increase of spontaneous activity in C-fibres (~23%) as compared with our model of total axotomy (≤10%) (Roza et al., 2003, 2006; Roza and Lopez-Garcia, 2008; Mazo et al., 2013). Following axotomy, neuronal phenotypes switch from a 'transmitting' to a 'regenerative state' triggering the activation of cellular components involved in neuronal survival and axonal regeneration. The regenerative process is mediated by trophic factors, such as NGF which is locally released at the site of injury (Heumann et al., 1987). Interestingly, NGF is involved in the induction and maintenance of chronic pain. For example, NGF induces C-fibre firing and sensitization in animal models (Moalem et al., 2005; Hirth et al., 2013) and hypersensitivity to mechanical stimuli when injected in humans (Deising et al., 2012; Rukwied et al., 2013). In addition, further insult on NGF-sensitized skin areas was able to provoke mild spontaneous pain (Rukwied et al., 2013). NGF influence on axonal excitability rely in its modulation of Nav and Kv channels (Zhang et al., 2002), including Kv7 (Jia et al., 2008). Following axotomy, NGF and other sensitizing substances may produce similar effects. In fact, the lack of tachyphylaxis to chemical stimulation described for axotomized fibres (Roza and Lopez-Garcia, 2008) could be taken as an indicator for nociceptor hyperexcitability. Supporting this interpretation, the levels of NFG immunoreactive fibres were larger in painful neuromas as compared with normal nerves or nonpainful relocated neuromas (Atherton et al., 2006).

Adequate nerve regeneration requires a permissive growth environment, including the sustained presence nerve growth factors and mechanical cues which are more likely found in partial nerve damage (Chen et al., 2007; Allodi et al., 2012).

4.2 Axotomized afferents with peripheral inputs

Ramón y Cajal (DeFelipe and Jones, 1991) already described sprouting from severed axons and/or their demyelinated nodes. Since then, several experimental studies in animal models and humans have shown that sprouting takes place in both intact and severed axons (Bajrovic et al., 2002; Rajan et al., 2003; Kovacic et al., 2007; Cobianchi et al., 2014), and this could explain our finding of units with dual inputs from the skin and the neuroma. If the sprout from an intact unit enters the neuroma, the CV of that branch should be equal or slower than the parental axon, which was not the case. The alternative sprouting from an axotomized unit along the intact neural tube towards the periphery seems more agreeable with our results regarding conduction velocity values. Besides, the rate of neural growth in mice is ~4 mm/day (Griffin et al., 2010) and most of the RF in these fibres run parallel to the peripheral nerve branches. In our collision experiments, the intervals needed to record two spikes were, by far, larger than the expected ones. As previously described in cutaneous nociceptors, antidromic propagation of an AP to their sister branches leads to a

decrease in the excitability of the terminals, which become refractory for even tens of milliseconds (Peng et al., 1999). But for some of our fibres, the refractory periods varied drastically depending on which site was stimulated first, indicating a differential channel distribution at each initiation site.

Alternatively, axotomized-induced demyelination could also favour electrical coupling between pairs of fibres at the axonal level, as suggested in early reports (Lisney and Pover, 1983; Blumberg and Janig, 1984; Meyer et al., 1985; Amir and Devor, 1992). The electrical coupling implies that the stimulation at the peripheral skin is able to cross-excite neighbouring fibres innervating the neuroma and vice versa. From our data, we cannot discern whether the responsiveness in the skin arises from a regenerated sprout or electrical coupling. Although a detailed evaluation of these phenomena was beyond the scope of our study, our *in vitro* model allows for a precise characterization in future studies.

4.3 Possible relation with sensory symptoms of pain in humans

In view of the described fibre cross-talk, the distinction between intact and injured units cannot only rely on the presence of a peripheral receptive field, at least when the partial damage is performed peripherally. Spontaneously active C-fibres were encountered among axotomized and 'putative intact' units in a similar proportion and with similar patterns and rate of discharge, hence both are likely contributors for positive symptoms of neuropathic pain. A constant discharge from a primary afferent, whether arising from the neuroma or the neighbouring intact branches, might well influence nociceptor encoding and central excitability; noteworthy, persistent peripheral input is a key factor for the maintenance of spontaneous pain in human patients (Haroutounian et al., 2014).

In addition, extraterritorial spread of sensory phenomena has been documented in patients and it is believed to depend on central sensitization (Tal and Bennett, 1994; Zanette et al., 2010). However, our data support the likelihood of a peripheral mechanism, which has been little explored to date.

4.4 M-current regulates ectopic spontaneous discharges in C-fibres

Retigabine acts as a potent opener of all Kv7 subunits expressed in neurons with good specificity when used at low concentration (Rundfeldt, 1997). Retigabine induces spike frequency adaptation and stabilizes the resting membrane potential in a number of neuronal types involved in pain transmission. It has been proven as an effective analgesic in different models of neuropathic pain; see Rivera-Arconada et al. (2009) for a review. Using electrophysiological techniques, it has been shown that retigabine blocks ectopic mechanical discharges from axotomized C-fibres from mice (Roza and Lopez-Garcia, 2008) and reduces excitability in unmyelinated fibres from human patients suffering from vascular disease or polyneuropathy (Lang et al., 2008). In our experiments, we have demonstrated that retigabine was able to reduce spontaneous discharges originating from both axotomized and putative intact units; hence, reinforcing the hypothesis that I_M modulation may be a peripheral target for the treatment of neuropathic pain.

However, responses to mechanical stimulation of the skin were preserved in the presence of retigabine. As previously described for lidocaine (Kirillova et al., 2011), retigabine also exhibits a differential effect on spontaneous activity and mechanical responsiveness, at least when evoked at distal sites from the damage. We should expect a greater action of retigabine on activity originating from sites in which Kv7 are prone to accumulate like axotimized endings (Roza et al., 2011; Cisneros et al., 2015). In contrast, intact receptor endings do not accumulate Kv7 channels and are not affected by retigabine. Fibres with a receptive field in the skin may develop spontaneous activity due to electrical coupling at demyelinated zones with axotomized fibre. Alternatively, axotomized fibres may grow and develop normal receptor endings while keeping spontaneous ectopic activity. Data from the collision experiments suggest differences in channel distribution between the neuroma and the terminals in the skin flap.

Our experiments suggest that by modulating I_M current, we could dampen specifically the aberrant discharge and still maintain 'normal' responsiveness. These observations are consistent with previous work from our laboratory (Roza and Lopez-Garcia, 2008).

5. Conclusions

Partial damage of a peripheral nerve increases the incidence of C-fibres with stable and relatively high rates of spontaneous activity in axotomized and intact units, allowing for pharmacological characterization. The enriched milieu in growth factors and mechanical guidance present at the site of injury might well favour fibre sprouting, functional

cross-talk and the development of spontaneous activity in both damaged and intact afferents. The effects of retigabine, which specifically inhibited ectopic spontaneous discharges, reinforce I_M modulation as a peripheral target to treat neuropathic pain.

Author contributions

L.B. carried out electrophysiological recordings and data analysis and contributed in writing of the manuscript. J.A.L. contributed with data interpretation and critical revision of the manuscript. C.R. carried out conception and design of the experiments, drafted and critically revised the manuscript and participated in the electrophysiological recordings, analysis and interpretation of data. All authors read and approved the final manuscript.

References

Allodi, I., Udina, E., Navarro, X. (2012). Specificity of peripheral nerve regeneration: Interactions at the axon level. *Prog Neurobiol* 98, 16–37.

Amir, R., Devor, M. (1992). Axonal cross-excitation in nerve-end neuromas: Comparison of A- and C-fibers. *J Neurophysiol* 68, 1160–1166.

Amir, R., Kocsis, J.D., Devor, M. (2005). Multiple interacting sites of ectopic spike electrogenesis in primary sensory neurons. *J Neurosci* 25, 2576–2585.

Atherton, D.D., Taherzadeh, O., Facer, P., Elliot, D., Anand, P. (2006). The potential role of nerve growth factor (NGF) in painful neuromas and the mechanism of pain relief by their relocation to muscle. *J Hand Surg Br* 31, 652–656.

Bajrovic, F., Kovacic, U., Pavcnik, M., Sketelj, J. (2002). Interneuronal signalling is involved in induction of collateral sprouting of nociceptive axons. *Neuroscience* 111, 587–596.

Blumberg, H., Janig, W. (1984). Discharge pattern of afferent fibers from a neuroma. *Pain* 20, 335–353.

Campbell, J.N., Meyer, R.A. (2006). Mechanisms of neuropathic pain. *Neuron* 52, 77–92.

Chen, Z.L., Yu, W.M., Strickland, S. (2007). Peripheral regeneration. *Annu Rev Neurosci* 30, 209–233.

Cisneros, E., Roza, C., Jackson, N., Lopez-Garcia, J.A. (2015). A new regulatory mechanism for Kv7. 2 protein during neuropathy: Enhanced transport from the soma to the axonal terminals of injured sensory neurons. *Front Cell Neurosci* 9, 470.

Cobianchi, S., de Cruz, J., Navarro, X. (2014). Assessment of sensory thresholds and nociceptive fiber growth after sciatic nerve injury reveals the differential contribution of collateral reinnervation and nerve regeneration to neuropathic pain. *Exp Neurol* 255C, 1–11.

DeFelipe, J., Jones, E.G. (1991). Part II First Section: Traumatic Degeneration and Regeneration of the Nerves. In *Cajal's Degeneration & Regeneration of the Nervous System*, J. DeFelipe, E. Jones, eds. (New York: Oxford University Press) pp. 66–304.

Deising, S., Weinkauf, B., Blunk, J., Obreja, O., Schmelz, M., Rukwied, R. (2012). NGF-evoked sensitization of muscle fascia nociceptors in humans. *Pain* 153, 1673–1679.

Devor, M. (2006). Sodium channels and mechanisms of neuropathic pain. *J Pain* 7, S3–S12.

Djouhri, L., Koutsikou, S., Fang, X., McMullan, S., Lawson, S.N. (2006). Spontaneous pain, both neuropathic and inflammatory, is related to frequency of spontaneous firing in intact C-fiber nociceptors. *J Neurosci* 26, 1281–1292.

Gorodetskaya, N., Constantin, C., Janig, W. (2003). Ectopic activity in cutaneous regenerating afferent nerve fibers following nerve lesion in the rat. *Eur J Neurosci* 18, 2487–2497.

Griffin, J.W., Pan, B., Polley, M.A., Hoffman, P.N., Farah, M.H. (2010). Measuring nerve regeneration in the mouse. *Exp Neurol* 223, 60–71.

Haroutounian, S., Nikolajsen, L., Bendtsen, T.F., Finnerup, N.B., Kristensen, A.D., Hasselstrom, J.B., Jensen, T.S. (2014). Primary afferent input critical for maintaining spontaneous pain in peripheral neuropathy. *Pain* 155, 1272–1279.

Heumann, R., Korsching, S., Bandtlow, C., Thoenen, H. (1987). Changes of nerve growth factor synthesis in nonneuronal cells in response to sciatic nerve transection. *J Cell Biol* 104, 1623–1631.

Hirth, M., Rukwied, R., Gromann, A., Turnquist, B., Weinkauf, B., Francke, K., Albrecht, P., Rice, F., Hagglof, B., Ringkamp, M., Engelhardt, M., Schultz, C., Schmelz, M., Obreja, O. (2013). Nerve growth factor induces sensitization of nociceptors without evidence for increased intraepidermal nerve fiber density. *Pain* 154, 2500–2511.

Hulse, R., Wynick, D., Donaldson, L.F. (2010). Intact cutaneous C fibre afferent properties in mechanical and cold neuropathic allodynia. *Eur J Pain* 14, 565.e1–565.e10.

Jia, Z., Bei, J., Rodat-Despoix, L., Liu, B., Jia, Q., Delmas, P., Zhang, H. (2008). NGF inhibits M/KCNQ currents and selectively alters neuronal excitability in subsets of sympathetic neurons depending on their M/KCNQ current background. *J Gen Physiol* 131, 575–587.

Kirillova, I., Teliban, A., Gorodetskaya, N., Grossmann, L., Bartsch, F., Rausch, V.H., Struck, M., Tode, J., Baron, R., Janig, W. (2011). Effect of local and intravenous lidocaine on ongoing activity in injured afferent nerve fibers. *Pain* 152, 1562–1571.

Kleggetveit, I.P., Namer, B., Schmidt, R., Helas, T., Ruckel, M., Orstavik, K., Schmelz, M., Jorum, E. (2012). High spontaneous activity of C-nociceptors in painful polyneuropathy. *Pain* 153, 2040–2047.

Klein, T., Magerl, W., Treede, R.D. (2006). Perceptual correlate of nociceptive long-term potentiation (LTP) in humans shares the time course of early-LTP. *J Neurophysiol* 96, 3551–3555.

Kovacic, U., Tomsic, M., Sketelj, J., Bajrovic, F.F. (2007). Collateral sprouting of sensory axons after end-to-side nerve coaptation–a longitudinal study in the rat. *Exp Neurol* 203, 358–369.

Lang, P.M., Fleckenstein, J., Passmore, G.M., Brown, D.A., Grafe, P. (2008). Retigabine reduces the excitability of unmyelinated peripheral human axons. *Neuropharmacology* 54, 1271–1278.

Lechner, S.G., Lewin, G.R. (2013). Hairy sensation. *Physiology (Bethesda)* 28, 142–150.

Lisney, S.J., Pover, C.M. (1983). Coupling between fibres involved in sensory nerve neuromata in cats. *J Neurol Sci* 59, 255–264.

Mazo, I., Rivera-Arconada, I., Roza, C. (2013). Axotomy-induced changes in activity-dependent slowing in peripheral nerve fibres: Role of hyperpolarization-activated/HCN channel current. *Eur J Pain* 17, 1281–1290.

Meyer, R.A., Raja, S.N., Campbell, J.N., Mackinnon, S.E., Dellon, A.L. (1985). Neural activity originating from a neuroma in the baboon. *Brain Res* 325, 255–260.

Moalem, G., Grafe, P., Tracey, D.J. (2005). Chemical mediators enhance the excitability of unmyelinated sensory axons in normal and injured peripheral nerve of the rat. *Neuroscience* 134, 1399–1411.

Passmore, G.M., Selyanko, A.A., Mistry, M., Al Qatari, M., Marsh, S.J., Matthews, E.A., Dickenson, A.H., Brown, T.A., Burbidge, S.A., Main, M., Brown, D.A. (2003). KCNQ/M currents in sensory neurons: Significance for pain therapy. *J Neurosci* 23, 7227–7236.

Peng, Y.B., Ringkamp, M., Campbell, J.N., Meyer, R.A. (1999). Electrophysiological assessment of the cutaneous arborization of Adelta-fiber nociceptors. *J Neurophysiol* 82, 1164–1177.

Pitcher, G.M., Henry, J.L. (2008). Governing role of primary afferent drive in increased excitation of spinal nociceptive neurons in a model of sciatic neuropathy. *Exp Neurol* 214, 219–228.

Rajan, B., Polydefkis, M., Hauer, P., Griffin, J.W., McArthur, J.C. (2003). Epidermal reinnervation after intracutaneous axotomy in man. *J Comp Neurol* 457, 24–36.

Rivera-Arconada, I., Lopez-Garcia, J.A. (2006). Retigabine-induced population primary afferent hyperpolarisation in vitro. *Neuropharmacology* 51, 756–763.

Rivera-Arconada, I., Roza, C., Lopez-Garcia, J.A. (2009). Enhancing m currents: A way out for neuropathic pain? *Front Mol Neurosci* 2, 10.
Roza, C., Lopez-Garcia, J.A. (2008). Retigabine, the specific KCNQ channel opener, blocks ectopic discharges in axotomized sensory fibres. *Pain* 138, 537–545.
Roza, C., Laird, J.M., Souslova, V., Wood, J.N., Cervero, F. (2003). The tetrodotoxin-resistant Na+ channel Nav1.8 is essential for the expression of spontaneous activity in damaged sensory axons of mice. *J Physiol* 550, 921–926.
Roza, C., Belmonte, C., Viana, F. (2006). Cold sensitivity in axotomized fibers of experimental neuromas in mice. *Pain* 120, 24–35.
Roza, C., Castillejo, S., Lopez-Garcia, J.A. (2011). Accumulation of Kv7.2 channels in putative ectopic transduction zones of mice nerve-end neuromas. *Mol Pain* 7, 58.
Rukwied, R., Weinkauf, B., Main, M., Obreja, O., Schmelz, M. (2013). Inflammation meets sensitization – An explanation for spontaneous nociceptor activity? *Pain* 154, 2707–2714.
Rundfeldt, C. (1997). The new anticonvulsant retigabine (D-23129) acts as an opener of K+ channels in neuronal cells. *Eur J Pharmacol* 336, 243–249.
Serra, J., Bostock, H., Sola, R., Aleu, J., Garcia, E., Cokic, B., Navarro, X., Quiles, C. (2012). Microneurographic identification of spontaneous activity in C-nociceptors in neuropathic pain states in humans and rats. *Pain* 153, 42–55.
Tal, M., Bennett, G.J. (1994). Extra-territorial pain in rats with a peripheral mononeuropathy: Mechano-hyperalgesia and mechano-allodynia in the territory of an uninjured nerve. *Pain* 57, 375–382.
Toia, F., Giesen, T., Giovanoli, P., Calcagni, M. (2015). A systematic review of animal models for experimental neuroma. *J Plast Reconstr Aesthet Surg* 68, 1447–1463.
Truini, A., Garcia-Larrea, L., Cruccu, G. (2013). Reappraising neuropathic pain in humans–how symptoms help disclose mechanisms. *Nat Rev Neurol* 9, 572–582.
Wu, G., Ringkamp, M., Hartke, T.V., Murinson, B.B., Campbell, J.N., Griffin, J.W., Meyer, R.A. (2001). Early onset of spontaneous activity in uninjured C-fiber nociceptors after injury to neighboring nerve fibers. *J Neurosci* 21, RC140.
Zanette, G., Cacciatori, C., Tamburin, S. (2010). Central sensitization in carpal tunnel syndrome with extraterritorial spread of sensory symptoms. *Pain* 148, 227–236.
Zhang, Y.H., Vasko, M.R., Nicol, G.D. (2002). Ceramide, a putative second messenger for nerve growth factor, modulates the TTX-resistant Na(+) current and delayed rectifier K(+) current in rat sensory neurons. *J Physiol* 544, 385–402.
Zimmermann, K., Hein, A., Hager, U., Kaczmarek, J.S., Turnquist, B.P., Clapham, D.E., Reeh, P.W. (2009). Phenotyping sensory nerve endings in vitro in the mouse. *Nat Protoc* 4, 174–196.

Supporting Information

Additional Supporting Information may be found in the online version of this article at the publisher's web-site:

Figure S1 Representative example of a collision experiment. (A) The electrical stimulation from the peripheral skin (site B; hollow arrow) or neuroma (site A, filled arrow) produced one AP that propagates orthodromically to the recording site R. Simultaneous stimulation from both sites – shown in the third panel – precludes the AP originated in the more distant site: collision is likely occurring at the peripheral segment. Increasing the interval between stimuli allows the AP propagation past the initiation site A (forth panel) or site B (fifth panel) then both AP reach the recording point R. The inset shows the averaged spike shape evoked from the skin and the neuroma. (B) Representation of the mechanical receptive fields in the skin of the axotomized fibres (in grey RF of the C-fibre used for this example in A, and punctate RF for A-fibres, $n = 6$). Black dots: sites for electrical stimulation. White dot: site for electrical stimulation for the mechano-insensitive unit. X: site for mechanical stimulation of the D-hair. Black cylinder represents the neuroma – stimulation site A-. *Marks the RF of the fibre which original recordings are shown in Fig. 3. Note the widespread distribution, sizes and the distance from neuroma.

Table S1 Conduction Velocity from axotomized fibres with inputs from the skin and interval values to avoid collision.

Table S2 Properties of C-fibres with spontaneous activity.

Figure S1

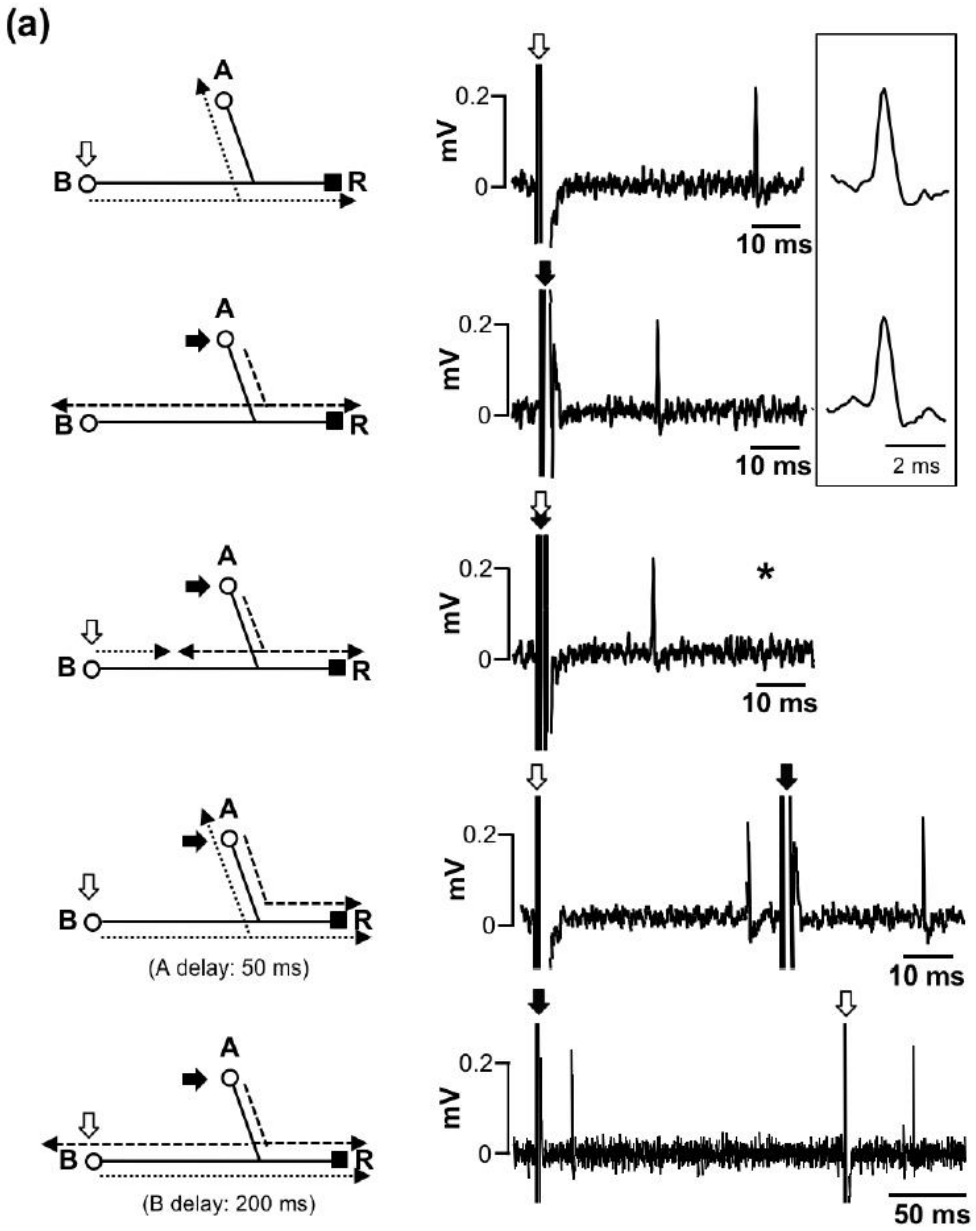

Supplementary Table 1. Conduction Velocity from axotomized fibers with inputs from the skin and interval values to avoid collision**.**

	CV (m/s) obtained from		Minimum Delay (ms)			
Unit	**Neuroma (A)**	**Skin (B)**	**Estimated**	**1st stim (A)**	**1st stim (B)**	**D.P.S.**
1*	0.78	0.55	10.0	200	50	36
2	1.29	0.88	6.8	30	n.t.	32
3	1.9	1.06	6.6	20	230	20
4*	2.34	1.56	10.9	15	20	43
5	4.82	1.28	5.5	20	16	22
6*	5.0	4.38	1.6	19	9	21
7	5.88	1.12	8.0	40	20	32
8	11.25	3.43	1.5	10	n.t.	42

Conduction velocity (CV) values from the skin were significantly slower that those calculated from the neuroma (Wilcoxon matched pair, $p < 0.05$). Fiber's CV recorded from the skin and the distance between both initiation sites were used to estimate the minimum delay to avoid collision. The recorded values were higher that the estimated, regardless which initiation site was stimulated first. * marks units with spontaneous activity. D.P.S days post surgery. n.t. not tested.

Supplementary Table 2. Properties of C-fibers with spontaneous activity

	C-fibers				
	nº of units	**CV**	**Mean Fq. (Hz)**	*nº ongoing*	*nº burst*
Axotomized					
Only Neuroma	$9^{\#1} + 3^{\#3}$	0.35 ± 0.04	0.53 ± 0.11	8	4
Projection to skin	$5^{\#1} + 1^{\#3}$	0.38 ± 0.08	0.26 ± 0.06	6	
Putative intacts	$12^{\#3}$	0.52 ± 0.03 *	0.28 ± 0.08	10	2

The table compares the mean discharge frequencies and CV of the whole population of C-fibers with ectopic spontaneous discharges recorded along Experiment #1 and Experiment #3 (which are indicated as $^{\#1}$ and $^{\#3}$ respectively ^{in} nº of units). The mean discharge frequency, which accounts for all of the units, regardless their patter of discharge (irregular ongoing vs burst), did not reach statistical significance. On the other hand, CV of "putative intact C-fibers" was significantly larger than axotomized C-units without projection to the skin (*$p < 0.05$, one-way ANOVA).

DISCUSSION

Natural compounds, such as coca leaves and opium, are purported analgesic treatments since 1500 B.C. (Sabatowski et al., 2005). However, in 2020 after decades of research on the molecular mechanisms of pain, we are still lacking adequate treatment options for chronic pain, a problem of serious concerns for the present and next generation of pain physicians and scientists. Although the knowledge on the pathophysiology of pain chronification has increased in the last decades, the lack of a breakthrough in medication might in part be due to the tools or methodological approaches that scientists use.

Regarding orofacial pain, retrograde labelling of tooth pulp afferents is a key method to investigate tooth nociceptors within TG neurons. For years, this method has been widely used in the rat (Eckert et al., 1997; Park et al., 2006; Vang et al., 2012), limiting the use of transgenic animals to elucidate specific transduction mechanisms. In the mouse, so far only Fluorogold (FG) was used to label tooth afferents (Chung et al., 2011; Lin et al., 2015; Michot et al., 2018), despite its neurotoxicity (Naumann et al., 2000). This is a limitation for the use of FG-labelled neurons for functional analysis in live cells, as they enter degenerative processes (Hu et al., 2013) that will probably affect the function or expression of ion channels. The reason why only FG was used in mice was that the restricted functional anatomy poses grave problems as the molars are too small to fit a sufficient amount of other, less bright fluorescent dyes. We demonstrated that retrograde labelling or molar teeth in the mouse is possible with enhanced new generation carbocyanines, with heightened affinity to neuronal membranes. We show that the dye does not produce cell death, and the number of stained cells and brightness is sufficient to perform various types of experiments in live neurons. Another important result from our study was that not only the area of the TG corresponding to the maxillary branch (V2) showed labelled neurons from maxillary molars, but also the mandibular (V3) and, to a very small degree, the ophthalmic area (V1), possibly as result of jaw development (Higashiyama and Kuratani, 2014). Hence, focusing on specific areas, V1, V2 or V3, in non-labelled TG alone is not recommended and will not be representative for specific neuron populations; therefore retrograde labelling with non-toxic dyes from the origin of the receptive fields is mandatory when studying subpopulations of trigeminal sensory neurons .

Several animal models have been developed in the last decades aiming to mimic the symptoms of neuropathic pain in patients. However, none of the existing preclinical models are unique and develop all the symptoms and alterations observed in a single patient. For example, allodynia and hyperalgesia are observed in most of the animal models (see (Jaggi et al., 2011) for a review), but spontaneous pain is difficult to assess in experimental models

(Tappe-Theodor and Rohini, 2014). Hence, choosing the adequate model based on the phenomena to study is fundamental to understand the underlying changes of chronic pain. The model described in this thesis provides for the first time a valid tool to study spontaneous activity in C-fibres *in vitro* due to their high incidence and firing rates. Additionally, this model allows a clear distinction of damaged and intact fibres (with their receptive fields) helping us to elucidate the contribution of each type of fibre to spontaneous activity and other phenomena, such as cross-excitation. As previously described, our results suggest an abnormal function of HCN and K_V7 channels after injury (Jiang et al., 2008; Mazo et al., 2013; Roza et al., 2011; Roza and Lopez-Garcia, 2008; Tsantoulas et al., 2017) as the cause of spontaneous activity in C-fibres. However, other channels implicated in membrane excitability such as Na_V or Ca_V are also altered in neuropathic conditions (Chen et al., 2018; Kang et al., 2018; Lai et al., 2002; Li et al., 2017, 2018; Roza et al., 2003). This suggests that spontaneous activity is probably caused by multiple coinciding mechanisms and not the modulation of a single channel alone, but most probably a combination of therapeutics with more than one target may alleviate spontaneous pain.

In summary, it is important to understand the limitations of scientific models and to apply adequate tools and preclinical models to investigate nociceptor characteristics in physiological and pathological conditions. In order to develop new therapeutic approaches to alleviate chronic pain it will be indispensable to recognize the functional differences of trigeminal, somatic, or visceral pain sensory populations.

CONCLUSIONS

Specific conclusions from Section I

1. Specific retrograde labelling from dental primary afferents in mice is feasible with non-toxic carbocyanine dyes in formulations of improved membrane diffusibility.
2. Cell bodies of neurons innervating the maxillary molars of the mouse are located in the territory of the mandibular and the maxillary branch in the TG.
3. Almost half of the dental primary afferents expressed TRPM8, and retrolabelled neurons responded to capsaicin in calcium imaging similar to non-retrolabelled neurons.
4. This method is now validated and available for future studies of molecular transduction mechanisms in nerves innervating teeth.

Specific conclusions from Section II

1. Both HCN and Kv7 channels contribute to the generation of ectopic spontaneous activity in C- and Aδ-nociceptors after nerve damage.
2. HCN channels shape the discharge firing pattern of C-nociceptors.
3. There was a high proportion of "putative intact" units that developed spontaneous activity and other ectopic behaviours (post-discharges, collision at the peripheral terminals) which may contribute to neuropathic pain.
4.

BIBLIOGRAPHY

Abe, J., Hosokawa, H., Okazawa, M., Kandachi, M., Sawada, Y., Yamanaka, K., Matsumura, K., & Kobayashi, S. (2005). TRPM8 protein localization in trigeminal ganglion and taste papillae. *Molecular Brain Research*, 136(1-2):91-98. https://doi.org/10.1016/j.molbrainres.2005.01.013

Ali, Z., Ringkamp, M., Hartke, T. V., Chien, H. F., Flavahan, N.A., Campbell, J. N., & Meyer, R. A. (1999). Uninjured C-fiber nociceptors develop spontaneous activity and alpha-adrenergic sensitivity following L6 spinal nerve ligation in monkey. *Journal of Neurophysiology*, 81(2):455-66. doi: 10.1152/jn.1999.81.2.455.

Amir, R., Kocsis, J. D., & Devor, M. (2005). Multiple interacting sites of ectopic spike electrogenesis in primary sensory neurons. *Journal of Neuroscience, 25(10): 2576–2585.*. https://doi.org/10.1523/JNEUROSCI.4118-04.2005

Attal, N. (2019). Pharmacological treatments of neuropathic pain: The latest recommendations. *Revue Neurologique,* 175 (2019), 46-50. https://doi.org/10.1016/j.neurol.2018.08.005

Averill, S., McMahon, S. B., Clary, D. O., Reichardt, L. F., & Priestley, J. V. (1995). Immunocytochemical Localization of trkA Receptors in Chemically Identified Subgroups of Adult Rat Sensory Neurons. *European Journal of Neuroscience,* 7(7): 1484–1494. https://doi.org/10.1111/j.1460-9568.1995.tb01143.x

Barabas, M. E., Kossyreva, E. A., & Stucky, C. L. (2012). TRPA1 Is Functionally Expressed Primarily by IB4-Binding, Non-Peptidergic Mouse and Rat Sensory Neurons. *PLoS ONE, 7(10):e47988*. https://doi.org/10.1371/journal.pone.0047988

Basbaum, A. I., & Bráz, J. M. (2009). Transgenic mouse models for the tracing of "pain" pathways. *Translational Pain Research: From Mouse to Man,* Chapter 7. https://doi.org/10.1201/9781439812105-c7

Bautista, D. M., Siemens, J., Glazer, J. M., Tsuruda, P. R., Basbaum, A. I., Stucky, C. L., Jordt, S. E., & Julius, D. (2007). The menthol receptor TRPM8 is the principal detector of environmental cold. *Nature,* 448(7150):204-8. https://doi.org/10.1038/nature05910

Bayliss, W. M. (1901). On the origin from the spinal cord of the vaso-dilator fibres of the hind-limb, and on the nature of these fibres. *The Journal of Physiology,* 26(3-4): 173–209. https://doi.org/10.1113/jphysiol.1901.sp000831

Bigal, M. E., & Lipton, R. B. (2009). Overuse of acute migraine medications and migraine chronification. *Current Pain and Headache Reports,* 13(4):301-7 . https://doi.org/10.1007/s11916-009-0048-3

Blackburn-Munro, G., & Jensen, B. S. (2003). The anticonvulsant retigabine attenuates nociceptive behaviours in rat models of persistent and neuropathic pain. *European Journal of Pharmacology,* 460(2-3):109-16. https://doi.org/10.1016/S0014-2999(02)02924-2

Bouhassira, D., & Attal, N. (2018). Emerging therapies for neuropathic pain: new molecules or new indications for old treatments? *Pain*, *159*(3), 576-582. https://doi.org/10.1097/j.pain.0000000000001136

Bouhassira, D., Attal, N., Alchaar, H., Boureau, F., Brochet, B., Bruxelle, J., Cunin, G., Fermanian, J., Ginies, P., Grun-Overdyking, A., Jafari-Schluep, H., Lantéri-Minet, M., Laurent, B., Mick, G., Serrie, A., Valade, D., & Vicaut, E. (2005). Comparison of pain syndromes associated with nervous or somatic lesions and development of a new neuropathic pain diagnostic questionnaire (DN4). *Pain,* 114(1-2):29-36. https://doi.org/10.1016/j.pain.2004.12.010

Breivik, H., Collett, B., Ventafridda, V., Cohen, R., & Gallacher, D. (2006). Survey of chronic pain in Europe: Prevalence, impact on daily life, and treatment. *European Journal of Pain,* 10(4): 287-333. https://doi.org/10.1016/j.ejpain.2005.06.009

Burchiel, K. J. (1984). Spontaneous impulse generation in normal and denervated dorsal root ganglia: sensitivity to alpha-adrenergic stimulation and hypoxia. *Experimental Neurology*, 85(2), 257–272. doi: 10.1016/0014-4886(84)90139-0.

Burgess, P. R., & Perl, E. R. (1967). Myelinated afferent fibres responding specifically to noxious stimulation of the skin. *The Journal of Physiology,* 190(3): 541–562. https://doi.org/10.1113/jphysiol.1967.sp008227

Byers, M. R. (1985). Terminal arborization of individual sensory axons in dentin and pulp of rat molars. *Brain Research,* 345(1):181-5. https://doi.org/10.1016/0006-8993(85)90851-0

Cadden, S. W., Lisney, S. J. W., & Matthews, B. (1983). Thresholds to electrical stimulation of nerves in cat canine tooth-pulp with Aβ-, Aδ- and C-fibre conduction velocities. *Brain Research,* 261(1): 31-41. https://doi.org/10.1016/0006-8993(83)91280-5

Cain, D. M., Khasabov, S. G., & Simone, D. A. (2001). Response properties of mechanoreceptors and nociceptors in mouse glabrous skin: An in vivo study. *Journal of Neurophysiology,* 85(4):1561-74 . https://doi.org/10.1152/jn.2001.85.4.1561

Campbell, J. N., Raja, S. N., Meyer, R. A., & Mackinnon, S. E. (1988). Myelinated afferents signal the hyperalgesia associated with nerve injury. *Pain,* 32(1):89-94. https://doi.org/10.1016/0304-3959(88)90027-9

Caterina, M. J., Leffler, A., Malmberg, A. B., Martin, W. J., Trafton, J., Petersen-Zeitz, K. R., Koltzenburg, M., Basbaum, A. I., & Julius, D. (2000). Impaired nociception and pain sensation in mice lacking the capsaicin receptor. *Science,* 288(5464):306-13. https://doi.org/10.1126/science.288.5464.306

Caterina, M. J., Schumacher, M. A., Tominaga, M., Rosen, T. A., Levine, J. D., & Julius, D. (1997). The capsaicin receptor: A heat-activated ion channel in the pain pathway. *Nature,* 39(3): 159-164. https://doi.org/10.1038/39807

Cavanaugh, D. J., Lee, H., Lo, L., Shields, S. D., Zylka, M. J., Basbaum, A. I., & Anderson, D. J. (2009). Distinct subsets of unmyelinated primary sensory fibers mediate behavioral responses to noxious thermal and mechanical stimuli. *Proceedings of the National Academy of Sciences of the United States of America,* 106(22):9075-80. https://doi.org/10.1073/pnas.0901507106

Chaplan, S. R., Guo, H.-Q., Lee, D., Luo, L., Liu, C., Kuei, C., Velumian, A. A., Butler, M. P., Brown, S. M., & Dubin, A. E. (2003). Neuronal hyperpolarization-activated pacemaker channels drive neuropathic pain. *The Journal of Neuroscience : The Official Journal of the Society for Neuroscience*, *23*(4), 1169–1178. https://doi.org/10.1523/JNEUROSCI.23-04-01169.2003

Chen, S., Wang, J., & Siegelbaum, S. A. (2001). Properties of hyperpolarization-activated pacemaker current defined by coassembly of HCN1 and HCN2 subunits and basal modulation by cyclic nucleotide. *The Journal of General Physiology*, *117*(5), 491–504. DOI: 10.1085/jgp.117.5.491

Chen, W., Chi, Y. N., Kang, X. J., Liu, Q. Y., Zhang, H. L., Li, Z. H., Zhao, Z. F., Yang, Y., Su, L., Cai, J., Liao, F. F., Yi, M., Wan, Y., & Liu, F. Y. (2018). Accumulation of Cav 3.2 t-type calcium channels in the uninjured sural nerve contributes to neuropathic pain in rats with spared nerve injury. *Frontiers in Molecular Neuroscience,* 11:24. https://doi.org/10.3389/fnmol.2018.00024

Chidchuangchai, W., Vongsavan, N., & Matthews, B. (2007). Sensory transduction mechanisms responsible for pain caused by cold stimulation of dentine in man. *Archives of Oral Biology,* 52(2):154-6. https://doi.org/10.1016/j.archoralbio.2006.09.009

Chung, G., Jung, S. J., & Oh, S. B. (2013). Cellular and molecular mechanisms of dental nociception. *Journal of Dental Research,* 92(11):948-55. https://doi.org/10.1177/0022034513501877

Chung, M. K., Lee, J., Duraes, G., & Ro, J. Y. (2011). Lipopolysaccharide-induced pulpitis up-regulates TRPV1 in trigeminal ganglia. *Journal of Dental Research,* 90(9): 1103-1107. https://doi.org/10.1177/0022034511413284

Cohen, S. P., Bhatia, A., Buvanendran, A., Schwenk, E. S., Wasan, A. D., Hurley, R. W., Viscusi, E. R., Narouze, S., Davis, F. N., Ritchie, E. C., Lubenow, T. R., & Hooten, W. M. (2018). Consensus Guidelines on the Use of Intravenous Ketamine Infusions for Chronic Pain From the American Society of Regional Anesthesia and Pain Medicine, the American Academy of Pain Medicine, and the American Society of Anesthesiologists. *Regional Anesthesia and Pain Medicine,* 43(5):521-546. https://doi.org/10.1097/AAP.0000000000000808

Colburn, R. W., Lubin, M. Lou, Stone, D. J., Wang, Y., Lawrence, D., D'Andrea, M. R. R., Brandt, M. R., Liu, Y., Flores, C. M., & Qin, N. (2007). Attenuated Cold Sensitivity in TRPM8 Null Mice. *Neuron,* 54(3):379-386. https://doi.org/10.1016/j.neuron.2007.04.017

Coste, B., Mathur, J., Schmidt, M., Earley, T. J., Ranade, S., Petrus, M. J., Dubin, A. E., & Patapoutian, A. (2010). Piezo1 and Piezo2 are essential components of distinct mechanically activated cation channels. *Science,* 330(6000):55-60. https://doi.org/10.1126/science.1193270

Daniluk, J., Cooper, J. A., Stender, M., & Kowalczyk, A. (2016). Survey of Physicians' Understanding of Specific Risks Associated with Retigabine. *Drugs Real World Outcomes,* 3(2):155-163. https://doi.org/10.1007/s40801-016-0068-3

Delmas, P., & Brown, D. A. (2005). Pathways modulating neural KCNQ/M (Kv7) potassium channels. *Nature Reviews Neuroscience*, *6*(11), 850–862. https://doi.org/10.1038/nrn1785

Devor, M., Govrin-Lippmann, R., & Angelides, K. (1993). Na+ channel immunolocalization in peripheral mammalian axons and changes following nerve injury and neuroma formation. *Journal of Neuroscience,* 13(5):1976-1992. https://doi.org/10.1523/jneurosci.13-05-01976.1993

Dhaka, A., Earley, T. J., Watson, J., & Patapoutian, A. (2008). Visualizing cold spots: TRPM8-expressing sensory neurons and their projections. *Journal of Neuroscience,* 28(3):566-75. https://doi.org/10.1523/JNEUROSCI.3976-07.2008

Dhaka, A., Murray, A. N., Mathur, J., Earley, T. J., Petrus, M. J., & Patapoutian, A. (2007). TRPM8 Is Required for Cold Sensation in Mice. *Neuron,* 54(3):371-378. https://doi.org/10.1016/j.neuron.2007.02.024

Djouhri, L., Malki, M. I., Zeidan, A., Nagi, K., & Smith, T. (2019). Activation of Kv7 channels with the anticonvulsant retigabine alleviates neuropathic pain behaviour in the streptozotocin rat model of diabetic neuropathy. *Journal of Drug Targeting,* 27(10):1118-1126. https://doi.org/10.1080/1061186X.2019.1608552

Du, X., & Gamper, N. (2013). Potassium channels in peripheral pain pathways: expression, function and therapeutic potential. *Current Neuropharmacology*, 11(6), 621–640. https://doi.org/10.2174/1570159X113119990042

Du, X., Gao, H., Jaffe, D., Zhang, H., & Gamper, N. (2018). M-type K + channels in peripheral nociceptive pathways. *British Journal of Pharmacology,* 175(12):2158-2172. https://doi.org/10.1111/bph.13978

Eckert, S. P., Taddese, A., & EW, M. (1997). Isolation and culture of rat sensory neurons having distinct sensory modalities. *Journal of Neuroscience Methods*, *77*(2), 183–190. https:// doi: 10.1016/s0165-0270(97)00125-8

Edvinsson, L., Ekman, R., Jansen, I., McCulloch, J., & Uddman, R. (1987). Calcitonin gene-related peptide and cerebral blood vessels: Distribution and vasomotor effects. *Journal of Cerebral Blood Flow and Metabolism,* 7(6):720-8. https://doi.org/10.1038/jcbfm.1987.126

Egbuniwe, O., Grover, S., Duggal, A. K., Mavroudis, A., Yazdi, M., Renton, T., Di Silvio, L., & Grant, A. D. (2014). TRPA1 and TRPV4 activation in human odontoblasts stimulates ATP release. *Journal of Dental Research,* 93(9):911-7. https://doi.org/10.1177/0022034514544507

El Karim, I. A., Linden, G. J., Curtis, T. M., About, I., McGahon, M. K., Irwin, C. R., & Lundy, F. T. (2011). Human odontoblasts express functional thermo-sensitive TRP channels: Implications for dentin sensitivity. *Pain,* 152(10):2211-23. https://doi.org/10.1016/j.pain.2010.10.016

Emery, E. C., Luiz, A. P., Sikandar, S., Magnúsdóttir, R., Dong, X., & Wood, J. N. (2016). In vivo characterization of distinct modality-specific subsets of somatosensory neurons using GCaMP. *Science Advances,* 2(11):e1600990. https://doi.org/10.1126/sciadv.1600990

Emery, E. C., Young, G. T., Berrocoso, E. M., Chen, L., & McNaughton, P. A. (2011). HCN2 ion channels play a central role in inflammatory and neuropathic pain. *Science,* 33(6048):1462-1466. https://doi.org/10.1126/science.1206243

Facer, P., Casula, M. A., Smith, G. D., Benham, C. D., Chessell, I. P., Bountra, C., Sinisi, M., Birch, R., & Anand, P. (2007). Differential expression of the capsaicin receptor TRPV1 and related novel receptors TRPV3, TRPV4 and TRPM8 in normal human tissues and changes in traumatic and diabetic neuropathy. *BMC Neurology,* 7:11 . https://doi.org/10.1186/1471-2377-7-11

Fang, X., Djouhri, L., McMullan, S., Berry, C., Okuse, K., Waxman, S. G., & Lawson, S. N. (2005). trkA is expressed in nociceptive neurons and influences electrophysiological properties via Nav1.8 expression in rapidly conducting nociceptors. *Journal of Neuroscience,* 25(19):4868-4878. https://doi.org/10.1523/JNEUROSCI.0249-05.2005

Farrell, S. M., Green, A., & Aziz, T. (2018). The current state of deep brain stimulation for chronic pain and its context in other forms of neuromodulation. *Brain Sciences,* 8(8):158. https://doi.org/10.3390/brainsci8080158

Fillmore, E. P., & Seifert, M. F. (2015). Anatomy of the Trigeminal Nerve. *Nerves and Nerve Injuries*. 1(22):319-347. Academic Press. https://doi.org/10.1016/B978-0-12-410390-0.00023-8

Forstenpointner, J., Otto, J., & Baron, R. (2018). Individualized neuropathic pain therapy based on phenotyping: are we there yet? *Pain,* 159(3):569-575. https://doi.org/10.1097/j.pain.0000000000001088

Franck, M. C. M., Stenqvist, A., Li, L., Hao, J., Usoskin, D., Xu, X., Wiesenfeld-Hallin, Z., & Ernfors, P. (2011). Essential role of Ret for defining non-peptidergic nociceptor phenotypes and functions in the adult mouse. *European Journal of Neuroscience,* 33(8):1385-400. https://doi.org/10.1111/j.1460-9568.2011.07634.x

Fried, K., Arvidsson, J., Robertson, B., Brodin, E., & Theodorsson, E. (1989). Combined retrograde tracing and enzyme/immunohistochemistry of trigeminal ganglion cell bodies innervating tooth pulps in the rat. *Neuroscience,* 33(1):101-9. https://doi.org/10.1016/0306-4522(89)90314-X

Galer, B. S., Rowbotham, M. C., Perander, J., & Friedman, E. (1999). Topical lidocaine patch relieves postherpetic neuralgia more effectively than a vehicle topical patch: Results of an enriched enrollment study. *Pain,* 80(3):533-8. https://doi.org/10.1016/S0304-3959(98)00244-9

Gauriau, C., & Bernard, J. F. (2002). Pain pathways and parabrachial circuits in the rat. *Experimental Physiology,* 87(2):251-8. https://doi.org/10.1113/eph8702357

Goldberg, D. S., & McGee, S. J. (2011). Pain as a global public health priority. *BMC Public Health,* 11:770. https://doi.org/10.1186/1471-2458-11-770

Goswami, S. C., Mishra, S. K., Maric, D., Kaszas, K., Gonnella, G. L., Clokie, S. J., Kominsky, H. D., Gross, J. R., Keller, J. M., Mannes, A. J., Hoon, M. A., & Iadarola, M. J. (2014). Molecular signatures of mouse TRPV1-lineage neurons revealed by RNA-seq transcriptome analysis. *Journal of Pain,* 15(12):1338-1359. https://doi.org/10.1016/j.jpain.2014.09.010

Gould, H. J., Gould, T. N., England, J. D., Paul, D., Liu, Z. P., & Levinson, S. R. (2000). A possible role for nerve growth factor in the augmentation of sodium channels in models of chronic pain. *Brain Research,* 854(1-2):19-29. https://doi.org/10.1016/S0006-8993(99)02216-7

Gracely, R. H., Lynch, S. A., & Bennett, G. J. (1992). Painful neuropathy: altered central processing maintained dynamically by peripheral input. *Pain,* 51(2):175-94. https://doi.org/10.1016/0304-3959(92)90259-E

Gracheva, E. O., Cordero-Morales, J. F., González-Carcacía, J. A., Ingolia, N. T., Manno, C., Aranguren, C. I., Weissman, J. S., & Julius, D. (2011). Ganglion-specific splicing of TRPV1 underlies infrared sensation in vampire bats. *Nature,* 476(7358):88-91. https://doi.org/10.1038/nature10245

Gracheva, E. O., Ingolia, N. T., Kelly, Y. M., Cordero-Morales, J. F., Hollopeter, G., Chesler, A. T., Sánchez, E. E., Perez, J. C., Weissman, J. S., & Julius, D. (2010). Molecular basis of infrared detection by snakes. *Nature,* 464(7291):1006-11. https://doi.org/10.1038/nature08943

Haas, E. T., Rowland, K., & Gautam, M. (2011). Tooth injury increases expression of the cold sensitive TRP channel TRPA1 in trigeminal neurons. *Archives of Oral Biology,* 56(12):1604-9. https://doi.org/10.1016/j.archoralbio.2011.06.014

Haroutounian, S., Nikolajsen, L., Bendtsen, T. F., Finnerup, N. B., Kristensen, A. D., Hasselstrøm, J. B., & Jensen, T. S. (2014). Primary afferent input critical for maintaining spontaneous pain in peripheral neuropathy. *Pain*, 155(7):1272-9. https://doi.org/10.1016/j.pain.2014.03.022

Henry, M. A., Luo, S., & Levinson, S. R. (2012). Unmyelinated nerve fibers in the human dental pulp express markers for myelinated fibers and show sodium channel accumulations. *BMC Neuroscience,* 13:29. https://doi.org/10.1186/1471-2202-13-29

Higashiyama, H., & Kuratani, S. (2014). On the maxillary nerve. *Journal of Morphology,* 275(1):17-38. https://doi.org/10.1002/jmor.20193

Hoeijmakers, J. G. J., Faber, C. G., Merkies, I. S. J., & Waxman, S. G. (2015). Painful peripheral neuropathy and sodium channel mutations. *Neuroscience Letters,* 596:51-9. https://doi.org/10.1016/j.neulet.2014.12.056

Hökfelt, T., Kellerth, J. O., Nilsson, G., & Pernow, B. (1975). Substance P: Localization in the central nervous system and in some primary sensory neurons. *Science,* 190(4217):889-90. https://doi.org/10.1126/science.242075

Hu, W., Liu, D., Zhang, Y., Shen, Z., Gu, T., Gu, X., & Gu, J. (2013). Neurological function following intra-neural injection of fluorescent neuronal tracers in rats. *Neural Regeneration Research,* 8(14):1253-1261. https://doi.org/10.3969/j.issn.1673-5374.2013.14.001

Huang, H., & Trussell, L. O. (2011). KCNQ5 channels control resting properties and release probability of a synapse. *Nature Neuroscience,* 14(7):840-847. https://doi.org/10.1038/nn.2830

Iwata, K., Tsuboi, Y., Toda, K., Yagi, J., Tsujimoto, C., & Sumino, R. (1991). Comparisons of the sensation perceived and intradental nerve activity following temperature changes in human teeth. *Experimental Brain Research,* 87(1):213-7. https://doi.org/10.1007/BF00228522

Jaggi, A., Jain, V., & Singh, N. (2011). Animal models of neuropathic pain. *Fundamental and Clinical Pharmacology*, 25(1), 1–28. https://doi.org/10.1111/j.1472-8206.2009.00801.x

Jankowski, M. P., Rau, K. K., & Koerber, H. R. (2017). Cutaneous TRPM8-expressing sensory afferents are a small population of neurons with unique firing properties. *Physiological Reports,* 5(7):e13234. https://doi.org/10.14814/phy2.13234

Jia, Z., Bei, J., Lise, R.-D., Liu, B., Jia, Q., Delmas, P., & Zhang, H. (2008). NGF Inhibits M/KCNQ Currents and Selectively Alters Neuronal Excitability in Subsets of Sympathetic Neurons Depending on their M/KCNQ Current Background. *The Journal of General Physiology*, 131(6): 575–587. https://doi.org/10.1085/jgp.200709924

Jiang, Y.-Q., Xing, G.-G., Wang, S.-L., Tu, H.-Y., Chi, Y.-N., Li, J., Liu, F.-Y., Han, J.-S., & Wan, Y. (2008). Axonal accumulation of hyperpolarization-activated cyclic nucleotide-gated cation channels contributes to mechanical allodynia after peripheral nerve injury in rat. *Pain*, 137(3):495–506. https://doi.org/10.1016/j.pain.2007.10.011

Johnsen, D., & Johns, S. (1978). Quantitation of nerve fibres in the primary and permanent canine and incisor teeth in man. *Archives of Oral Biology,* 23(9):825-9. https://doi.org/10.1016/0003-9969(78)90163-2

Jordt, S. E., Bautista, D. M., Chuang, H. H., McKemy, D. D., Zygmunt, P. M., Högestätt, E. D., Meng, I. D., & Julius, D. (2004). Mustard oils and cannabinoids excite sensory nerve fibres through the TRP channel ANKTM1. *Nature,* 427(6971):260-5. https://doi.org/10.1038/nature02282

Josephson, A., Widenfalk, J., Trifunovski, A., Widmer, H. R., Olson, L., & Spenger, C. (2001). GDNF and NGF family members and receptors in human fetal and adult spinal cord and dorsal root ganglia. *Journal of Comparative Neurology,* 440(2):204-17. https://doi.org/10.1002/cne.1380

Jung, S., Jones, T. D., Lugo, J. N., Sheerin, A. H., Miller, J. W., D'Ambrosio, R., Anderson, A. E., & Poolos, N. P. (2007). Progressive dendritic HCN channelopathy during epileptogenesis in the rat pilocarpine model of epilepsy. *Journal of Neuroscience,* 27(47):13012-13021. https://doi.org/10.1523/JNEUROSCI.3605-07.2007

Jyväsjärvi, E., & Kniffki, K. D. (1987). Cold stimulation of teeth: a comparison between the responses of cat intradental A delta and C fibres and human sensation. *The Journal of Physiology,* 391:193-207. https://doi.org/10.1113/jphysiol.1987.sp016733

Kang, X. J., Chi, Y. N., Chen, W., Liu, F. Y., Cui, S., Liao, F. F., Cai, J., & Wan, Y. (2018). Increased expression of CaV3.2 T-type calcium channels in damaged DRG neurons contributes to neuropathic pain in rats with spared nerve injury. *Molecular Pain,* 14:1744806918765808. https://doi.org/10.1177/1744806918765808

Karashima, Y., Damann, N., Prenen, J., Talavera, K., Segal, A., Voets, T., & Nilius, B. (2007). Bimodal action of menthol on the transient receptor potential channel TRPA1. *Journal of Neuroscience,* 27(37):9874-9884. https://doi.org/10.1523/JNEUROSCI.2221-07.2007

Karashima, Y., Talavera, K., Everaerts, W., Janssens, A., Kwan, K. Y., Vennekens, R., Nilius, B., & Voets, T. (2009). TRPA1 acts as a cold sensor in vitro and in vivo. *Proceedings of the National Academy of Sciences of the United States of America,* 106(4):1273-1278. https://doi.org/10.1073/pnas.0808487106

Karim, B. F. A., & Gillam, D. G. (2013). The efficacy of strontium and potassium toothpastes in treating dentine hypersensitivity: A systematic review. *International Journal of Dentistry,* 2013:573258. https://doi.org/10.1155/2013/573258

Khaliq, W., Alam, S., Puri, N. K., & Hobson, A. (2013). Topical lidocaine for the treatment of postherpetic neuralgia. *Cochrane Database of Systematic Reviews,* (2):CD004846. https://doi.org/10.1002/14651858.CD004846.pub3

Kim, H. Y., Chung, G., Jo, H. J., Kim, Y. S., Bae, Y. C., Jung, S. J., Kim, J. S., & Oh, S. B. (2011). Characterization of Dental Nociceptive Neurons. *Journal of Dental Research*, 90(6):771–776. https://doi.org/10.1177/0022034511399906

Kim, Y. S., Jung, H. K., Kwon, T. K., Kim, C. S., Cho, J. H., Ahn, D. K., & Bae, Y. C. (2012). Expression of transient receptor potential Ankyrin 1 in human dental pulp. *Journal of Endodontics,* 38(8):1087-92. https://doi.org/10.1016/j.joen.2012.04.024

Kleggetveit, I., Namer, B., Schmidt, R., Hel\r as, T., Rückel, M., Ørstavik, K., Schmelz, M., & Jørum, E. (2012). High spontaneous activity of C-nociceptors in painful polyneuropathy. *Pain*, 153(10): 2040–2047. https://doi.org/10.1016/j.pain.2012.05.017

Kobayashi, K., Fukuoka, T., Obata, K., Yamanaka, H., Dai, Y., Tokunaga, A., & Noguchi, K. (2005). Distinct expression of TRPM8, TRPA1, and TRPV1 mRNAs in rat primary afferent neurons with aδ/c-fibers and colocalization with trk receptors. *The Journal of Comparative Neurology*, 493(4): 596–606. https://doi.org/10.1002/cne.20794

Lai, J., Gold, M. S., Kim, C. S., Biana, D., Ossipov, M. H., Hunterc, J. C., & Porreca, F. (2002). Inhibition of neuropathic pain by decreased expression of the tetrodotoxin-resistant sodium channel, NaV1.8. *Pain,* 95(1-2):143:52. https://doi.org/10.1016/S0304-3959(01)00391-8

Lawson, S. N. (2002). Phenotype and function of somatic primary afferent nociceptive neurones with C-, Aδ- or Aα/β-fibres. *Experimental Physiology,* 87(2):239-244. https://doi.org/10.1113/eph8702350

Lawson, S. N., & Waddell, P. J. (1991). Soma neurofilament immunoreactivity is related to cell size and fibre conduction velocity in rat primary sensory neurons. *The Journal of Physiology,* 435:41-63. https://doi.org/10.1113/jphysiol.1991.sp018497

Lawson, S. N., Fang, X., & Djouhri, L. (2019). Nociceptor subtypes and their incidence in rat lumbar dorsal root ganglia (DRGs): focussing on C-polymodal nociceptors, Aβ-nociceptors, moderate pressure receptors and their receptive field depths. *Current Opinion in Physiology,* 11:125-146. https://doi.org/10.1016/j.cophys.2019.10.005

Levy, D., & Strassman, A. M. (2002). Mechanical response properties of A and C primary afferent neurons innervating the rat intracranial dura. *Journal of Neurophysiology,* 88(6):3021-31. https://doi.org/10.1152/jn.00029.2002

Li, C. L., Li, K. C., Wu, D., Chen, Y., Luo, H., Zhao, J. R., Wang, S. S., Sun, M. M., Lu, Y. J., Zhong, Y. Q., Hu, X. Y., Hou, R., Zhou, B. B., Bao, L., Xiao, H. S., & Zhang, X. (2016). Somatosensory neuron types identified by high-coverage single-cell RNA-sequencing and functional heterogeneity. *Cell Research,* 26(1):83-102. https://doi.org/10.1038/cr.2015.149

Li, C., Wang, S., Chen, Y., & Zhang, X. (2018). Somatosensory Neuron Typing with High-Coverage Single-Cell RNA Sequencing and Functional Analysis. *Neuroscience Bulletin,* 34(1):200-207. https://doi.org/10.1007/s12264-017-0147-9

Li, Y., North, R. Y., Rhines, L. D., Tatsui, C. E., Rao, G., Edwards, D. D., Cassidy, R. M., Harrison, D. S., Johansson, C. A., Zhang, H., & Dougherty, P. M. (2018). DRG voltage-gated sodium channel 1.7 is upregulated in paclitaxel-induced neuropathy in rats and in humans with neuropathic pain. *Journal of Neuroscience,* 38(5):1124-1136. https://doi.org/10.1523/JNEUROSCI.0899-17.2017

Li, Y., Tatsui, C., Rhines, L. D., North, R. Y., Harrison, D. S., Cassidy, R. M., Johansson, C. A., Kosturakis, A. K., Edwards, D. D., Zhang, H., & Dougherty, P. M. (2017). Dorsal root ganglion neurons become hyperexcitable and increase expression of voltage-gated T-type calcium channels (Cav3.2) in paclitaxel-induced peripheral neuropathy. *Pain,* 158(3), 417-429. https://doi.org/10.1097/j.pain.0000000000000774

Liedgens, H., Obradovic, M., De Courcy, J., Holbrook, T., & Jakubanis, R. (2016). A burden of illness study for neuropathic pain in Europe. *ClinicoEconomics and Outcomes Research,* 8:113-26. https://doi.org/10.2147/CEOR.S81396

Light, A. R., & Perl, E. R. (1979). Reexamination of the dorsal root projection to the spinal dorsal horn including observations on the differential termination of coarse and fine fibers. *Journal of Comparative Neurology,* 186(2):117-31. https://doi.org/10.1002/cne.901860202

Lin, J.-J., Du, Y., Cai, W.-K., Kuang, R., Chang, T., Zhang, Z., Yang, Y.-X., Sun, C., Li, Z.-Y., & Kuang, F. (2015). Toll-like receptor 4 signaling in neurons of trigeminal ganglion contributes to nociception induced by acute pulpitis in rats. *Scientific Reports,* 5:12549. https://doi.org/10.1038/srep12549

Linley, J. E., Rose, K., Patil, M., Robertson, B., Akopian, A. N., & Gamper, N. (2008). Inhibition of M current in sensory neurons by exogenous proteases: A signaling pathway mediating inflammatory nociception. *Journal of Neuroscience,* 28(44):11240-9. https://doi.org/10.1523/JNEUROSCI.2297-08.2008

Ljungdahl, Å., Hökfelt, T., Nilsson, G., & Goldstein, M. (1978). Distribution of substance P-like immunoreactivity in the central nervous system of the rat-II. Light microscopic localization in relation to catecholamine-containing neurons. *Neuroscience,* 3(10):945-976. https://doi.org/10.1016/0306-4522(78)90117-3

Luo, L., L, C., Brown, S. M., Ao, H., Lee, D. H., Higuera, E. S., Dubin, A. E., & Chaplan, S. R. (2007). Role of peripheral hyperpolarization-activated cyclic nucleotide-modulated channel pacemaker channels in acute and chronic pain models in the rat. *Neuroscience*, 144(4), 1477–1485. https://doi.org/10.1016/j.neuroscience.2006.10.048

Madrid, R., De La Peña, E., Donovan-Rodriguez, T., Belmonte, C., & Viana, F. (2009). Variable threshold of trigeminal cold-thermosensitive neurons is determined by a balance between TRPM8 and Kv1 potassium channels. *Journal of Neuroscience,* 29(10):3120-3131. https://doi.org/10.1523/JNEUROSCI.4778-08.2009

Madrid, R., Donovan-Rodríguez, T., Meseguer, V., Acosta, M. C., Belmonte, C., & Viana, F. (2006). Contribution of TRPM8 channels to cold transduction in primary sensory neurons and peripheral nerve terminals. *Journal of Neuroscience,* 26(48):12512-25. https://doi.org/10.1523/JNEUROSCI.3752-06.2006

Manteniotis, S., Lehmann, R., Flegel, C., Vogel, F., Hofreuter, A., Schreiner, B. S. P., Altmüller, J., Becker, C., Schöbel, N., Hatt, H., & Gisselmann, G. (2013). Comprehensive RNA-Seq expression analysis of sensory ganglia with a focus on ion channels and GPCRs in trigeminal ganglia. *PLoS ONE,* 8(11):e79523. https://doi.org/10.1371/journal.pone.0079523

Mäntyselkä, P., Kumpusalo, E., Ahonen, R., Kumpusalo, A., Kauhanen, J., Viinamäki, H., Halonen, P., & Takala, J. (2001). Pain as a reason to visit the doctor: A study in Finnish primary health care. *Pain,* 89(2-3):175-80. https://doi.org/10.1016/S0304-3959(00)00361-4

Matzner, O., & Devor, M. (1994). Hyperexcitability at sites of nerve injury depends on voltage-sensitive Na+ channels. *Journal of Neurophysiology,* 72(1):349-59. https://doi.org/10.1152/jn.1994.72.1.349

Mazo, I., Rivera-Arconada, I., López-García, J. A., & Roza, C. (2013). Axotomy-induced changes in activity-dependent slowing in peripheral nerve fibres: Role of hyperpolarization-activated/HCN channel current. *European Journal of Pain*, 17(9), 1281–1290. https://doi.org/10.1002/j.1532-2149.2013.00302.x

McCarthy, P. W., & Lawson, S. N. (1990). Cell type and conduction velocity of rat primary sensory neurons with calcitonin gene-related peptide-like immunoreactivity. *Neuroscience,* 28(3):745-53. https://doi.org/10.1016/0306-4522(90)90169-5

McKemy, D. D. (2007). TRPM8: The Cold and Menthol Receptor. *TRP Ion Channel Function in Sensory Transduction and Cellular Signaling Cascades*. Chapter 13. Boca Raton (FL). CRC Press/Taylor & Francis.

McKemy, D. D., Neuhausser, W. M., & Julius, D. (2002). Identification of a cold receptor reveals a general role for TRP channels in thermosensation. *Nature,* 416(6876):52-58. https://doi.org/10.1038/nature719

Michot, B., Lee, C. S., & Gibbs, J. L. (2018). TRPM8 and TRPA1 do not contribute to dental pulp sensitivity to cold. *Scientific Reports,* 8(1):13198. https://doi.org/10.1038/s41598-018-31487-2

Miglani, S., Aggarwal, V., & Ahuja, B. (2010). Dentin hypersensitivity: Recent trends in management. *Journal of Conservative Dentistry,* 13(4):218-24. https://doi.org/10.4103/0972-0707.73385

Momin, A., Cadiou, H., Mason, A., & A, M. P. (2008). Role of the hyperpolarization-activated current Ihin somatosensory neurons. *The Journal of Physiology*, 586(24), 5911–5929. https://doi.org/10.1113/jphysiol.2008.163154

Montell, C., & Rubin, G. M. (1989). Molecular characterization of the drosophila trp locus: A putative integral membrane protein required for phototransduction. *Neuron,* 2(4):1313-23. https://doi.org/10.1016/0896-6273(89)90069-X

Moparthi, L., Survery, S., Kreir, M., Simonsen, C., Kjellbom, P., Högestätt, E. D., Johanson, U., & Zygmunt, P. M. (2014). Human TRPA1 is intrinsically cold- and chemosensitive with and without its N-terminal ankyrin repeat domain. *Proceedings of the National Academy of Sciences of the United States of America,* 111(47):16901. https://doi.org/10.1073/pnas.1412689111

Murthy, S. E., Loud, M. C., Daou, I., Marshall, K. L., Schwaller, F., Kühnemund, J., Francisco, A. G., Keenan, W. T., Dubin, A. E., Lewin, G. R., & Patapoutian, A. (2018). The mechanosensitive ion channel Piezo2 mediates sensitivity to mechanical pain in mice. *Sci Transl Med*, 10(462): eaat9897. https://doi.org/10.1126/scitranslmed.aat9897

Nagi, S. S., Marshall, A. G., Makdani, A., Jarocka, E., Liljencrantz, J., Ridderström, M., Shaikh, S., O'Neill, F., Saade, D., Donkervoort, S., Reghan Foley, A., Minde, J., Trulsson, M., Cole, J., Bönnemann, C. G., Chesler, A. T., Catherine Bushnell, M., McGlone, F., & Olausson, H. (2019). An ultrafast system for signaling mechanical pain in human skin. *Science Advances,* 5(7):eaaw1297. https://doi.org/10.1126/sciadv.aaw1297

Nagy, J. I., & Hunt, S. P. (1982). Fluoride-resistant acid phosphatase-containing neurones in dorsal root ganglia are separate from those containing substance P or somatostatin. *Neuroscience,* 7(1):89-97. https://doi.org/10.1016/0306-4522(82)90155-5

Närhi, M. (1990). The neurophysiology of the teeth. *Dental clinics of North America,* 34(3):439-48.

Närhi, M., Jyväsjärvi, E., Virtanen, A., Huopaniemi, T., Ngassapa, D., & Hirvonen, T. (1992). Role of intradental A- and C-type nerve fibres in dental pain mechanisms. *Proceedings of the Finnish Dental Society. Suomen Hammaslääkäriseuran toimituksia,* 88(Suppl 1):507-16.

Naumann, T., Härtig, W., & Frotscher, M. (2000). Retrograde tracing with Fluoro-Gold: Different methods of tracer detection at the ultrastructural level and neurodegenerative changes of back-filled neurons in long-term studies. *Journal of Neuroscience Methods,* 103(1):11-21. https://doi.org/10.1016/S0165-0270(00)00292-2

Nyström, B., & Hagbarth, K. E. (1981). Microelectrode recordings from transected nerves in amputees with phantom limb pain. *Neuroscience Letters,* 27(2):211-6. https://doi.org/10.1016/0304-3940(81)90270-6

Ochoa, J. L. (2010). Intraneural microstimulation in humans. *Neuroscience Letters,* 110(6):1509-29. https://doi.org/10.1016/j.neulet.2009.10.007

Okumura, R., Shima, K., Muramatsu, T., Nakagawa, K. I., Shimono, M., Suzuki, T., Magloire, H., & Shibukawa, Y. (2005). The odontoblast as a sensory receptor cell? The expression of TRPV1 (VR-1) channels. *Archives of Histology and Cytology,* 68(4):251-7. https://doi.org/10.1679/aohc.68.251

Paik, S. K., Park, K. P., Lee, S. K., Ma, S. K., Cho, Y. S., Kim, Y. K., Rhyu, I. J., Ahn, D. K., Yoshida, A., & Bae, Y. C. (2009). Light and electron microscopic analysis of the somata and parent axons innervating the rat upper molar and lower incisor pulp. *Neuroscience,* 162(4):1279-86. https://doi.org/10.1016/j.neuroscience.2009.05.046

Paik, Sang Kyoo, Lee, D. S., Kim, J. Y., Bae, J. Y., Cho, Y. S., Ahn, D. K., Yoshida, A., & Bae, Y. C. (2010). Quantitative ultrastructural analysis of the neurofilament 200-positive axons in the rat dental pulp. *Journal of Endodontics,* 36(10):1638-42. https://doi.org/10.1016/j.joen.2010.05.005

Pajot, J., Pelissier, T., Sierralta, F., Raboisson, P., & Dallel, R. (2000). Differential effects of trigeminal tractotomy on Aδ- and C-fiber-mediated nociceptive responses. *Brain Research,* 8(1-2):289-292. https://doi.org/10.1016/S0006-8993(00)02157-0

Park, C.-K., Kim, M., Fang, Z., Li, H., Jung, S., Choi, S.-Y., Lee, S., Park, K., Kim, J., & Oh, S. (2006). Functional expression of thermo-transient receptor potential channels in dental primary afferent neurons: implication for tooth pain. *The Journal of Biological Chemistry*, 281(25), 17304–17311. https://doi.org/10.1074/jbc.M511072200

Passmore, G. M., Reilly, J. M., Thakur, M., Keasberry, V. N., Marsh, S. J., Dickenson, A. H., & Brown, D. A. (2012). Functional significance of M-type potassium channels in nociceptive cutaneous sensory endings. *Frontiers in Molecular Neuroscience,* 5:63. https://doi.org/10.3389/fnmol.2012.00063

Peier, A. M., Moqrich, A., Hergarden, A. C., Reeve, A. J., Andersson, D. A., Story, G. M., Earley, T. J., Dragoni, I., McIntyre, P., Bevan, S., & Patapoutian, A. (2002). A TRP channel that senses cold stimuli and menthol. *Cell,* 108(5):705-15. https://doi.org/10.1016/S0092-8674(02)00652-9

Prato, V., Taberner, F. J., Hockley, J., Callejo, G., Arcourt, A., Tazir, B., Hammer, L., Schad, P., Heppenstall, P. A., Smith, E. S., & Lechner, S. G. (2017). Functional and Molecular Characterization of Mechanoinsensitive "Silent" Nociceptors. *Cell Reports*, 21(11), 3102–3115. https://doi.org/10.1016/j.celrep.2017.11.066

Raja, S. N., Meyer, R. A., & Campbell, J. N. (1988). Peripheral mechanisms of somatic pain. *Anesthesiology,* 68(4):571-90. https://doi.org/10.1097/00000542-198804000-00016

Ramón Y Cajal, S., DeFelipe, J., Jones, E. G., & May, R. M. (2012). Cajal's Degeneration and Regeneration of the Nervous System. *Cajal's Degeneration and Regeneration of the Nervous System*. https://doi.org/10.1093/acprof:oso/9780195065169.001.0001

Ray, P., Torck, A., Quigley, L., Wangzhou, A., Neiman, M., Rao, C., Lam, T., Kim, J. Y., Kim, T. H., Zhang, M. Q., Dussor, G., & Price, T. J. (2018). Comparative transcriptome profiling of the human and mouse dorsal root ganglia: An RNA-seq-based resource for pain and sensory neuroscience research.. *Pain,* 159(7):1325-1345. https://doi.org/10.1097/j.pain.0000000000001217

Rexed, B. (1952). The cytoarchitectonic organization of the spinal cord in the cat. *Journal of Comparative Neurology,* 96(3):414-95. https://doi.org/10.1002/cne.900960303

Reynolds, D. V. (1969). Surgery in the rat during electrical analgesia induced by focal brain stimulation. *Science,* 164(3878):444-5. https://doi.org/10.1126/science.164.3878.444

Rose, K., Ooi, L., Dalle, C., Robertson, B., Wood, I. C., & Gamper, N. (2011). Transcriptional repression of the M channel subunit Kv7.2 in chronic nerve injury. *Pain,* 152(4):742-54. https://doi.org/10.1016/j.pain.2010.12.028

Rostock, C., Schrenk-Siemens, K., Pohle, J., & Siemens, J. (2018). Human vs. Mouse Nociceptors – Similarities and Differences. *Neuroscience,* 387:13-27. https://doi.org/10.1016/j.neuroscience.2017.11.047

Roza, C., Castillejo, S., & López-García, J.A. Accumulation of Kv7.2 channels in putative ectopic transduction zones of mice nerve-end neuromas. *Molecular Pain*, 7(1), 58. https://doi.org/10.1186/1744-8069-7-58

Roza, C., & Lopéz-García, J. A. (2008). Retigabine, the specific KCNQ channel opener, blocks ectopic discharges in axotomized sensory fibres. *Pain*, 138(3), 537–545. https://doi.org/10.1016/j.pain.2008.01.031

Roza, C., Laird, J. M. A., Souslova, V., Wood, J. N., & Cervero, F. (2004). The Tetrodotoxin-Resistant Na+ Channel Nav1.8 is Essential for the Expression of Spontaneous Activity in Damaged Sensory Axons of Mice. *The Journal of Physiology*, 550(3), 921–926. https://doi.org/10.1113/jphysiol.2003.046110

Sabatowski, R., Schafer, D., Kasper, S., Brunsch, H., & Radbruch, L. (2005). Pain Treatment: A Historical Overview. *Current Pharmaceutical Design,* 10(7):701-16. https://doi.org/10.2174/1381612043452974

Santoro, B., Chen, S., Lüthi, A., Pavlidis, P., Shumyatsky, G. P., Tibbs, G. R., & Siegelbaum, S. A. (2000). Molecular and functional heterogeneity of hyperpolarization-activated pacemaker channels in the mouse CNS. *Journal of Neuroscience,* 20(14):5264-75. https://doi.org/10.1523/jneurosci.20-14-05264.2000

Saria, A. (1984). Substance P in sensory nerve fibres contributes to the development of oedema in the rat hind paw after thermal injury. *British Journal of Pharmacology,* 82(1):217-22. https://doi.org/10.1111/j.1476-5381.1984.tb16461.x

Sato, M., Sobhan, U., Tsumura, M., Kuroda, H., Soya, M., Masamura, A., Nishiyama, A., Katakura, A., Ichinohe, T., Tazaki, M., & Shibukawa, Y. (2013). Hypotonic-induced stretching of plasma membrane activates transient receptor potential vanilloid channels and sodium-calcium exchangers in mouse odontoblasts. *Journal of Endodontics,* 39(6):779-787. https://doi.org/10.1016/j.joen.2013.01.012

Schlegel, T., Sauer, S. K., Handwerker, H. O., & Reeh, P. W. (2004). Responsiveness of C-fiber nociceptors to punctate force-controlled stimuli in isolated rat skin: Lack of modulation by inflammatory mediators and flurbiprofen. *Neuroscience Letters,* 361(1-3):163-7. https://doi.org/10.1016/j.neulet.2003.12.073

Schmalbruch, H. (1986). Fiber composition of the rat sciatic nerve. *The Anatomical Record,* 215(1):71-81. https://doi.org/10.1002/ar.1092150111

Schmidt, R., Schmelz, M., Forster, C., Ringkamp, M., Torebjork, E., & Handwerker, H. (1995). Novel classes of responsive and unresponsive C nociceptors in human skin. *Journal of Neuroscience,* 15(1):333-41. https://doi.org/10.1523/jneurosci.15-01-00333.1995

Seal, R. P., Wang, X., Guan, Y., Raja, S. N., Woodbury, C. J., Basbaum, A. I., & Edwards, R. H. (2009). Injury-induced mechanical hypersensitivity requires C-low threshold mechanoreceptors. *Nature,* 462(7273):651-5. https://doi.org/10.1038/nature08505

Seifert, R., Scholten, A., Gauss, R., Mincheva, A., Lichter, P., & Kaupp, U. B. (1999). Molecular characterization of a slowly gating human hyperpolarization-activated channel predominantly expressed in thalamus, heart, and testis. *Proceedings of the National Academy of Sciences of the United States of America,* 96(16):9391-6. https://doi.org/10.1073/pnas.96.16.9391

Serra, J., Bostock, H., Solà, R., Aleu, J., García, E., Cokic, B., Navarro, X., & Quiles, C. (2012). Microneurographic identification of spontaneous activity in C-nociceptors in neuropathic pain states in humans and rats. *Pain*, 153(1), 42–55. https://doi.org/10.1016/j.pain.2011.08.015

Sessle, B. J. (2000). Acute and chronic craniofacial pain: Brainstem mechanisms of nociceptive transmission and neuroplasticity, and their clinical correlates. *Critical Reviews in Oral Biology and Medicine,* 11(1):57-91. https://doi.org/10.1177/10454411000110010401

Shigenaga, Y., Okamoto, T., Nishimori, T., Suemune, S., Nasution, I. D., Chen, I. C., Tsuru, K., Yoshida, A., Tabuchi, K., Hosoi, M., & Tsuru, H. (1986). Oral and facial representation in the trigeminal principal and rostral spinal nuclei of the cat. *Journal of Comparative Neurology,* 244(1):1-18. https://doi.org/10.1002/cne.902440102

Silverman, J. D., & Kruger, L. (1988a). Acid phosphatase as a selective marker for a class of small sensory ganglion cells in several mammals: Spinal cord distribution, histochemical properties, and relation to fluoride-resistant acid phosphatase (FRAP) of rodents. *Somatosensory and Motor Research,* 5(3):219-46. https://doi.org/10.3109/07367228809144628

Silverman, J. D., & Kruger, L. (1988b). Lectin and neuropeptide labeling of separate populations of dorsal root ganglion neurons and associated "nociceptor" thin axons in rat testis and cornea whole-mount preparations. *Somatosensory and Motor Research,* 5(3):259-67. https://doi.org/10.3109/07367228809144630

Solé-Magdalena, A., Martínez-Alonso, M., Coronado, C. A., Junquera, L. M., Cobo, J., & Vega, J. A. (2018). Molecular basis of dental sensitivity: The odontoblasts are multisensory cells and express multifunctional ion channels. *Annals of Anatomy,* 215:20-29. https://doi.org/10.1016/j.aanat.2017.09.006

Story, G. M., Peier, A. M., Reeve, A. J., Eid, S. R., Mosbacher, J., Hricik, T. R., Earley, T. J., Hergarden, A. C., Andersson, D. A., Hwang, S. W., McIntyre, P., Jegla, T., Bevan, S., & Patapoutian, A. (2003). ANKTM1, a TRP-like channel expressed in nociceptive neurons, is activated by cold temperatures. *Cell,* 112(6):819-29. https://doi.org/10.1016/S0092-8674(03)00158-2

Stucky, C. L., & Lewin, G. R. (1999). Isolectin B4-positive and -negative nociceptors are functionally distinct. *Journal of Neuroscience,* 19(15):6497-505. https://doi.org/10.1523/jneurosci.19-15-06497.1999

Study, R. E., & Kral, M. G. (1996). Spontaneous action potential activity in isolated dorsal root ganglion neurons from rats with a painful neuropathy. *Pain,* 65(2-3):235-42. https://doi.org/10.1016/0304-3959(95)00216-2

Takahashi, N., & Mori, Y. (2011). TRP channels as sensors and signal integrators of redox status changes. *Frontiers in Pharmacology,* 2:58. https://doi.org/10.3389/fphar.2011.00058

Tappe-Theodor, A., & Rohini, K. (2014). Studying ongoing and spontaneous pain in rodents - challenges and opportunities. *European Journal of Neuroscience*, 39(11), 1881–1890. https://doi.org/10.1111/ejn.12643

Tatulian, L., Delmas, P., Abogadie, F. C., & Brown, D. A. (2001). Activation of expressed KCNQ potassium currents and native neuronal M-type potassium currents by the anti-convulsant drug retigabine. *Journal of Neuroscience,* 21(15):5535-45. https://doi.org/10.1523/jneurosci.21-15-05535.2001

Thakur, M., Crow, M., Richards, N., Davey, G. I. J., Levine, E., Kelleher, J. H., Agley, C. C., Denk, F., Harridge, S. D. R., & McMahon, S. B. (2014). Defining the nociceptor transcriptome. *Frontiers in Molecular Neuroscience,* 7:87. https://doi.org/10.3389/fnmol.2014.00087

Thut, P. D., Wrigley, D., & Gold, M. S. (2003). Cold transduction in rat trigeminal ganglia neurons in vitro. *Neuroscience,* 119(4):1071-83. https://doi.org/10.1016/S0306-4522(03)00225-2

Todd, A. J. (2002). Anatomy of primary afferents and projection neurones in the rat spinal dorsal horn with particular emphasis on substance P and the neurokinin 1 receptor. *Experimental Physiology,* 87(2):245-9. https://doi.org/10.1113/eph8702351

Todd, A. J. (2010). Neuronal circuitry for pain processing in the dorsal horn. *Nature Reviews Neuroscience,* 11(12):823-836. https://doi.org/10.1038/nrn2947

Todd, A. J., Wang, F., Todd, A. J., & Wang, F. (2018). Central Nervous System Pain Pathways. *The Oxford Handbook of the Neurobiology of Pain*. Oxford University Press. https://doi.org/10.1093/oxfordhb/9780190860509.013.5

Touska, F., Winter, Z., Mueller, A., Vlachova, V., Larsen, J., & Zimmermann, K. (2016). Comprehensive thermal preference phenotyping in mice using a novel automated circular gradient assay. *Temperature,* 3(1):77-91. https://doi.org/10.1080/23328940.2015.1135689

Treede, R. D., Rief, W., Barke, A., Aziz, Q., Bennett, M. I., Benoliel, R., Cohen, M., Evers, S., Finnerup, N. B., First, M. B., Giamberardino, M. A., Kaasa, S., Korwisi, B., Kosek, E., Lavand'Homme, P., Nicholas, M., Perrot, S., Scholz, J., Schug, S., Smith, B.H., Svensson, P., Vlaeyen, J.W.S, Wang, S. J. (2019). Chronic pain as a symptom or a disease: The IASP Classification of Chronic Pain for the International Classification of Diseases (ICD-11). *Pain,* 160(1):19-27. https://doi.org/10.1097/j.pain.0000000000001384

Trowbridge, H. O. (1985). Intradental sensory units: Physiological and clinical aspects. *Journal of Endodontics,* 11(11):489-498. https://doi.org/10.1016/S0099-2399(85)80222-3

Truini, A., Galeotti, F., Haanpaa, M., Zucchi, R., Albanesi, A., Biasiotta, A., Gatti, A., & Cruccu, G. (2008). Pathophysiology of pain in postherpetic neuralgia: A clinical and neurophysiological study. *Pain,* 140(3):405-10. https://doi.org/10.1016/j.pain.2008.08.018

Truini, A., Padua, L., Biasiotta, A., Caliandro, P., Pazzaglia, C., Galeotti, F., Inghilleri, M., & Cruccu, G. (2009). Differential involvement of A-delta and A-beta fibres in neuropathic pain related to carpal tunnel syndrome. *Pain,* 145(1-2):105-9. https://doi.org/10.1016/j.pain.2009.05.023

Truini, A. (2017). A Review of Neuropathic Pain: From Diagnostic Tests to Mechanisms. *Pain and Therapy,* 6(Suppl 1):5-9. https://doi.org/10.1007/s40122-017-0085-2

Truini, A., Luis, García-Larrea, L., & Cruccu, G. (2013). Reappraising neuropathic pain in humans —how symptoms help disclose mechanisms. *Nature Reviews Neurology*, 9(10), 1–11. https://doi.org/10.1038/nrneurol.2013.180

Tsantoulas, C., Lainez, S., Wong, S., Mehta, I., Vilar, B., & McNaughton, P. A. (2017). Hyperpolarization-activated cyclic nucleotide-gated 2 (hcn2) ion channels drive pain in mouse models of diabetic neuropathy. *Science Translational Medicine,* 9(409):eaam6072. https://doi.org/10.1126/scitranslmed.aam6072

Tsumura, M., Sobhan, U., Sato, M., Shimada, M., Nishiyama, A., Kawaguchi, A., Soya, M., Kuroda, H., Tazaki, M., & Shibukawa, Y. (2013). Functional expression of TRPM8 and TRPA1 channels in rat odontoblasts. *PLoS ONE,* 8(12):e82233. https://doi.org/10.1371/journal.pone.0082233

Usoskin, D., Furlan, A., Islam, S., Abdo, H., Lönnerberg, P., Lou, D., Hjerling-Leffler, J., Haeggström, J., Kharchenko, O., Kharchenko, P. V., Linnarsson, S., & Ernfors, P. (2015). Unbiased classification of sensory neuron types by large-scale single-cell RNA sequencing. *Nature Neuroscience,* 18(1):145-153. https://doi.org/10.1038/nn.3881

Van Hecke, O., Austin, S. K., Khan, R. A., Smith, B. H., & Torrance, N. (2014). Neuropathic pain in the general population: A systematic review of epidemiological studies. *Pain,* 155(4):654-62. https://doi.org/10.1016/j.pain.2013.11.013

Vandewauw, I., De Clercq, K., Mulier, M., Held, K., Pinto, S., Van Ranst, N., Segal, A., Voet, T., Vennekens, R., Zimmermann, K., Vriens, J., & Voets, T. (2018). A TRP channel trio mediates acute noxious heat sensing. *Nature,* 555(7698):662-666. https://doi.org/10.1038/nature26137

Vang, H., Chung, G., Kim, H. Y., Park, S.-B., Jung, S. J., Kim, J.-S., & Oh, S. B. (2012). Neurochemical Properties of Dental Primary Afferent Neurons. *Experimental Neurobiology,* 21(2):68-74. https://doi.org/10.5607/en.2012.21.2.68

Viana, F. (2016). TRPA1 channels: molecular sentinels of cellular stress and tissue damage. *Journal of Physiology,* 594(15):4151-69. https://doi.org/10.1113/JP270935

Vollert, J., Maier, C., Attal, N., Bennett, D. L. H., Bouhassira, D., K, E.-K. E., Finnerup, N. B., Freynhagen, R., Gierthmühlen, J., Haanpää, M., Hansson, P., Hüllemann, P., Jensen, T. S., Magerl, W., Ramirez, J. D., Rice, A. S. C., Sigrid, S.-H., Segerdahl, M., Serra, J., … Baron, R. (2017). Stratifying patients with peripheral neuropathic pain based on sensory profiles. *Pain*, 158(8), 1446–1455. https://doi.org/10.1097/j.pain.0000000000000935

Walton, R. E., & Nair, P.N.R. (1995). Neural elements in dental pulp and dentin. *Oral Surgery, Oral Medicine, Oral Pathology, Oral Radiology And Endodontology,* 80(6):710-719. https://doi.org/10.1016/S1079-2104(05)80256-2

Wemmie, J. A., Taugher, R. J., & Kreple, C. J. (2013). Acid-sensing ion channels in pain and disease. *Nature Reviews Neuroscience,* 14(7):461-71. https://doi.org/10.1038/nrn3529

West, N. X., Lussi, A., Seong, J., & Hellwig, E. (2013). Dentin hypersensitivity: Pain mechanisms and aetiology of exposed cervical dentin. *Clinical Oral Investigations,* 17(Suppl 1):9-19. https://doi.org/10.1007/s00784-012-0887-x

Wiesenfeld-Hallin, Z., Hökfelt, T., Lundberg, J. M., Forssmann, W. G., Reinecke, M., Tschopp, F. A., & Fischer, J. A. (1984). Immunoreactive calcitonin gene-related peptide and substance P coexist in sensory neurons to the spinal cord and interact in spinal behavioral responses of the rat. *Neuroscience Letters,* 52(1-2):199-204. https://doi.org/10.1016/0304-3940(84)90374-4

Wijayasinghe, N., Ringsted, T. K., Bischoff, J. M., Kehlet, H., & Werner, M. U. (2016). The role of peripheral afferents in persistent inguinal postherniorrhaphy pain: A randomized, double-blind, placebo-controlled, crossover trial of ultrasound-guided tender point blockade. *British Journal of Anaesthesia,* 116(6)829-37). https://doi.org/10.1093/bja/aew071

Winter, Z., Gruschwitz, P., Eger, S., Touska, F., & Zimmermann, K. (2017). Cold temperature encoding by cutaneous TRPA1 and TRPM8-carrying fibers in the mouse. *Frontiers in Molecular Neuroscience,* 10:209. https://doi.org/10.3389/fnmol.2017.00209

Woolf, C. J. (2011). Central sensitization: Implications for the diagnosis and treatment of pain. *Pain,* 152(Suppl 3):2-15. https://doi.org/10.1016/j.pain.2010.09.030

Wu, G., Ringkamp, M., Hartke, T. V, Murinson, B. B., Campbell, J. N., Griffin, J. W., & Meyer, R. A. (2001). Early onset of spontaneous activity in uninjured C-fiber nociceptors after injury to neighboring nerve fibers. *Journal of Neuroscience*, 21(8), RC140. https://doi.org/10.1523/JNEUROSCI.21-08-j0002.2001

Wu, G., Ringkamp, M., Murinson, B. B., Pogatzki, E. M., Hartke, T. V, Weerahandi, H. M., Campbell, J. N., Griffin, J. W., & Meyer, R. A. (2002). Degeneration of myelinated efferent fibers induces spontaneous activity in uninjured C-fiber afferents. *Journal of Neuroscience*, 22(17), 7746–7753. https://doi.org/10.1523/JNEUROSCI.22-17-07746.2002

Wulff, H., Castle, N. A., & Pardo, L. A. (2009). Voltage-gated potassium channels as therapeutic targets. *Nature Reviews Drug Discovery,* 8(12):982-1001. https://doi.org/10.1038/nrd2983

Wuttke, T. V., Jurkat-Rott, K., Paulus, W., Garncarek, M., Lehmann-Horn, F., & Lerche, H. (2007). Peripheral nerve hyperexcitability due to dominant-negative KCNQ2 mutations. *Neurology,* 69(22):2045-53. https://doi.org/10.1212/01.wnl.0000275523.95103.36

Young, G. T., Emery, E. C., Mooney, E. R., Tsantoulas, C., & A, M. P. (2014). Inflammatory and neuropathic pain are rapidly suppressed by peripheral block of hyperpolarisation-activated cyclic nucleotide-gated ion channels. *Pain*, 155(9):1708-19. https://doi.org/10.1016/j.pain.2014.05.021

Zhang, M., Wang, Y., Geng, J., Zhou, S., & Xiao, B. (2019). Mechanically Activated Piezo Channels Mediate Touch and Suppress Acute Mechanical Pain Response in Mice. *Cell Reports,* 26(6):1419-1431. https://doi.org/10.1016/j.celrep.2019.01.056

Zhang, Y., Bo, X., Schoepfer, R., Holtmaat, A. J. D. G., Verhaagen, J., Emson, P. C., Lieberman, A. R., & Anderson, P. N. (2005). Growth-associated protein GAP-43 and L1 act synergistically to promote regenerative growth of Purkinje cell axons in vivo. *Proceedings of the National Academy of Sciences of the United States of America,* 102(41):14883-8. https://doi.org/10.1073/pnas.0505164102

Zhuo, M., & Gebhart, G. F. (1997). Biphasic modulation of spinal nociceptive transmission from the medullary raphe nuclei in the rat. *Journal of Neurophysiology,* 78(2):746-58. https://doi.org/10.1152/jn.1997.78.2.746

Zimmermann, K., Lennerz, J. K., Hein, A., Link, A. S., Stefan Kaczmarek, J., Delling, M., Uysal, S., Pfeifer, J. D., Riccio, A., & Clapham, D. E. (2011). Transient receptor potential cation channel, subfamily C, member 5 (TRPC5) is a cold-transducer in the peripheral nervous system. *Proceedings of the National Academy of Sciences of the United States of America,* 108(44):18114-9. https://doi.org/10.1073/pnas.1115387108

Zylka, M. J., Rice, F. L., & Anderson, D. J. (2005). Topographically distinct epidermal nociceptive circuits revealed by axonal tracers targeted to Mrgprd. *Neuron,* 45(1):17-25. https://doi.org/10.1016/j.neuron.2004.12.015

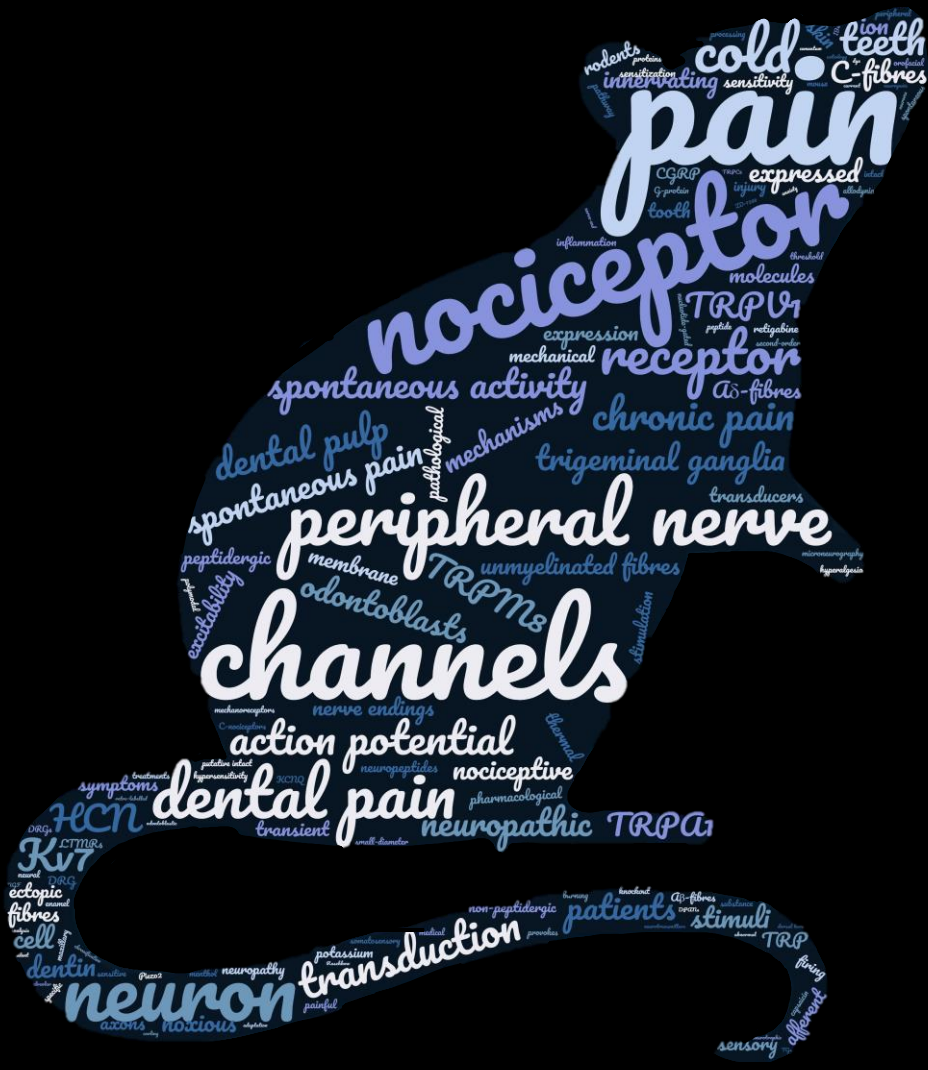

Funding:

GOBIERNO DE ESPAÑA

DFG Deutsche Forschungsgemeinschaft

interdisziplinäres Zentrum für Klinische Forschung Erlangen

Dr. Pfleger ARZNEIMITTEL